Influence of Hydrophobically Modified Polyelectrolytes on Nanoparticle Synthesis in Self-Organized Systems and in Water

Dissertation

zur Erlangung des akademischen Grades
"doctor rerum naturalium" (Dr. rer. nat.)
in der Wissenschaftsdisziplin
Kolloid- und Polymerchemie

eingereicht an der Mathematisch-Naturwissenschaftlichen Fakultät
der Universität Potsdam

von

Carine Note

geboren am 02.03.1979 in Saint-Saulve

Potsdam, im September 2006

"L'Homme n'est qu'un roseau,
le plus faible de la nature,
mais c'est un roseau pensant".

Blaise Pascal, Pensées, 1670

ABSTRACT

The formation of colloids by the controlled reduction, nucleation, and growth of inorganic precursor salts in different media has been investigated for more than a century. Recently, the preparation of ultrafine particles has received much attention since they can offer highly promising and novel options for a wide range of technical applications (nanotechnology, electrooptical devices, pharmaceutics, etc). The interest derives from the well-known fact that properties of advanced materials are critically dependent on the microstructure of the sample. Control of size, size distribution and morphology of the individual grains or crystallites is of the utmost importance in order to obtain the material characteristics desired.

Several methods can be employed for the synthesis of nanoparticles. On the one hand, the reduction can occur in diluted aqueous or alcoholic solutions. On the other hand, the reduction process can be realized in a template phase, e.g. in well-defined microemulsion droplets. However, the stability of the nanoparticles formed mainly depends on their surface charge and it can be influenced with some added protective components. Quite different types of polymers, including polyelectrolytes and amphiphilic block copolymers, can for instance be used as protecting agents.

The reduction and stabilization of metal colloids in aqueous solution by adding self-synthesized hydrophobically modified polyelectrolytes were studied in much more details. The polymers used are hydrophobically modified derivatives of poly(sodium acrylate) and of maleamic acid copolymers as well as the commercially available branched poly(ethyleneimine).

The first notable result is that the polyelectrolytes used can act alone as both reducing and stabilizing agent for the preparation of gold nanoparticles. The investigation was then focused on the influence of the hydrophobic substitution of the polymer backbone on the reduction and stabilization processes. First of all, the polymers were added at room temperature and the reduction process was investigated over a longer time period (up to 8 days). In comparison, the reduction process was realized faster at higher temperature, i.e. 100°C. In both cases metal nanoparticles of colloidal dimensions can be produced. However, the size and shape of the

individual nanoparticles mainly depends on the polymer added and the temperature procedure used.

In a second part, the influence of the prior mentioned polyelectrolytes was investigated on the phase behaviour as well as on the properties of the inverse micellar region (L_2 phase) of quaternary systems consisting of a surfactant, toluene-pentanol (1:1) and water. The majority of the present work has been made with the anionic surfactant sodium dodecylsulfate (SDS) and the cationic surfactant cetyltrimethylammonium bromide (CTAB) since they can interact with the oppositely charged polyelectrolytes and the microemulsions formed using these surfactants present a large water-in-oil region.

Subsequently, the polymer-modified microemulsions were used as new templates for the synthesis of inorganic particles, ranging from metals to complex crystallites, of very small size. The water droplets can indeed act as nanoreactors for the nucleation and growth of the particles, and the added polymer can influence the droplet size, the droplet-droplet interactions, as well as the stability of the surfactant film by the formation of polymer-surfactant complexes.

One further advantage of the polymer-modified microemulsions is the possibility to stabilize the primary formed nanoparticles via a polymer adsorption (steric and/or electrostatic stabilization). Thus, the polyelectrolyte-modified nanoparticles formed can be redispersed without flocculation after solvent evaporation.

The results of this thesis have been or will be published in due course:

1-   C. Note, J. Koetz, S. Kosmella, B. Tiersch, "Hydrophobically modified polyelectrolytes used as reducing and stabilizing agent for the formation of gold nanoparticles", Colloid Polym. Sci. 283 (2005) 1334-1342.

2-   C. Note, J. Koetz, S. Kosmella, "Influence of hydrophobically modified polyelectrolytes on CTAB-based w/o microemulsions", Colloid Surf. A 288 (1-3) (2006) 158-164.

3-   C. Note, S. Kosmella, J. Koetz, "Poly(ethyleneimine) as reducing and stabilizing agent for the formation of gold nanoparticles ", Colloid Surf. A (2006) in press.

4-   C. Note, J. Koetz, S. Kosmella, "Structural changes in poly(ethyleneimine) modified microemulsions", J. Colloid Interface Sci. (2006) in press.

5-   C. Note, J. Ruffin, J. Koetz, "The influence of polyampholytes on the phase behaviour of microemulsion used as template for the nanoparticles formation", J. Disp. Sci. Techn. Special Issue, 28 (2007) 1, accepted.

TABLE OF CONTENTS

AOT	Sodium bis(2-ethylhexyl) sulfosuccinate
c	Concentration of a solution [$mol \cdot L^{-1}$ or wt %]
$c_{s,t}$	Total surfactant concentration [$mmol \cdot dm^{-3}$]
$c_{s,b}$	Concentration of bound surfactant [$mmol \cdot dm^{-3}$]
$c_{s,f}$	Concentration of free surfactant [$mmol \cdot dm^{-3}$]
CAC	Critical aggregation concentration
CDI	Dicyclohexylcarbodiimine
CMC	Critical micellization concentration
Cryo-SEM	Cryo-high resolution Scanning Electron Microscopy
CTAB	Cetyltrimethylammonium bromide
d	Distance between two particles [nm]
D	Mean diameter of a particle [nm] measured by DLS
d_{mean}	Mean diameter of a particle calculated from TEM micrographs [nm]
DADMAC	N,N'-diallyl-N,N'-dimethylammonium chloride
D_2O	Deuterium oxide
DSC	Differential Scanning Calorimetry
DLS	Dynamic Light Scattering
H_o	Spontaneous curvature
HM-PEL	Hydrophobically modified polyelectrolyte
IR	Infrared Spectroscopy
k_B	Bolzmann constant [$J \cdot K^{-1}$]
Ku	Binding constant of a surfactant to a polymer [$dm^3 \cdot mmol^{-1}$]
L_1	Oil-in-water microemulsion
L_2	Water-in-oil microemulsion
Mn	Number average molar mass of a polymer [$g \cdot mol^{-1}$]
M_w	Weight average molar mass of a polymer [$g \cdot mol^{-1}$]
n	Refractive index of a solution
NMP	1-methyl-2-pyrrolidone
NMR	Nuclear Magnetic Resonance Spectroscopy
O/W	Oil-in-water
PAA	Poly(sodium acrylate)
PA3C4	Poly(sodium acrylate) modified by 3% of butylamine
PA10C4	Poly(sodium acrylate) modified by 10% of butylamine
PA20C4	Poly(sodium acrylate) modified by 20% of butylamine
PalH	Poly-(N,N'-dially-N,N'-dimethylammonium-alt-maleamic carboxylate)

PalBu	Poly-(N,N'-dially-N,N'-dimethylammonium-alt-N-n-butyl-maleamic carboxylate)
PalOc	Poly-(N,N'-dially-N,N'-dimethylammonium-alt-N-n-octyl-maleamic carboxylate)
PalPh	Poly-(N,N'-dially-N,N'-dimethylammonium-alt-N-phenyl-maleamic carboxylate)
PEI	Poly(ethyleneimine)
PEL	Polyelectrolyte
PEO-PPO-PEO	Poly(ethylene oxide)-poly(propylene oxide)-poly(ethylene oxide) copolymer
$\mathbf{p_p}$	Packing parameter
r	Mass ratio between two solutions
$\mathbf{R_h}$	Hydrodynamic radius of a scattering object [nm] (DLS)
$\mathbf{R_w}$	Water/surfactant weight ratio in microemulsion
SB	3-(N-N'-dimethyldodecylammonio) propanesulphonate
SDS	Sodium dodecylsulphate
t	Time [s]
T	Temperature [°C or K]
TEM	Transmission Electron Microscopy
UV	Ultraviolet
UV-vis	Ultraviolet/visible Light Spectroscopy
$\mathbf{V_{att}}$	Van der Waals attraction energy between two particles [$J \cdot m^{-2}$]
$\mathbf{V_{rep}}$	Electrostatic repulsion energy between two particles [$J \cdot m^{-2}$]
$\mathbf{V_s}$	Steric repulsion energy between two particles [$J \cdot m^{-2}$]
W/O	Water-in-oil
δ	Adsorbed layer thickness of polymer [nm]
ε	Relative dielectric constant
$\dot{\gamma}$	Shear rate [s^{-1}]
η	Shear viscosity of a microemulsion [Pas]
[η]	Intrinsic viscosity of a polymer solution [$cm^3 \cdot g^{-1}$]
λ	Wavelength [nm]
μ	Dynamic viscosity of a solution [cP]
σ	Standard deviation of the mean particle diameter [nm]
τ	shear stress [Pa]
ω	Surfactant/oil weight ratio in microemulsion
ξ	Zeta potential [mV]
ΔH	Enthalpy change [$kJ \cdot mol^{-1}$]
Θ	Scattering angle [°] (DLS)
Ω	Angular velocity [$rad \cdot s^{-1}$]

1. INTRODUCTION

This introductory part aims at giving a general overview of the scientific concepts relevant for the experimental work described later in this thesis. It is divided in four main chapters.

Chapter 1.1. gives a brief discussion of the theoretical background of surfactant science, and describes the general characteristics of amphiphilic self-organizing systems.

An introduction to the concept of microemulsion is presented in the Chapter 1.2., as well as an overview of their particular properties, and their intensive uses nowadays in every-day-life applications.

Chapter 1.3. focuses on the principle of the formation of inorganic particles, ranging from metals to complex crystallites, especially in microemulsion systems. How to understand and influence the stability of colloidal systems are questions that will be also approached in this part.

Finally, Chapter 1.4. presents the main challenges of this work, i.e. the interests of using polymers and hydrophobically modified polyelectrolytes to control the synthesis and the stabilization of nanoparticles in aqueous systems and/or in microemulsion nanoreactors.

1.1.   Surfactants in solution

Surfactant is an abbreviation for surface-active agent, which literally means active at a surface. In other words, a surfactant is characterized by its tendency to adsorb at surfaces or interfaces. Thus, surfactants can modify the physico-chemical properties of the surfaces or interfaces of the system in which they are contained.

The general structure of a surfactant consists of two parts: an hydrophobic or non polar moiety, generally named the "tail", and an hydrophilic or polar part, the "head"-group. Due to its special structural characteristics, or namely its amphiphilic properties, a surfactant molecule can adsorb for instance at liquid-liquid interfaces, resulting in a reduction of the interfacial tension between the two phases. Figure 1.1-1 shows a commonly used schematic illustration of a surfactant molecule and its adsorption at a water-oil interface.
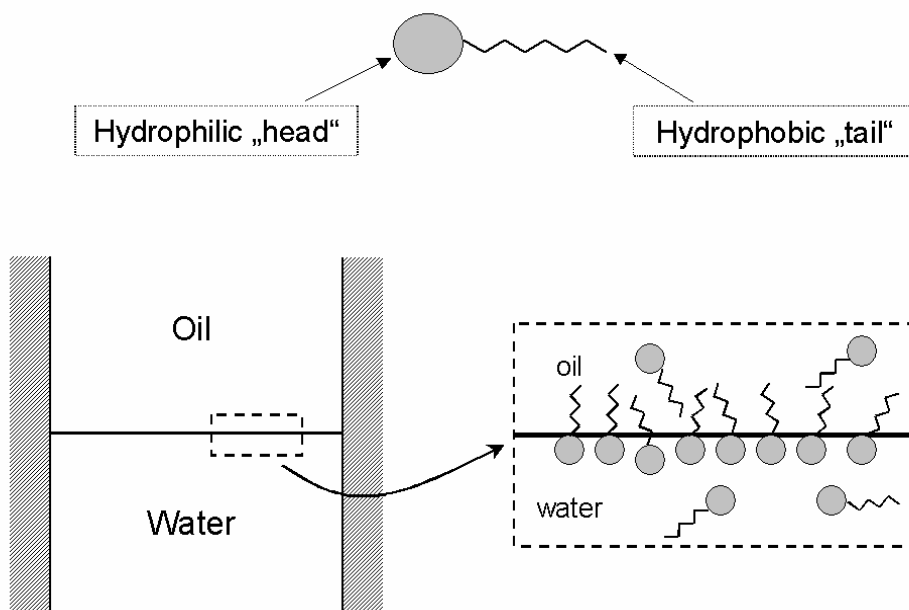
Figure 1.1-1: Schematic illustration of a surfactant molecule and of a macroscopic oil-water interface, where surfactant molecules are in a dynamic equilibrium. From ref. [1].
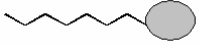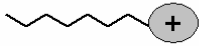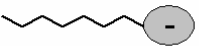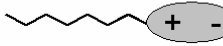
1.1.1. Classification of surfactants

The primary classification of surfactants is based on the charge of the hydrophilic head group. One can thus distinguish between nonionic, cationic, anionic or zwitterionic (dipolar) groups of surfactants (see Table. 1.1-1). The hydrophobic tail of the surfactant is generally made of hydrocarbon chains containing between 8 and 20 carbon atoms, but may also be

polydimethylsiloxane or fluorocarbon. Otherwise, another possible classification consists in referring the surfactant according to its chemical structure.

Table. 1.1-1: Classification of surfactants based on the charge of the head group.

Scheme	Type of surfactant	Example and Structure	
	nonionic	$C_{10}E_4$ (Decyltetraethylene glycol ether)	$CH_3-[CH_2]_8-CH_2-[O-CH_2-CH_2]_4-OH$
	cationic	CTAB (Cetyltrimethyl-ammonium bromide)	$CH_3-[CH_2]_{15}-N^+(CH_3)_3$ Br^-
	anionic	SDS (Sodium dodecylsulphate)	$CH_3-[CH_2]_{11}-O-S(=O)_2-O^-$ Na^+
	zwitterionic	SB (3-[N-N'-dimethyl-dodecylammonio] propanesulphonate)	$CH_3-[CH_2]_{11}-N^+(CH_3)_2-[CH_2]_3-S(=O)_2-O^-$

1.1.2. Aggregation of surfactants
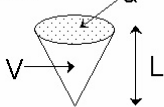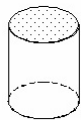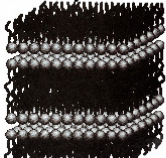
In very diluted solutions, surfactants dissolve and exist as single molecules, but when their concentration exceeds a certain value, the so-called critical micellization concentration (CMC), the molecules of surfactant spontaneously self-organize into a variety of aggregates. The CMC is one of the most important characteristics of a surfactant, in consideration of their practical use. Different factors, as the chemical structure and nature of the surfactant, the temperature, or the presence of other compounds or impurities, can principally influence the CMC value.

The morphology of the aggregates formed after the CMC is directly related to the molecular structure of the surfactant used. The orientation of the molecules at the interface can be expressed by the packing parameter [2, 3] (p_p), which represents the ratio between the effective areas occupied by the hydrophobic and hydrophilic parts of the surfactant. This parameter is given by the following equation:

$$p_p = V/aL$$

where *V* stands for the volume of the hydrophobic portion of the surfactant molecule, L is the length of the hydrocarbon chain, and *a* is the effective area per head group (see Table. 1.1-2).

Table. 1.1-2: Aggregation of amphiphilic molecules: mean (dynamic) packing shapes of surfactants and the structures they form (* From ref. [1]).

Surfactant		p_p (=V/aL)	Critical packing shape	Structures formed*
Single-chained surfactants with large head-group areas		< 1/3	Cone	Spherical micelles
Single-chained surfactants with small head-group areas		$1/3<p_p<1/2$	Truncated cone	Cylindrical micelles
Double-chained surfactants with large head-group areas		$1/2<p_p<1$	Truncated cone	Flexible bilayers, vesicles
Double-chained surfactants with small head-group areas		~ 1	Cylinder	Planar bilayers
Double-chained surfactants with small head-group areas		> 1	Inverted truncated cone or wedge	Inverted micelles

Nowadays, surfactants have become indispensable, and are used in many fields of applications: in the manufacture of detergents, soaps, shampoos, cosmetics, paints, pesticides, etc. All major types of surfactants, alkylbenzene sulphonates, alkyl sulphates, alcohol ethoxylates, etc., have been extensively used for decades. Their routes of preparation have been carefully optimised and their physicochemical behaviour is relatively well understood. Besides the constant challenge of finding new ways to minimize the manufacturing cost for existing surfactants, the market pull for "greener" products has been a primary objective for the development of new surfactants in recent years.

1.2.   Microemulsions

An emulsion is a mixture of two immiscible substances. One substance (the dispersed phase) is dispersed in the other (the continuous phase). Examples of emulsions include butter, margarine or mayonnaise.

Emulsification is the process by which emulsions are prepared. Under intense stirring, fine droplets of one phase in the other may form. However, without any stabilizing agent, such emulsions are not stable, and the droplets will coalesce immediately as stirring is stopped. In order to ensure reasonable stability of the dispersed system, the interface has to be "protected" by an emulsifying agent, for instance by a surfactant.

From the thermodynamic point of view, we can distinguish two types of emulsions. Systems that are thermodynamically stable are called microemulsions, while metastable (or kinetically stable) systems are known as macroemulsions.

Microemulsions are transparent, isotropic, thermodynamically stable dispersions of two immiscible fluids, commonly water and oil, stabilized by amphiphilic molecules [4-6], and involve a smaller scale range (from 10 to 100 nm) than macroemulsions. In some cases, short-chain alcohols can be added to the mixture to enhance the solubilization properties of the surfactant and are referred as cosurfactants [7].

1.2.1. From spherical droplets to bicontinuous structure

From a structural point of view, microemulsions are formed by very small-dispersed droplets of one phase in an external phase, with a monomolecular layer of amphiphilic molecules located at the interface.

Noteworthy, surfactant-water-oil mixtures can form different types of microemulsions.

In an oil-rich microemulsion, water as the dispersed medium, is solubilized in small droplets surrounded by a membrane of surfactant (and co-surfactant) molecules, as shown schematically in Figure 1.2-1. These structures are known as water-in-oil (**W/O**) microemulsion, or inverse-microemulsion, or **L₂** phase.
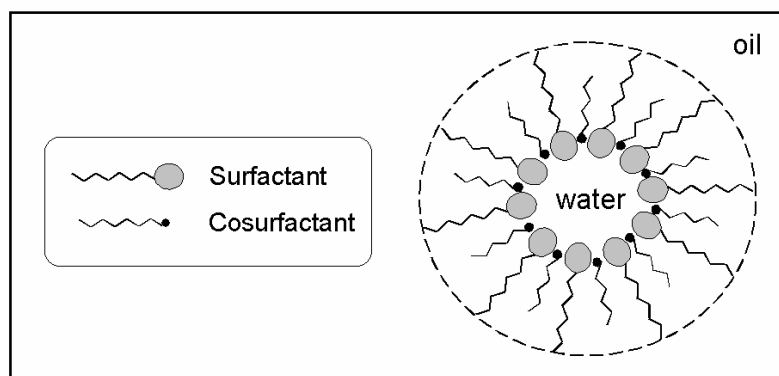
Figure 1.2-1: Schematic structure of a water-in-oil microemulsion.

In the case of an oil-in-water (**O/W**) microemulsion, or **L$_1$** phase, oil droplets are solubilized in an external aqueous phase, as represented on Figure 1.2-2.
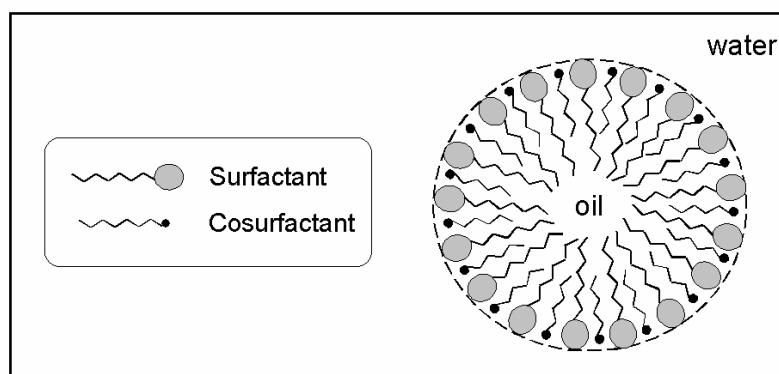
Figure 1.2-2: Schematic structure of an oil-in-water microemulsion.

A comparable, though quantitatively different, approach to analyse aggregates uses the curvature concept. In this case, the decisive parameter is the spontaneous curvature of the interfacial surfactant film **H$_0$** = 1/R$_m$ (R$_m$ is the micelle radius) [8-10]. Indeed, the interface bends to optimise the interaction energy with both water and oil phases, and the curvature of the oil-water interface of a microemulsion may therefore vary from highly curved towards oil, to zero mean curvature, to highly curved towards water.

Thus, in particular cases, a **bicontinuous** microemulsion, can be formed, which can be explained by a change of the spontaneous curvature of the surfactant film to zero. This structure is usually represented by a sponge-like phase, where both solvents form domains extending over macroscopic distances (Figure 1.2-3).

Different parameters can also influence more or less the spontaneous interfacial curvature. They include the temperature (for non-ionic surfactants) [11], the ionic strength (for ionic

6

surfactants), the nature of the oil, the surfactant structure (chain length, branching, head group) or the presence of cosurfactants.
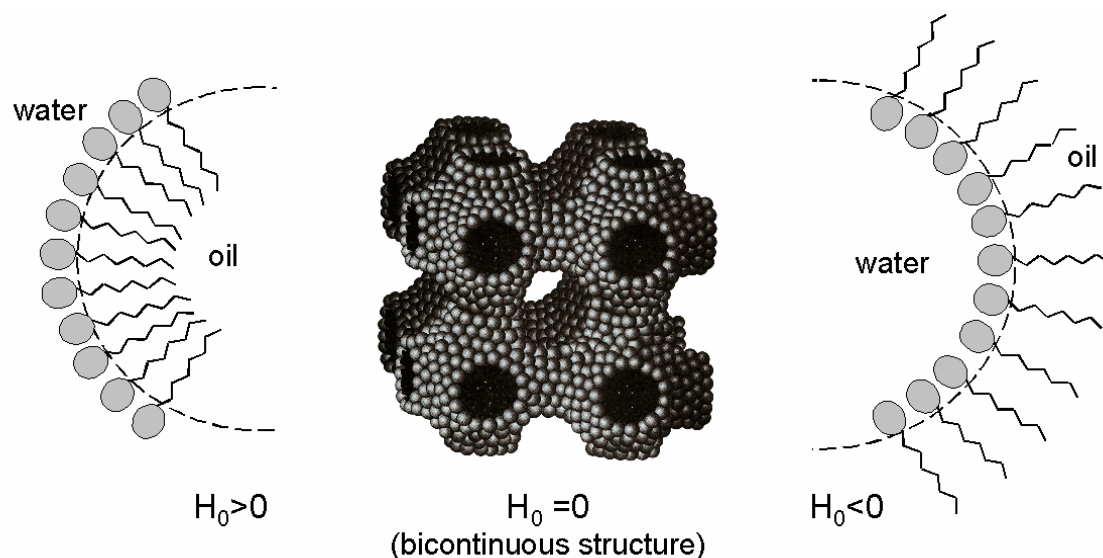
Figure 1.2-3: Evolution of the interfacial curvature of microemulsion systems according to the parameter H_0.

1.2.2. Microemulsion phase diagrams

A triangular phase diagram is the usual graphical representation of microemulsion systems, at well-defined temperature and pressure, with varying composition.
It is geometrically represented by an equilateral triangle, where the tops of the triangle correspond to the pure components, and each side represents possible compositions of binary mixtures. Any point inside the diagram represents a ternary mixture in specific proportions of each component.

In practical applications, more complicated systems, comprising more than three components, are often used. Thus, the difficulty of representing these systems increases with the number of variables. A four-components system requires for instance a three-dimensional representation. To overcome this problem, two components are usually considered as one, according to their weight or volume ratio, thus generating a single "pseudo-component". In the following studies, the fixed [oil]/[cosurfactant] ratio will be used for the representation of the microemulsion phase diagrams, as the cosurfactant is directly soluble in the oil phase. Figure 1.2-4 shows how four-component systems may be represented in a "pseudo-ternary" phase diagram.
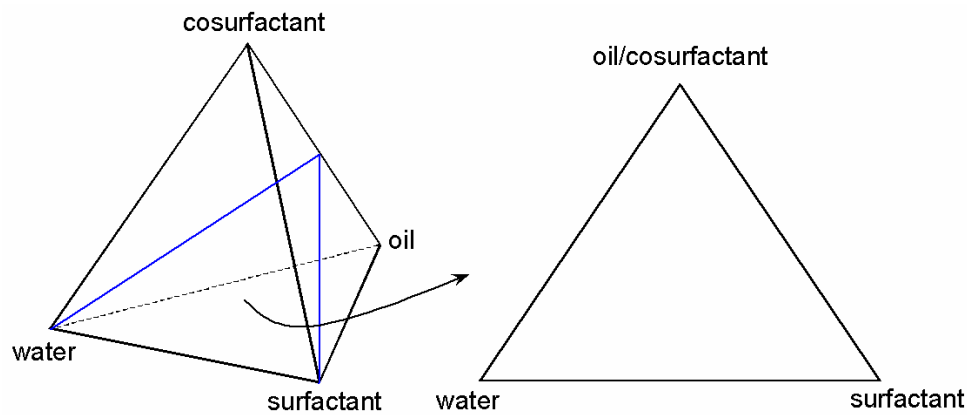
Figure 1.2-4: Schematic representation of a four-component system in a "pseudo-ternary" phase diagram.

Figure 1.2-5 shows a ternary phase diagram of a four-components system SDS/toluene-pentanol/water, in which the single phases O/W microemulsions and W/O microemulsions are represented.

In this partial phase diagram, an illustration of a defined composition is also given for the point X, which has the following composition (SDS/oil/water)=(60/30/10).
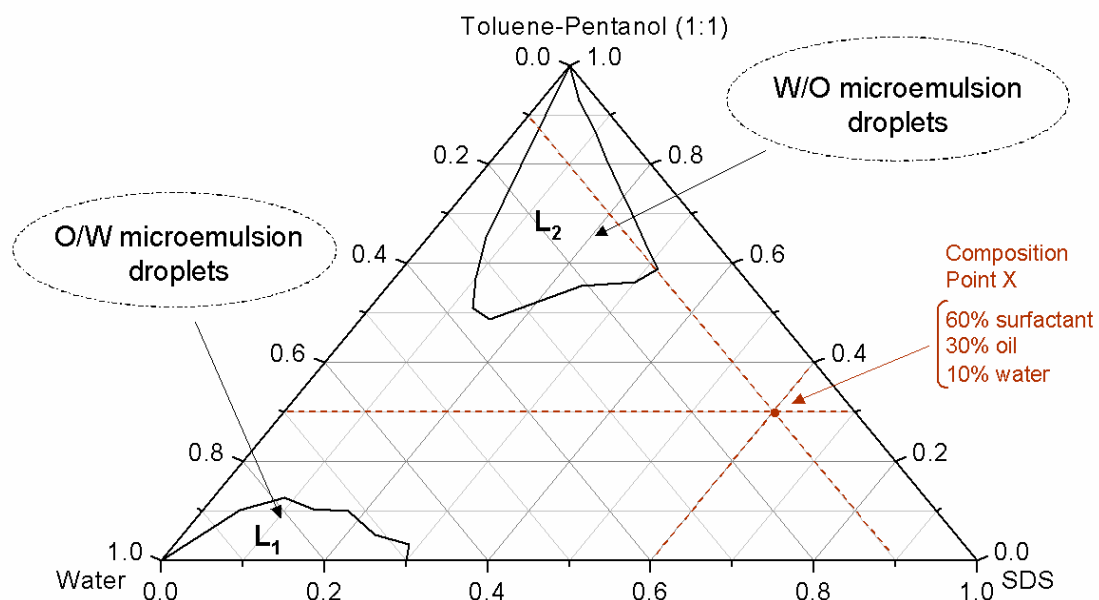
Figure 1.2-5: Example of a partial ternary phase diagram, showing the L_1 and L_2 phases of the system SDS/toluene-pentanol/water and a defined composition at point X.

In the large majority of systems, the regions of the L_1-phase and the L_2-phase are well separated in the phase diagram [6, 12, 13]. However, in some cases, a connection between these

8

both regions, i.e., a common isotropic phase connecting the water corner and the oil corner, can exist, and is defined as a bicontinuous microemulsion [14, 15].

1.2.3. Chemical reactions in microemulsion

Microemulsions, being micro-heterogeneous mixtures of oil, water, surfactant, are excellent solvents for non-polar organic compounds as well as inorganic salts. Over the last decades, there has been an increasing interest in solubilizing various additives, varying from inorganic compounds [16-18] to biological molecules [19-21] within the microemulsion systems. This capacity of microemulsions to solubilize a wide range of substances in a one-phase formulation has also been of interest for many technical applications. Microemulsions are, for instance, used in industrial cleaning processes, lubricants, in pharmaceutical or cosmetic formulations. Additionally, relatively new areas of applications such as extraction processes, biotechnology, textile dyeing, preparation of nanostructured materials can also be mentioned [22].

Recently, microemulsions have been used as reaction media for a variety of chemical reactions.

In organic chemistry, the great utility of microemulsions as solvents lies in their ability to solubilize polar and non-polar substances and to compartmentalise and concentrate reagents. Moreover, microemulsions may be used to overcome reactant solubility problems, and may also increase the reaction rate [23-25].

Microemulsions are also of interest as media for inorganic reactions, and water-in-oil microemulsions have been successfully used for the preparation of small particles of metals and inorganic salts, as it will be further discussed in Chapter 1.3.

Finally, microemulsions can be used in polymerisation reactions to obtain ultra-fine particles containing very high molecular weight polymers [26], or in bioorganic synthesis as minireactors for condensation and hydrolysis reactions [27, 28].

The different types of reactions in microemulsion mentioned above can all be seen as emerging technologies of considerable interest.

1.3. Preparation of nanoparticles

Nanoparticles are of great scientific interest as they are effectively a bridge between bulk materials and atomic or molecular structures. The interesting and sometimes unexpected properties of nanoparticles are partly due to the aspects of the surface of the material. When the size of a material approaches the nano-scale, the confinement of the electrons in the small volume influences the electronic structure of the material, and hence its properties. Moreover, the high percentage of atoms at the surface of a nanomaterial becomes significant. It can for instance arise 50% for particles with a diameter around 3 nm. As a result, an extreme reactivity, as well as a high surface energy are generated.

1.3.1. Metal particles and their application

Colloidal noble metals, e.g. gold and silver, have been well known for a long time. Already the alchemists tried to use the colloidal gold (aurum potabile) as an "elixir of life". Later, colloidal gold has been used for colouring glass, as to be seen in old cathedrals. In the last decades, the preparation of ultra-fine metal particles attracted again significant attention because of their special optical, electronic, magnetic, and catalytic properties when the particle size is fixed between 5 and 50 nm [29-33]. For example, 5 nm sized gold nanoparticles exhibit intense photoluminescence [34]. Also, the unusual size dependent chemical and physical properties make them attractive for various new fields of application, such as e.g. electron-dense labelling agents in histochemistry and cytochemistry [35, 36], in catalysis, nanotechnologies, electro-optical devices and pharmaceutics [37, 38].

1.3.2. Stability of colloidal systems

Stabilizing or destabilizing a colloidal solution is of considerable importance in many industrial processes, and several studies have been developed to understand the forces implicated in the stability of colloids.

By considering a colloid-colloid system, the long-range interactions have to be particularly taken into account. These interactions mainly consist of van der Waals, electrostatic, and steric forces [1, 39].

The van der Waals attraction V_{attr} may be combined with the electrostatic repulsion V_{rep} or the steric repulsion V_{st} to give two main types of energy-distance curves.

In the classical DLVO theory (from Boris Derjaguin and Lev Landau, 1941; Evert Verwey, and Theo Overbeek, 1948), colloidal stability is determined by a balance between double-layer repulsion V_{rep}, which increases exponentially with decreasing distance d between the particles, and van der Waals attraction V_{attr}. The type of energy-distance curves resulting is illustrated in Figure 1.3-1 (a). One can observe that the curve displays two minima, a deep primary minimum at short distance and a shallow secondary minimum at higher distance, separated by a potential energy barrier. If the system reaches the primary minimum, the coagulation process is typically irreversible. In addition, the secondary minimum may be deep enough to avoid the coagulation and the higher the value of the barrier, the more kinetically stable the suspension. If the energy barrier far exceeds the value " 25 $k_B T$" (k_B is Boltzmann's constant and T the absolute temperature), the primary minimum becomes inaccessible and the system is kinetically stable.
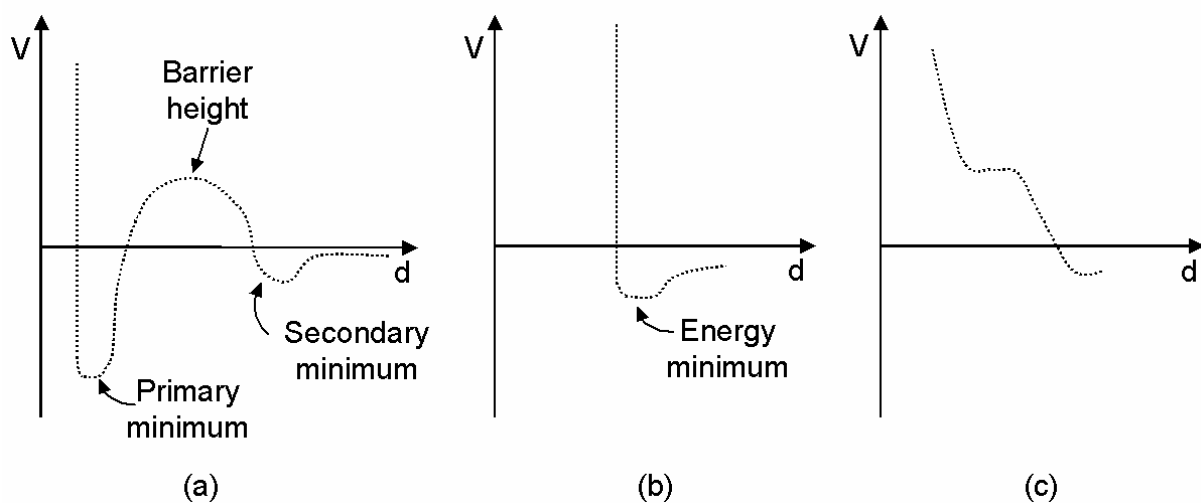
Figure 1.3-1: Schematic representation of the energy-distance curves for three cases of stabilization: (a) electrostatic; (b) steric; (c) electrosteric.

When dealing with polymer-colloid systems, emphasis has to be put additionally on the steric interactions due to the macromolecular nature of polymers.

Thus, the basis of the theory of steric stabilization (Napper, 1983) is formed by the combination of V_{attr} with V_{st}, and the form of the energy-distance curve is shown in Figure 1.3-1 (b). In this case, only one minimum is observed at a separation distance comparable to twice the adsorbed-layer thickness (δ). One has to note that the depth of the minimum

increases with increasing δ, so that thermodynamic stability is reached for particles containing thick layer, particularly in dilute dispersions.

The stability of the system, when steric interactions occur, is strongly influenced by the thickness and the density of the adsorption-layer. Thus, temperature, molecular weight, etc, are parameters which can influence the polymer adsorption-layer and hence the stability of the colloidal system.

Finally, for polyelectrolytes, the stabilization process is mainly influenced by the simultaneous electrostatic and purely steric effects. Therefore, a third type of energy-distance curve is shown in Figure 1.3-1 (c), in which the total interaction is the sum of V_{attr}, V_{rep} and $V_{st.}$

1.3.3. Formation of inorganic nanoparticles

Several methods can be employed for the synthesis of metal colloids [40]. Concerning the formation of gold nanoparticles, different in situ methods can be applied for reducing a diluted tetrachloroaureate solution. The reduction can occurred in diluted aqueous or alcoholic solutions by adding organic reducing agents (e.g. sodium salt of citric acid used by Faraday [41]) to the refluxed aqueous solution of the $HAuCl_4$ precursor, or by using the reducing agent borohydride BH_4^-.

Another way of preparing gold nanoparticles is to use photoreduction by UV irradiation, or by refluxing alcoholic solutions of the precursor (alcohol reduction) [42]. Often, the borohydride reduction is a fast reduction method performed at room temperature and leads to small spherical particles in contrast to the slow reduction by UV irradiation resulting in significant larger particles [43]. However, the reduction speed can be adjusted via the pH, too [44].

The reduction process can also be realized in different types of template phases, e.g. in polymer gel templates [45, 46], in polymer dendrimers [47, 48] or in other polymeric nanoenvironments [49, 50]. Another possibility is the use of well-defined microemulsion droplets as templates, as discussed in more details in Chapter 1.3.4.

Nanosized particles of cadmium sulphide are of special interest as semiconductors. There is a particular need of extremely small particles for this application since the material properties are strongly dependent on the size of the crystallites. The formation of CdS particles can be illustrated by the following reaction:

$$CdCl_2 + Na_2S \rightarrow CdS + 2\ NaCl$$
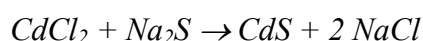
The hexagonal ferrite $BaFe_{12}O_{19}$ has traditionally been used in permanent magnets because of its high intrinsic coercivity and fairly large crystal anisotropy. For this material, control of the homogeneity, as well as particle size and shape is needed, to optimise its magnetic characteristics. The classical method to prepare barium ferrite consists of firing mixtures of iron oxide and barium carbonate at high temperatures.

Barium sulphate nanoparticles are frequently used clinically as radiocontrast agent for X-ray imaging and other diagnostic procedures. Their formation can be illustrated by the following reaction:

$$BaCl_2 + Na_2SO_4 \rightarrow BaSO_4 + 2\ NaCl$$
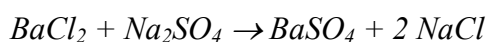
Nevertheless, whatever the particles prepared or the method used, the nanoparticles formed can be quite unstable in solution, hence it is necessary to provide new methods to avoid their aggregation.

In Chapter 1.4., it will be shown that the most common strategy consists of protecting the nanoparticles with special agents that can adsorb at the particle surface and prevent their agglomeration.

1.3.4. Microemulsions as reactor for the formation of nanoparticles

One important feature of water-in-oil microemulsions is their abillity to solubilize guest molecules such as inorganic precursor salts.

In recent years, microemulsions, particularly the W/O type, have become of interest as a medium for synthesis of inorganic particles, ranging from metals to complex crystallites, of very small size [51-55]. The water droplets, in which core the precursor salts are dissolved, can indeed act as nanoreactors for the nucleation and growth of the particles, and the size of the aqueous core should control the final size of the nanoparticles. As evocated before, the extremely small size of these particles opens new fields of application such as catalysts [56, 57], semiconductors [58, 59], electrooptical devices [60], or advanced ceramics [61].

Table 1.3.1 gives examples of areas where the microemulsion technique is already used.

Table 1.3-1: Applications of the microemulsion technique to prepare small inorganic particles. From ref [62].

Semiconductors	CdS, CdSe
Superconductors	Y-Ba-Cu-O, Bi-Pb-Sr-Ca-Cu-O
Catalysts	Pt, Pd, Rh
Magnetic particles	Fe or Fe alloys, $BaFe_{12}O_{19}$

The method using microemulsions as nanoreactors can be described as follows: two reagents soluble in water, but insoluble in the oil phase, are involved. The first reagent is dissolved in the water core of the droplets of the W/O microemulsion A, and the second reagent in the water core of the droplets of the W/O microemulsion B. The two microemulsions are then mixed together. Due to their small size, the droplets are subject to Brownian motion, and collide continuously with each other. As a result of the continuous coalescence and de-coalescence process, the content of the water pools of microemulsions A and B will enter in contact and reaction will occur inside the droplets. This principle is schematised in Figure 1.3-2.
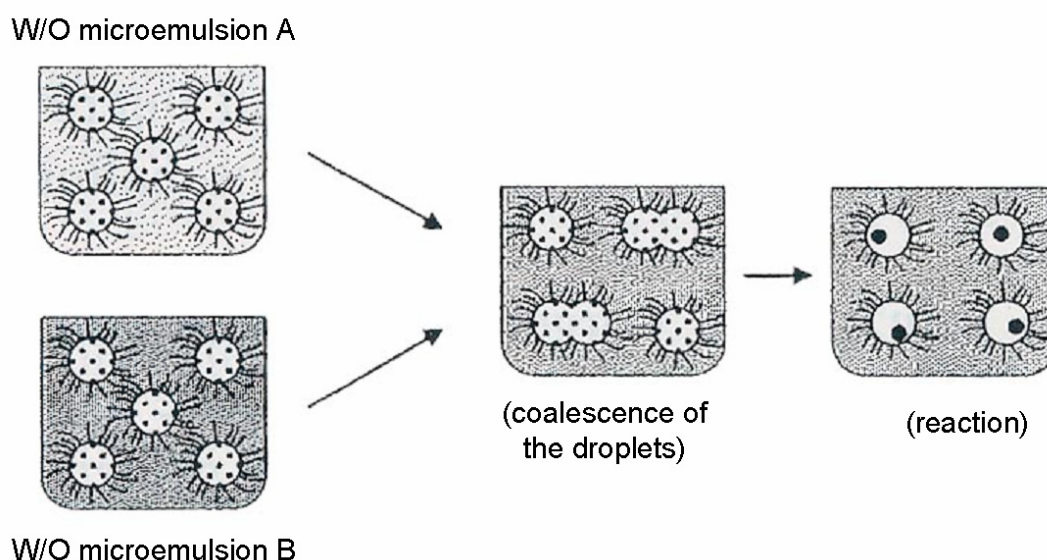
Figure 1.3-2: Principle of nanoparticles formation in water-in-oil microemulsion droplets. From ref. [63].

A detailed review about the preparation of metal nanoparticles in water-in-oil microemulsions was recently published [55].

However, in most cases the stability of the surfactant film is not strong enough to avoid the continuous growth of the particles out of the droplets. Another problem is the recovery of the nanoparticles from the reverse micelles while avoiding aggregation of the particles.

1.4.   Polyelectrolytes: promising protective agents

Polyelectrolytes are a fascinating topic in polymer chemistry due to the broad spectrum of possible molecular structures and the strong dependence of their properties in solution or dispersion to the surrounding medium. Noteworthy, they are strongly related to the processes of life, play an important role in many branches of modern technology, and are a valuable tools in solving environmental water and soil problems.
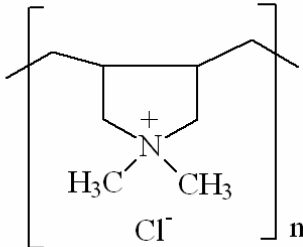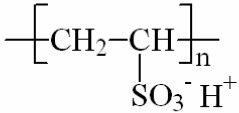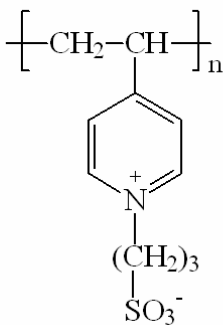
1.4.1. General description of polyelectrolytes

Polyelectrolytes (PEL) consist of a "macro-ion", i.e. a macromolecule carrying covalently bound anionic or cationic groups, and low-molecular "counterions" securing for electro-neutrality [64].

The "polyampholytes", a subgroup of PEL, are carrying both anionic and cationic groups covalently bound to the macromolecule. They are represented in nature by an abundant number of proteins, but can also be obtained by various synthetic routes.

Table 1.4-1 shows examples of different commonly used polyelectrolytes.

Table 1.4-1: Examples of different charged PEL.

Cationic PEL	Anionic PEL	Polyampholyte
Poly-(N,N'-diallyl-N,N'-dimethylammonium chloride) PDADMAC	*Poly(vinylsulfonic acid) PVS*	*Polymeric sulfobetaine*

In general, polyelectrolytes are soluble in water and other polar solvents but not in apolar solvents. The presence of charged groups influences their aqueous solubility, but also both intramolecular and intermolecular interactions. Intramolecular repulsions between the charged groups lead to a more extended conformation of the chain compared to the corresponding neutral polymer.

In contrast to the multiple possibilities of polymer backbone structure, the number of chemical structures for ionic sites of PEL is rather limited and is detailed in Table 1.4-2.

Table 1.4-2: Structures of ionic sites of PEL. From ref. [64].

Anionic sites	Cationic sites
$-COO^-$	$-NH_3^+$
$-CSS^-$	$=NH_2^+$
$-OSO_3^-$	
$-SO_3^-$	$\equiv NH^+$
$-OPO_3^{2-}$	$-NR_3^+$

Beside the ionic strength of the ionic site, another decisive parameter for the characterization of a polyelectrolyte is the density of charges along the polymer chain, which is defined as the average distance between ionic sites, taking into account chain bond geometry. The regularity of distribution of ionic sites along the chain, as well as the location of the charged sites within the molecular geometry of the macro-ion, are also influencing parameters for the PEL properties, for example, with regard to the solubility.
One has also to mention the strong influence of the species of low molecular counter-ions on the properties of the whole system in solution, especially on the solubility and structure formation of the PEL considered.

Finally, a further important parameter for the characterization of PEL is the pH of the medium, which affects strongly the properties of some PEL in solution, as the pH determines the degree of dissociation of a given ionic group and thus the actual charge density of the PEL used. Thus, polymers like poly(acrylic acid) or poly(ethyleneimine) are usually classified as PEL, in spite of the fact that they form a polyion-counterion system only in a limited pH range, and remain as an undissociated polyacid in the acid range (see Figure 1.4-1) or an undissociated polybase in the alkaline range respectively. This behaviour is typical for weak polyelectrolytes [64].

$$\text{\small{wwwCH}}_2-\text{CH}\text{\small{www}} \rightleftharpoons \text{\small{wwwCH}}_2-\text{CH}\text{\small{www}} + H^+$$
$$\qquad\qquad | \qquad\qquad\qquad\qquad | $$
$$\qquad\quad COOH \qquad\qquad\qquad COO^-$$
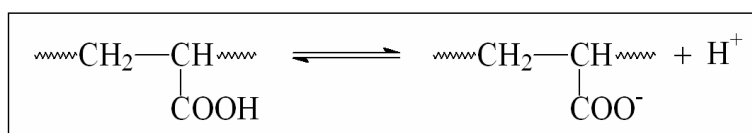
Figure 1.4-1: Dissociation equilibrium of poly(acrylic acid).

Polyelectrolytes can be synthetic, like poly(acrylic acid), polystyrene sulphonate, or they can have a biological source, like DNA or charged polysaccharides. Today's commercial polyelectrolytes are synthesized via well-known methods of polymer chemistry: free-radical polymerisation, ionic polymerisation, polycondensation, polyaddition and polymer modification. But numerous important PEL also come from nature, such as proteins (gelatine) or pectins. Furthermore, some PEL result from a chemical modification of nonionic natural polymers such as cellulose, chitosan or starch.

1.4.2. Hydrophobically modified polyelectrolytes

Water-soluble polymers bearing hydrophobic groups represent another interesting class of polymers. They have attracted much attention in recent years because of their resemblance to biological systems as well as their strong tendency for self-organization in aqueous environments due to hydrophobic interactions [65-67]. Different models have already been proposed to explain the self-organization of hydrophobically modified (HM) polymers. For example, the frequently used model of the "local micelle", also called microdomains, introduced by Strauss [68-71], assumes an intramolecular aggregation of a limited number of neighbouring hydrophobic side chain as shown by Figure 1.4-2.
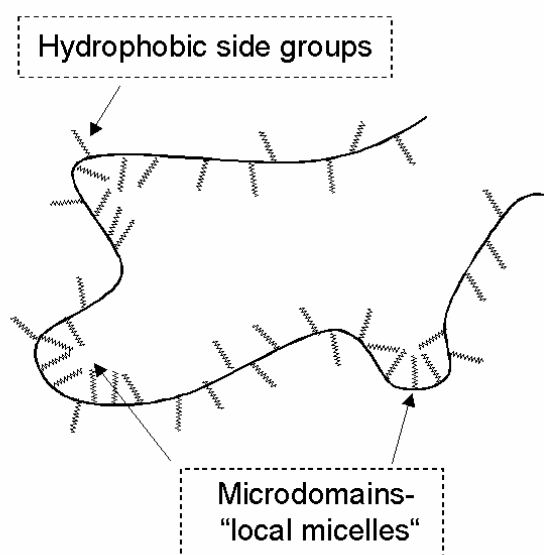
Figure 1.4-2: Model of microdomains formed by hydrophobically modified polymers.

On the one hand, PEL with a small number of hydrophobic groups are well known as thickeners in enhanced oil recovery due to intermolecular aggregations, resulting in an increase in viscosity.

On the other hand, PEL with a large number of surfactant moieties linked to the polymer backbone are known as "micellar polymers" or "polysoaps" [72]. Typical properties of aqueous polysoaps are very low viscosities up to high polymer contents, which is a marked difference from ordinary PEL, and relatively high solubilization performances. There is a considerable practical interest in micellar polymers due to their many attractive properties and thus potential uses, especially as protective colloids, but also as emulsifiers, surfactants, wetting agents, lubricants, viscosity modifiers, pharmaceutics and cosmetic formulation ingredients, etc.

However, whether a polymer behaves as a thickener or as a polysoap depends mainly on the amount and length of the hydrophobic chains.

The synthesis of HM-PEL can be achieved by different routes. Copolymerisation of hydrophilic and hydrophobic vinyl monomers, or polymerisation of surfactants containing vinyl groups are possible syntheses employed for this purpose [64].

1.4.3. Polyelectrolyte-surfactant systems

Surfactants and water-soluble polymers find a wide range of applications, as described previously. In practice, the combination of polymers and surfactants is relevant for use in diverse products such as paints, detergents, cosmetics, pesticide formulations, etc. They are mostly employed to achieve different effects -colloidal stability, emulsification, rheology control- but in some cases a synergistic effect is sought.

When a surfactant is added to a dilute polymer solution, one can often observe a cooperative self-assembly process below the CMC of the pure amphiphile solution. A micelle-like aggregate is formed, which interacts with the polymer coil. The formation of these polymer-bound micelles occurs at the so-called critical aggregation concentration (CAC), which varies with the nature of the surfactant and the polymer.

The stabilization of these aggregates is provided by interactions with the polymer chain, and the nature of these interactions varies from system to system. By using hydrophobically modified polymers, a more specific micelle-polymer interaction can be observed. Indeed, the

side chains will strengthen the polymer-polymer interactions and also serve as a strong binding site for micelles, as demonstrated on Figure 1.4-3.

In the case of charged polymers, the polyelectrolytes will bind micelles of opposite charge electrostatically [73].

Polymer molecules

Added surfactant

Added surfactant

Hydrophobic side groups
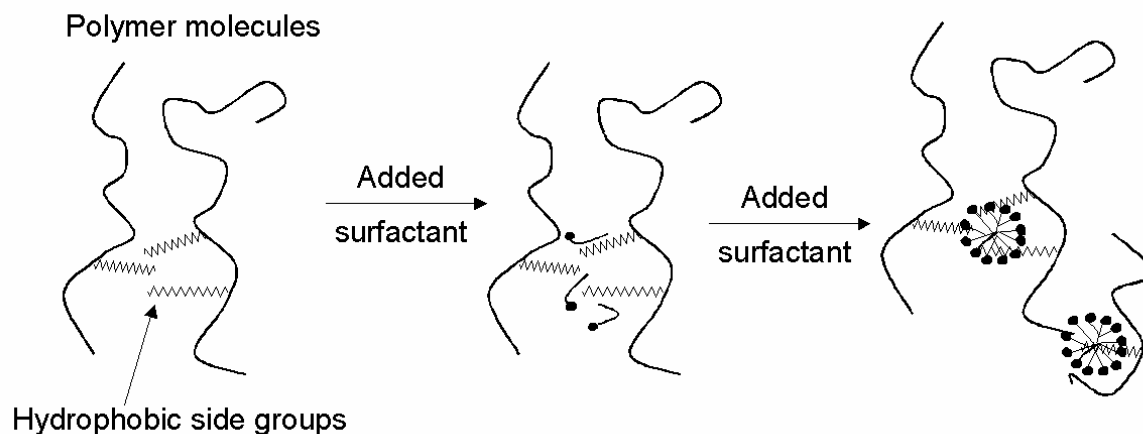
Figure 1.4-3: Self-association of hydrophobically modified water-soluble polymer chains and surfactant molecules.

The interactions between polymer and surfactant are essentially influenced by the properties of both polymer and surfactant. A number of methods have been employed to study the interactions between polyelectrolytes and surfactants in solution such as surface tension, electrical conductivity, viscosity, electrophoresis and so on [74]. The use of surfactant selective electrodes has lead to great progress in the study of polymer-surfactant interactions, too [75, 76].

1.4.4. Polyelectrolytes in microemulsion systems

Recently, a topic that has found an increasing interest, is the incorporation of polyelectrolytes into microemulsions [77-80]. It is indeed well established that the added polymer can influence the droplet size [81-83], the droplet-droplet interactions [84-86], as well as the stability [87] and the flexibility of the interface [87, 88] by the formation of polymer-surfactant complexes, as described previously.

Again, the use of HM-PEL is of interest in microemulsion to stabilize the surfactant film. In addition to electrostatic interactions between the surfactant head group and the polymer, hydrophobic interactions between the surfactant tail and the hydrophobic side chains have to be taken into account. These additional hydrophobic-hydrophobic interactions affect the

surfactant film stability (Figure 1.4-4) and lead generally to an increase of the solubilization capacity of the microemulsion droplets.
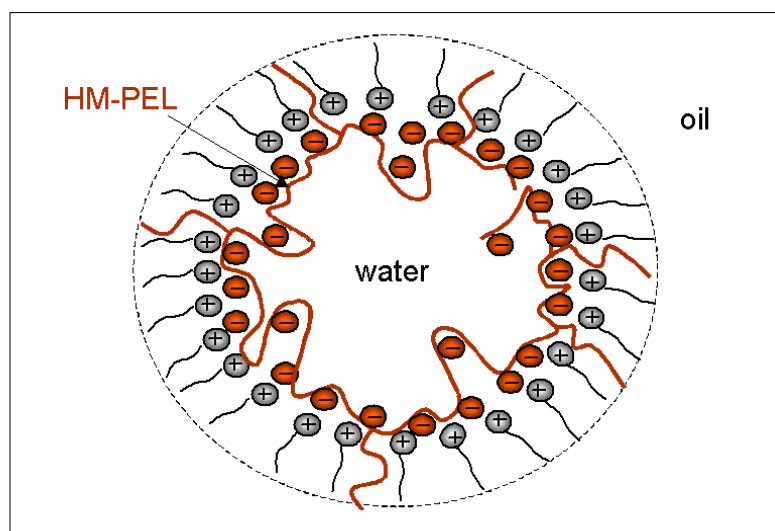
Figure 1.4-4: Influence of HM-PEL on the surfactant film of a W/O microemulsion system.

Several theoretical [89-92] and experimental [93, 94] studies have shown that the individual structure of a surfactant dispersion, that means a droplet or sponge-like one, is mainly determined by the surfactant film bending elasticity. The presence of a polymer, interacting with the surfactant layer, can deeply affect the structure and phase behaviour of these systems. For instance, the presence of poly(N-vinyl-2-pyrrolidone) [95, 96] or poly(ethylene glycol) [97] induces the formation of a bicontinuous channel in the SDS/xylene-pentanol/water system. Similar results were observed by Bellocq by adding poly(ethylene glycol) into the AOT/isooctane/water system [98].

Finally, the presence of the polymer can strongly influence the rate of exchange of material between two colliding droplets of a microemulsion system, i.e. the percolation phenomenon, as well as the attractions between the droplets.

In recent years, the use of polymer-modified microemulsions for the synthesis of nanoparticles has received considerable attention [96, 99-101]. The polymers can indeed be involved in the nanoparticles formation by increasing the film stability of the microemulsion droplets due to polymer-surfactant interactions and can influence the control of the particle size.

One further advantage of the polymer-modified microemulsions is the possibility to stabilize the primary formed nanoparticles in the droplets via a polymer adsorption (steric or electrostatic stabilization, see chapter 1.4.4) [102, 103].

Finally, in presence of polymers, aggregation phenomena, occurring during the drying-process, are well prevented (due to steric or electrostatic stabilization), and monodisperse polymer-modified-nanoparticles can be redispersed without flocculation after solvent evaporation [104].

1.4.5. Adsorption of polyelectrolytes in colloidal systems

If a polymer has any affinity for a surface, it usually adsorbs strongly on it and in practice often irreversibly.

The polymer adsorption can be promoted through specific effects. A block copolymer, for instance, with a higher surface activity, will have a strong tendency for adsorption. Besides, a polymer chain can be grafted to a surface by a covalent bond. In the case of polyelectrolytes, they will adsorb strongly on an oppositely charged surface.

Chain configuration at the surface depends on the forces that bring the polymer down to the surface. In the case of polyelectrolytes, electrostatic forces governed mainly the adsorption and the conformation of the polymer in solution, so that surface conformation depends strongly on salt concentration in aqueous medium. In pure water, adsorption is very strong and the PEL adopts a conformation that provides an optimal match between polymer and surface charges. As the salt concentration is increased, the effective strength of the electrostatic interactions is decreased, and the polymer can gain conformational entropy by extending somewhat into the solution.

Due to their ability to adsorb on surfaces, polymers play an important role in colloid chemistry and can be used to influence the interactions between colloidal particles and hence their stability.

Quite different types of polymers, including polyelectrolytes and amphiphilic block copolymers, can be used as protecting agents [105-107]. The most commonly used polymers are poly(1-vinylpyrrolidone), poly(ethylene glycol) or their copolymers [105-108]. Moreover, the choice of polyelectrolytes as stabilizers has also been of interest for the stabilization of nanoparticles due to the several advantages that these macromolecules can offer. Pugh and al.

have confirmed the stabilization of colloidal particles by the use of polyelectrolytes, which can combine both steric and electrostatic effects [109]. Figure 1.4-5 summarizes the different types of stabilization, which can be inferred to influence the stability of a colloidal system.
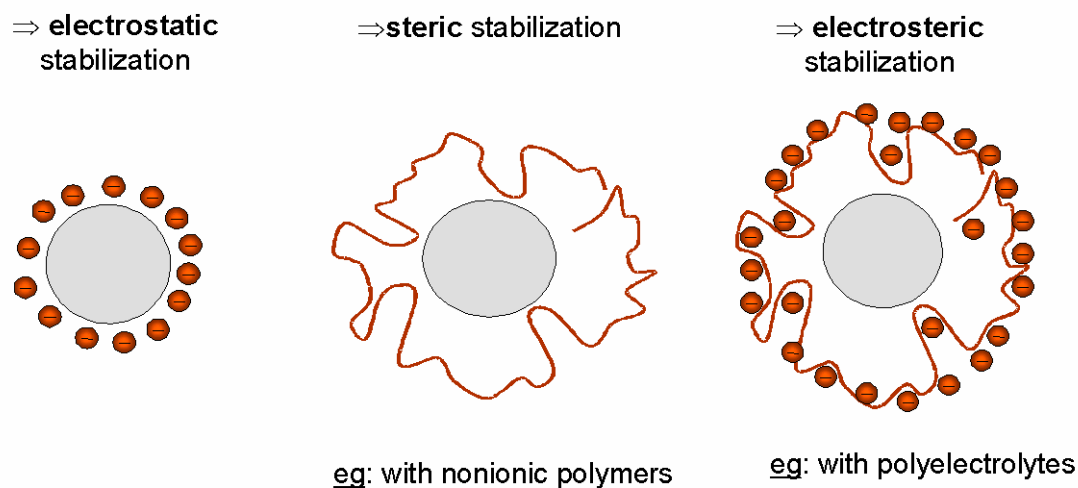
Figure 1.4-5: Different types of stabilization of a colloidal system.

1.4.6. Polyelectrolytes as reducing and stabilizing agents

It was recently shown that polyelectrolytes, in addition to their properties as stabilizing agent, can act also as reducing agent for the formation of gold nanoparticles.

Thus, protected gold particles have successfully been obtained with linear polyethyleneimine that serves as reducing and protective agent [110]. However, the linear polyethyleneimine has some special features, such as its solubility in water: the polymer becomes soluble in water only at pH < 7, or by heating to higher temperatures (> 70°C).

It was newly demonstrated that polyanions, i.e. polyacrylates, can act as reducing agents, too, when the precursor solution was refluxed [111].

Another example for a single-step synthesis and stabilization of metal nanoparticles was shown by adding pluronic copolymers with PEO-PPO-PEO blocks [112].

The advantage of this method is the combination of the reduction and stabilization processes of the nanoparticles in one step, and with only one component.

Moreover, variations of different parameters, such as concentration, pH, temperature, type of reducing agent, etc, can affect the size of the nanoparticles produced, as well as their morphology [113].

1.5. Objectives and motivation

In the context described previously, the general aim of this work is the synthesis of inorganic particles with colloidal dimensions below 10 nm.

For the stabilization of the nanoparticles, quite different types of polymers, including polyelectrolytes and amphiphilic block copolymers, can be used. The most commonly used polymers are poly(1-vinylpyrrolidone), poly(ethylene glycol) or their copolymers. In the present work, more "exotic" polyelectrolytes as stabilizing agent are targeted.

The main objectives of this work are:

- Synthesis of hydrophobically modified polyelectrolytes by varying the type of polymer, its charge, as well as the degree of substitution and the nature of the hydrophobic group, in order to obtain a large panel of compounds.

- Incorporation of the charged polymers in microemulsion systems.

- Checking the influence of the polymer on the phase behaviour of the microemulsion.

- Use of the polymer-modified microemulsions droplets as new template for the nucleation and growth of colloidal particles.

- Checking the influence of the PEL on the particle size and stability within the core of the microemulsion.

- Examination of the role of the polyelectrolyte adsorption layer for the recovery of the nanoparticles from the microemulsion.

- Use of the polyelectrolytes as reducing and stabilizing agent for the synthesis of gold nanoparticles in aqueous solution and in microemulsion.

1.6. References

[1] Evans D.F., Wennerström H., *The Colloidal Domain where physics, chemistry, biology, and technology meet*, VCH Publishers, 1994.

[2] Israelachvili J.N., Mitchell D.J., Ninham B.W., J. Chem. Soc. Faraday transactions II 72 (9) (1976) 1525.

[3] Mitchell D.J., Ninham B.W., J. Chem. Soc. Faraday transactions II 77 (4) (1981) 601.

[4] Langevin D., Acc. Chem. Res. 21 (7) (1988) 255.

[5] Prince L.M., *Microemulsions*, Ed. Academic New York, 1977.

[6] Shah O., Micelles, *Microemulsions and Monolayers*, Science and Technology, Marcel Dekker Inc., New York, 1998.

[7] Stilbs P., Rapacki K., Lindman B., J. Colloid Interface Sci. 95 (1983) 585.

[8] Helfrich W., Z. Naturforsch. C 28 (1973) 693.

[9] Strey R., Colloid Polymer Sci. 272 (1994) 1005.

[10] Chen S.H., Lee D., Chang S.L., J. Mol. Struct. 296 (1993) 259.

[11] Garza C., Carbajal-Tinoco M.D., Castillo R., J. Colloid Interface Sci. 280 (2004) 276.

[12] Söderman O., Walderhaug H., Lindman B., J. Phys. Chem. 89 (1985) 1795.

[13] Bagger-Jorgensen H., Olsson U., Iliopoulos I., Mortensen K., Langmuir 13 (1997) 5820.

[14] Fontell K., Khan A., Lindström B., Maciejewska D., Puang-Ngern S., Colloid Polym. Sci. 269 (1991) 727.

[15] Jahn W., Strey R., J. Phys. Chem. 92 (1988) 2294.

[16] Hait S.K., Sanyal A., Moulik S.P., J. Phys. Chem. B 106 (2002) 12642.

[17] Alvarez E., Garcia-Rio L., Leis J.R., Mejuto J.C., Navaza J.M., J. Chem. Eng. Data 43 (1998) 123.

[18] Dasilva-Carvalhal J., Garcia-Rio L., Gomez-Diaz D., Mejuto J.C., Rodrigeuz-Dafonate P., Langmuir 19 (2003) 5975.

[19] Klyachko N.L., Levashov A.V., Curr. Opin. Colloid Interface Sci. 8 (2003) 179.

[20] Luisi P.L., Magid L.J., CRC Crit. Rev. Biochem. 20 (1986) 409.

[21] Goto A., Ibuki Y., Goto R., in: A.G. Volkov (Ed.), *Interfacial Catalysis* Dekker, New York, 2002, p.391.

[22] Solans C., Kunieda H., *Industrial Applications of Microemulsions*, Surfactant Science Series 66, Marcel Dekker Inc., New York Basel Hong Kong, 1997.

[23] Menger F.M., Elrington A.R., J. Am. Chem. Soc. 113 (1991) 9621.

[24] Holmberg K., Oh S.G., Kizling J., Prog. Colloid Polym. Sci. 100 (1996) 281.

[25] Chhatre A.S., Joshi R.A., Kulkarni B.D., J. Colloid Interface Sci. 158 (1993) 183.

[26] Candau F., in *Scientific Methods for the Study of Polymer Colloids and their Applications*, Kluwer Academic Publishers, Dordrecht, The Netherlands, 1990, p.73.

[27] Hahn D., Rhee J.S., Biotechnol. Bioeng. 28 (1986) 1250.

[28] Rees G.D., Nascimento M.G., Jenta T.R.J., Robinson B.H., Biochim. Biophys. Acta, 1073 (1991) 493.

[29] Demaille C., Brust M., Tsionsky M., Bard A.J., Analytical Chemistry 69 (13) (1997) 2323.

[30] Hayward R.C., Saville D.A., Aksay I.A., Nature 404 (2000) 56.

[31] Braun E., Eichen Y., Sivan U., Ben-Yoseph G., Nature 391 (1998) 775.

[32] Chen M., Yamaruro S., Farrell D., Majetich S.A., J Applied Physics 93 (2003) 7551.

[33] Ciebien J.F., Cohen R.E., Duran A., Supramol. Sci. 5 (1998) 31.

[34] Wilcoxon J.P., Martin J.E., Parsapour F., Wiedenman B., Kelley D.F., J. Chem. Phys. 108 (21) (1998) 9137.

[35] Hayat M.A.(Ed) *Colloidal Gold: Principles, Methods and Applications*, Academic Press San Diego, 1989.

[36] Hyatt A.D., Eaton B.T. *Immuno-Gold Electron Microscopy in Virus Diagnosis and Research,* CRC Press, Boca Raton, 1993.

[37] Quinn M., Mills G.J., Phys. Chem. 98 (1994) 9840.

[38] Wei Y., Cao C., Jin R., Mirkin C.A., Science 297 (2002) 1536.

[39] Tadros Th.F., *Solid/Liquid Dispersions*, Academic Press Inc. London, 1987.

[40] Roucoux A., Schulz J., Patin H., Chem. Rev. 102 (2002) 3757.

[41] Faraday M., Philos. Trans. R. Soc. London 147 (1857) 145.

[42] Esumi K., Suzuki A., Aihara N., Usui K., Torigoe K., Langmuir 14 (1998) 3157.

[43] Mayer A.B.R., Mark J.E., Eur. Polym. J. 34 (1) (1998) 103.

[44] Sidorov S.N., Bronstein L.M., Valetsky P.M., Hartmann J., Cölfen H., Schnablegger H., Antonietti M., J. Colloid Interface Sci. 212 (1998) 197.

[45] Caruso R.A., Giersig M., Willig F., Antonietti M., Langmuir 14 (1998) 6333.

[46] Caruso R.A., Antonietti M., Giersig M., Hentze H.P., Jia J., Chem. Mater. 13 (2001) 1114.

[47] Faul C.F.J., Antonietti M., Hentze H.P., Smarsly B., Colloids Surf. 212 (2-3) (2003) 115.

[48] Grohn F., Kim G., Bauer A.J., Amis E.J., Macromolecules 34 (7) (2001) 2179.

[49] Saito H., Okamura S., Ishizu K., Polymer 33 (1992) 1099.

[50] Chan Y.N.C., Schrock R.R., Cohen R.E., Chem. Mater. 4 (1992) 24.

[51] Barnickel P., Wokaun A., Sager W., Eicke H.F., J. Colloid Interface Sci. 148 (1) (1992) 80.

[52] Curri M.L., Agostiano A., Catalano M., Chiavarone L., J. Phys. Chem. B 104 (2000) 8391.

[53] Lin J., Zhou W., O'Connor C.J., Mater. Lett. 49 (2001) 282.

[54] Chen F., Xu G.Q., Hor A., Mater. Lett. 57 (2003) 3282.

[55] Capek I., Adv. Colloid Inter. Sci. 110 (2004) 49.

[56] Beck D.D., Siegel R.W., J. Matter. Res.7 (1992) 2840.

[57] Mayer A.B.R., Mark J. E., Colloid Polym. Sci. 275 (1997) 333.

[58] Moffitt M., Eisenberg A., Chem. Mater. 7 (1995) 1178.

[59] Holmes J.D., Bhargava P.A., Korgel B.A., Johnston K.P., Langmuir 15 (1999) 6613.

[60] Brus L., Appl. Phys. A 53 (1991) 465.

[61] Herrig H., Hempelmann R., Mater. Lett. 27 (1996) 287.

[62] Jönsson B., Lindman B., Holmberg K., Kronberg B., in *Surfactants and Polymers in Aqueous Solution*, John Wiley & Sons Inc., New York, 1998.

[63] Dörfler H.D., in *Grenzflächen und Kolloid-Disperse Systeme*, Springer-Verlag, Berlin, 2002, p.547.

[64] Dautzenberg H., Jaeger W., Koetz J., Philipp B., Seidel C., Stscherbina D., *Polyelectrolytes*, Carl Hanser Verlag, Munich, 1994, p.133.

[65] Tanford C., *The hydrophobic effect*, Wiley, New York, 1973.

[66] Evans D.F., Langmuir 4 (1988) 3.

[67] Blockzijl W., Engberts J.B.F.N., Angew. Chem. Int. Eng. Ed 32 (1993) 1545.

[68] Dubin P.L, Strauss U.P., in *Polyelectrolytes and Their Applications*, Rembaum A., Sélégny E. (eds), Reidel D. Publishers, Dordrecht (NL), 1975, p.3.

[69] Strauss U.P., in *Polymers in Aqueous Media*, Glass J.E. (ed), Adv. Chemistry Series 223, Am. Chem. Soc., Washington DC, 1989, p.317.

[70] Strauss U.P., Barbieri B.W., Macromolecules 15 (1982) 1347

[71] Zdanowicz V.S., Strauss U.P., Macromolecules 26 (1993) 4770.

[72] Laschewsky A., Adv. Polym. Sci. 124 (1995) 1.

[73] Dawydoff W., Linow K.L., Philipp B., Acta Polym. 38 (1987) 307.

[74] Liu J., Takisawa N., Kodama H., Shirahama K., Langmuir 14 (1998) 4489.

[75] Hayakawa K., Santerre J.P., Kwak J.C.T., Macromolecules 16 (1983) 1642.

[76] Liu J., Takisawa N., Shirahama K., J. Phys. Chem. 101 (1997) 7520.

[77] Bagger-Jorgensen H., Olsson U., Iliopoulos I., Mortensen K., Langmuir 13 (1997) 5820.

[78] Lianos P., Phys. Chem. 100 (1996) 5155.

[79] Plucinski P., Reitmeir J., Coll. Surf. A 122 (1997) 75.

[80] Beitz T., Koetz J., Friberg S.E., Progr. Colloid Polym. Sci. 111 (1998) 100.

[81] Suarez M.J., Levy H., Lang J., J. Phys. Chem. 97 (1993) 9808.

[82] Lianos P., Modes S., Staikos G., Brown W., Langmuir 8 (1992) 1054.

[83] Papoutsi D., Lianos P., Brown W., Langmuir 10 (1994) 3402.

[84] Gonzalez-Blanco C., Rodriguez L.J., Velazquez M.M., Langmuir 13 (1997) 1938.

[85] Kabalnov A., Olsson U., Thuresson K., Wennerström H., Langmuir 10 (1994) 4509.

[86] Suarez M.J., Lang J., J. Phys. Chem. 99 (1995) 4626.

[87] Meier W., Langmuir 12 (1996) 1188.

[88] Lal J., Auvray L., J. Phys. II 4 (1994) 2119.

[89] De Gennes P.G., Taupin C., J. Phys. Chem. 86 (1982) 2294.

[90] Huse D., Liebler S., J. Phys. (Paris) 49 (1988) 605.

[91] Andelman D., Cates M.E., Roux D., Safran S.A., J. Phys. Chem. 87 (1987) 7229.

[92] Wennestroem H., Olsson U., Langmuir 9 (1993) 365.

[93] Porte G., Appell J., Bassereau P., Marignan J., J. Phys. (Paris) 50 (1989) 1335.

[94] Hervé P., Roux D., Bellocq A.M., Nallet F., Gulik-Krzywicki T., J. Phys. II 3 (1993) 1255.

[95] Koetz J., Beitz T., Kosmella S., Tiersch B., Proceedings CESIO 5th World Surfactant Congress Firenze, Italy, vol. 1 (2000) 499-506.

[96] Beitz T., Koetz J., Wolf G., Kleinpeter E., Friberg S.E., J. Colloid Interface Sci. 240 (2001) 581.

[97] Koetz J., Andres S., Kosmella S., Tiersch B., Composite Interfaces 13 (4-6) (2006) 461.

[98] Bellocq A.M., Langmuir 14 (1998) 3730.

[99] Jacobs B., Sottmann T., Strey R., Allgaier J., Willner L., Richter D., Langmuir 15 (1999) 6707.

[100] Lang J., J. Phys. Chem. 100 (1996) 5156.

[101] Maugey M., Bellocq A.M., Langmuir 15 (1999) 8602.

[102] Koetz J., Saric M., Kosmella S., Tiersch B., Progr. Colloid Polym. Sci.129 (2004) 1.

[103] Koetz J., Bahnemann J., Lucas G., Tiersch B., Kosmella S., Coll. Surf. A: Phys. Eng. Aspects 250 (2004) 423.

[104] Koetz J., Bahnemann J., Kosmella S., M. Peter, WO 2004/056928 A3.

[105] Mayer A.B.R., Mark J.E., Polymer 41 (2000) 1627.

[106] Mayer A.B.R., Mark J.E., Colloid Polym. Sci. 275 (1997) 333.

[107] Corbierre M.K., Cameron N.S., Lennox R.B., Langmuir 20 (2004) 2867.

[108] Kim F., Connor S., Song H., Kuykendall T., Yang P., Angew. Chem. Int. Ed 43 (2004) 3673.

[109] Pugh T.L., Heller W.J., Polym. Science 47 (149) (1960) 219.

[110] Sun X., Dong S., Wang E., Polymer 45 (2004) 2181.

[111] Hussain I., Brust M., Papworth A.J., Cooper A.I., Langmuir 19 (2003) 4831.

[112] Sakai T., Alexandridis P., Langmuir 208 (2004) 426.

[113] Sidorov S.N., Bronstein L.M., Valetsky P.M., Hartmann J., Cölfen H., Schnablegger H., Antonietti M., J. Colloid Interface Sci. 212 (1998) 197.

2.   SYNTHESIS OF HYDROPHOBICALLY MODIFIED POLYELECTROLYTES AND THEIR CHARACTERIZATION

As described in the previous chapter, hydrophobically modified polyelectrolytes are of great interest because of their scientific and technological significance.

In the past decade, a large number of investigations in photophysics and photochemistry focusing on water-soluble polymers with pendent hydrophobic aromatic groups have been published [1-3]. Amphiphilic-associating polyelectrolytes appear also to be promising emulsifiers since they offer the opportunity to combine both electrosteric and viscosifying stabilization mechanisms [4-6]. Within these interesting potential uses, polyampholytes may also serve as models or mimics of proteins, especially when bearing hydrophobic fragments that give them amphiphilic properties [7, 8].

In the present chapter, polyelectrolytes functionalised by hydrophobic groups were prepared with the purpose to incorporate them in microemulsion systems (Chapter 3.) and/or to use them as stabilizing and/or reducing agent in the nanoparticle formation process (Chapter 4.).

2.1. Hydrophobically modified poly(sodium acrylates)

First of all, the experiments were focused on a frequently used anionic polyelectrolyte, i.e. the poly(sodium acrylate) (PAA). Indeed, this polymer can be hydrophobically modified, as described in the literature [9, 10].

2.1.1. Polymer synthesis

Thus, commercially available poly(acrylic acid), with an weight-average molar mass M_w of 5.100 g/mol, has been hydrophobically modified with various degrees of grafting x (x=3; x=10; x=20 mol%) of butylamine introduced randomly along the chain, as shown on the reaction scheme 2.1-1.
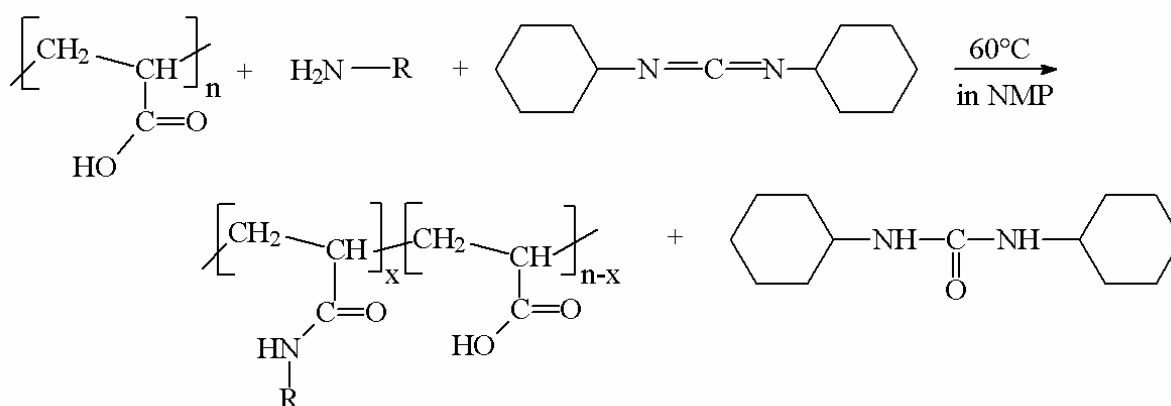
Scheme. 2.1-1: Synthesis scheme for the preparation of hydrophobically modified poly(acrylic acid)s.

One can note that the polymers formed are referred as follows: the polymers named PA3C4, PA10C4 and PA20C4 are a PAA respectively modified by 3, 10, or 20% of butylamine along the polymer backbone.
The detailed protocol of the synthesis is reported in Chapter 5.3.

2.1.2. Characterization of the polymers

^{1}H-NMR spectroscopy is a useful method to confirm the modification of the polyelectrolytes. The spectra of the modified polymers in D_2O were compared to the one of the unmodified PAA (Appendix 1, Figure A1-1) [11].

First of all, the results show characteristic peaks due to the presence of an amide chain. Around 0.8 ppm (peak ε) the typical chemical shift of the methyl end group of the grafted chain can be observed. Moreover, the chemical shift at 3.05 ppm (peak χ) is characteristic for the first ethyl group of the grafted chain: the peak deshielding is due to the presence of the amide group. Additionally, when the percentage of grafting increases, the intensity of the peaks χ and ε increases, as expected.

As a second method, IR spectroscopy can also successfully be used to detect the substitution of polyelectrolytes. The infrared spectrum of the PAA sample, in the form of KBr pellets [12], is shown in Appendix 1, Figure A1-2 a. The spectrum shows the characteristic stretching absorption band of the carbonyl group C=O at 1720 cm^{-1}. Bending vibrations of ─CH$_2$─ and CH─CO group are respectively located at 1457 and 1417 cm^{-1}. Additional bands at 1241 and 1164 cm^{-1} can be related to the coupling between inplane OH bending and C─O stretching vibrations of neighbouring carboxyl groups. The infrared spectra of the modified polymers (Figure A1-2 b-d) show significant changes in comparison to the PAA. The most characteristic absorption band of the amide group located at 1569 cm^{-1} can be correlated to the C=O band.

The elemental analysis permits to calculate the degree of grafting of polyacrylamides via the carbon/nitrogen (C/N) ratio. The results are summarized in Table 2.1-1. It is shown that the yield of incorporation is above 80% of the theoretically expected value, indicating a successful chemical modification.

Table 2.1-1: Degree of hydrophobic substitution of the PAA calculated from elemental analysis.

	C/N ratio		Degree of substitution (mol%)
	theoretical	measured	(calculated from C/N ratio)
PA3C4	89.2	106.2	2.50%
PA10C4	29.1	30.4	9.50%
PA20C4	16.3	18.6	16.90%

In the case of polyelectrolytes, potentiometric pH titrations are of relevance to analyse the degree of functionalization, acidity constants, as well as conformational changes in dependence of the degree of neutralization. Potentiometric titrations were consequently

carried out with the hydrophobically modified polymers in comparison to the non-modified PAA.

Taking into account that the degree of neutralization (α') of a weak acid correlates with the ion concentration, the pK_a value can be calculated by means of the Henderson-Hasselbalch equation:

$$pK_a = pH + \log \left[(1-\alpha')/(\alpha')\right]$$

The dissociation behaviour of polyacids can be described in a similar way, but the resulting pK_a value depends on the degree of dissociation (α) and is only an apparent one (pK_{app}) [13]:

$$pK_{app} = pH + \log \left[(1-\alpha)/(\alpha)\right]$$

The pK_a^0 value can be obtained by plotting pK_{app} versus α and by extrapolating to $\alpha \rightarrow 0$ [14].

The potentiometric titration curves of the non-modified polyacrylic acid in comparison to the hydrophobically modified polymer (PA3C4) in water are given in Figure 2.1-1. The potentiometric results for PA10C4 and PA20C4 are given in Appendix 1 (respectively Figure A1-3 and A1-4).
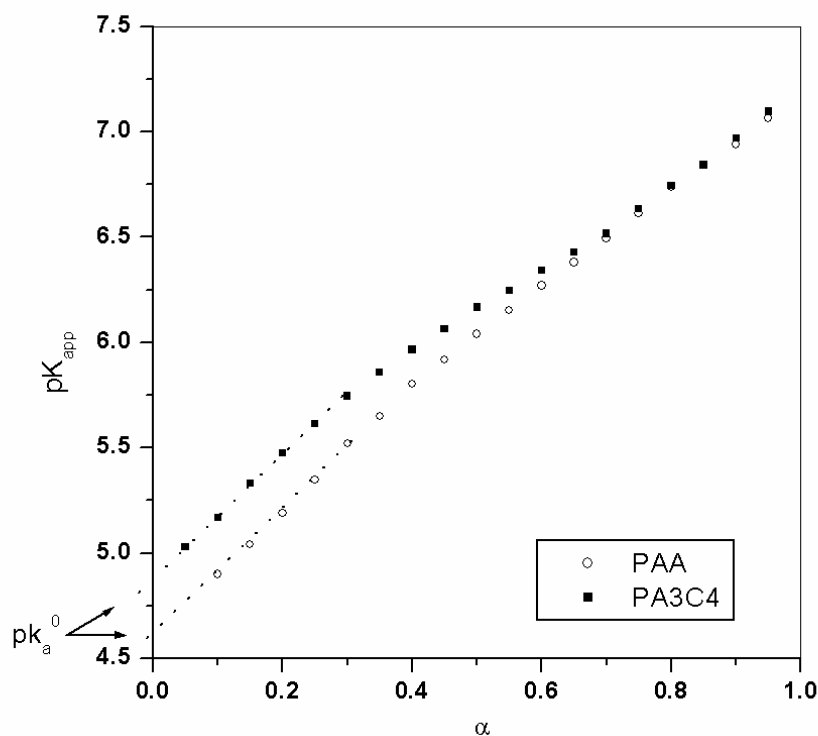
Figure 2.1-1: Potentiometric titration of (○) PAA and (■) PA3C4 in water.

First of all it can be noticed that the pK_a^0 value of 4.6 obtained for the non- modified PAA is in full agreement with the reference value of 4.6 [15]. Moreover it is well known that an increase of the hydrophobicity around the carboxyl group induces an increase in the pK_a^0 value [16]. Similar effects can be also induced by conformational changes [17].

The experimental data show that the incorporation of the hydrophobic side chains indeed leads to an increase of the pK_a^0 value (to 4.8 for a 3% modified PAA for instance). These results can be also related to a decrease of the acidity.

2.2. Hydrophobically modified polyampholytes

The most frequently used synthetic route to polymers in industry is the free radical polymerisation. In the world, more than 50% of all plastics produced are prepared via radical polymerisation processes, since this method exhibits number of advantages for the polymerisation of vinylic monomers [18]. Free radical polymerisation is easy to perform, applicable under mild conditions to various type of monomers and is compatible with many solvents [19]. It is inert toward water, but sensitive to the presence of oxygen.

For instance, maleic acid and some allyl or diallyl amine derivates are known to copolymerise via free radical polymerisation to yield highly alternating structures [20-22].

The present study was focused on the copolymerisation of diallyl amine and N-substituted-maleamic acid derivates, for which the hydrophobicity of the resulting polymer chain can be tuned by varying the chain length of the N-substituted-maleamic acid monomer. This is schematised in Figure 2.2-1.

In such copolymers, the hydrophilic ammonium groups promotes the water solubility of the polymer, whereas the hydrophobic units may induce aggregation to form organized domains.
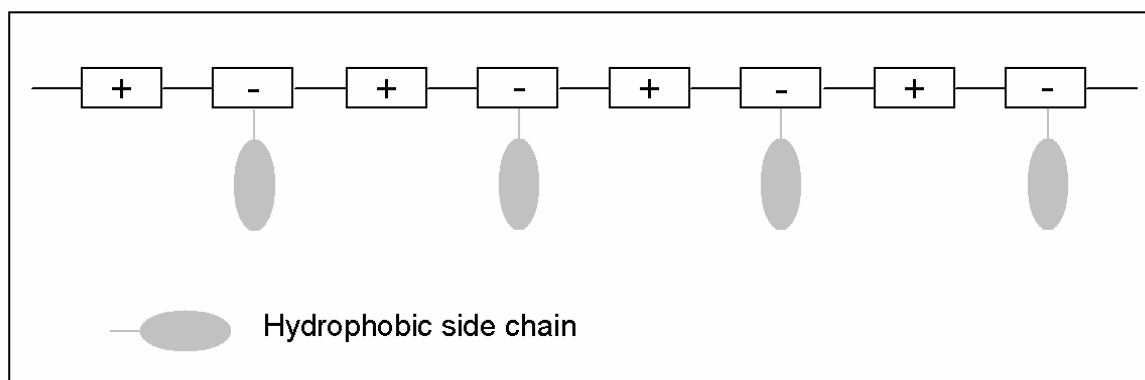
Figure 2.2-1: Schematic structure of an alternating polyampholyte with hydrophobic side chains.

2.2.1. Monomer synthesis

The commercial N,N'-diallyl-N,N'-dimethylammonium chloride (DADMAC) was used as cationic monomer for the copolymerisation and used as received (Figure 2.2-2).
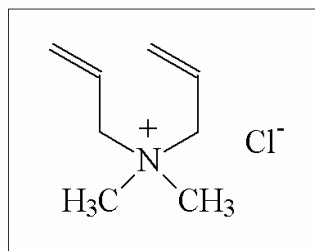
Figure 2.2-2: Chemical structure of DADMAC.

The N-substituted-maleamic acid monomers were prepared by amination of the maleic anhydride, as described in the literature [23].

The amine compounds used were the n-butylamine, the n-octylamine, and the aniline. Unsubstituted maleamic acid is commercially available and was used as received. The general chemical reaction, as well as the resulting monomer structures are shown in Table 2.2-1. The detailed protocols of the reactions are described in Chapter 5.4.1.

Table 2.2-1: Preparation and structures of the N-substituted maleamic acids.
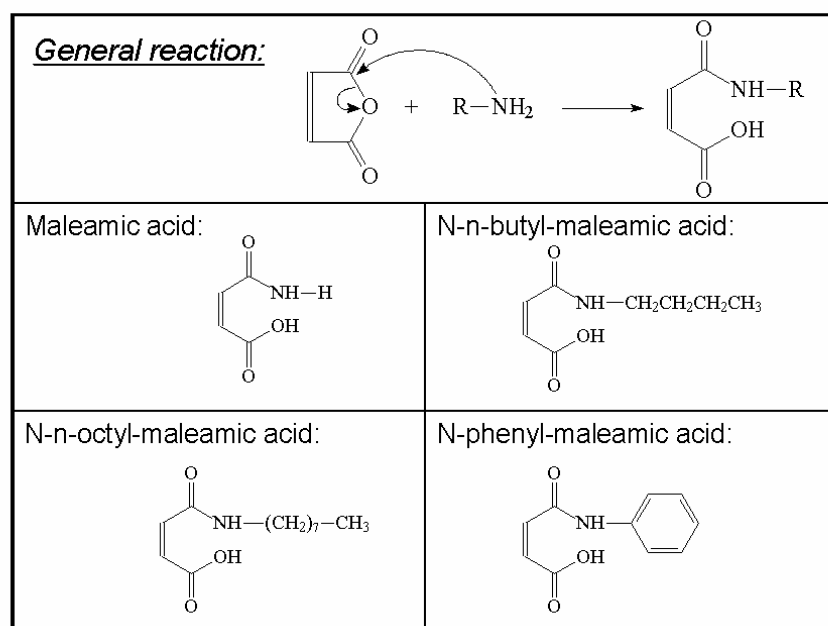
After reaction and recrystallisation, the monomers were characterized by elemental analysis and ^{1}H-NMR spectroscopy (see Chapter 5.4.1).

2.2.2. Polymerisation conditions

The following reaction parameters have to be controlled and optimised during the copolymerisation [20, 24, 25]:

• the monomer ratio

• the monomer concentration

• the initiator concentration

• the temperature

• the ionic strength (salt concentration)

• the pH value

The initial molar ratio between the monomers was kept constant to 1:1 [20, 24]. The optimised conditions for the polymerisation are taken from the literature [20-25], and are summarized in the reaction procedures in Chapter 5.4.2.

Concerning the ionic strength, both monomers bear a counter ion. To avoid the influence of these species during the reaction, the maleamic acid monomers were used in their acid form and the N,N'-diallyl-N,N'-dimethylammonium chloride was converted in its hydroxide form. Thus, a salt between the monomers, free from counter ions, was formed as depicted on Scheme 2.2-1.
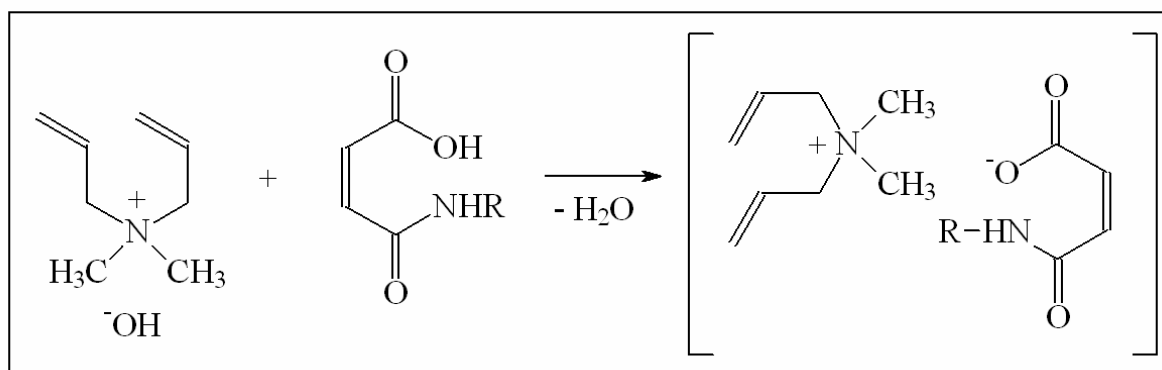
Scheme 2.2-1: Preparation of the monomer salt.

Finally, the monomer solution was polymerised, as shown in Scheme 2.2-2.
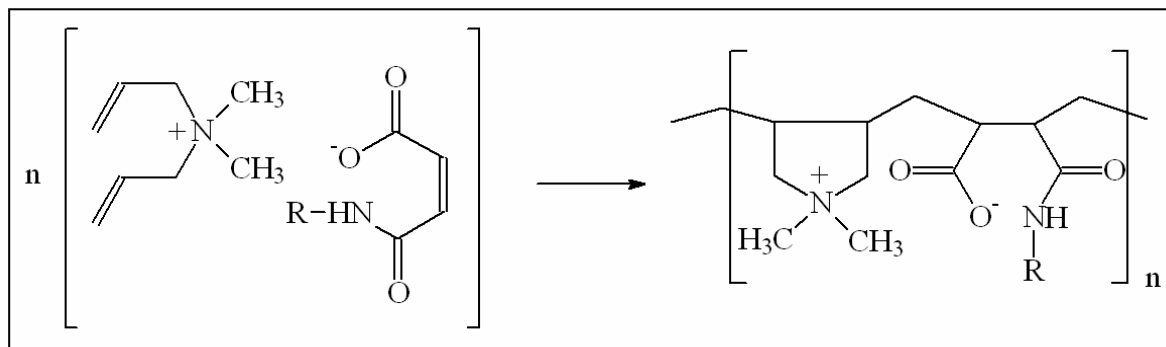
Scheme 2.2-2: Copolymerisation of the N,N'-diallyl-N,N'-dimethylammonium-(N-substituted-maleamic acid carboxylate) salt solution (idealized structure).

2.2.3. Radical polymerisation

Typically, the mechanism of a free radical polymerisation can be divided in three major steps, namely the initiation, the propagation and the termination [18].

Initiation:

The first step of the initiation consists of the homolytic dissociation by thermal reaction of the initiator, i.e. the 4,4'-Azobis-(4-cyano-pentanoic acid) (V501), to generate two radicals I• (Scheme 2.2-3).
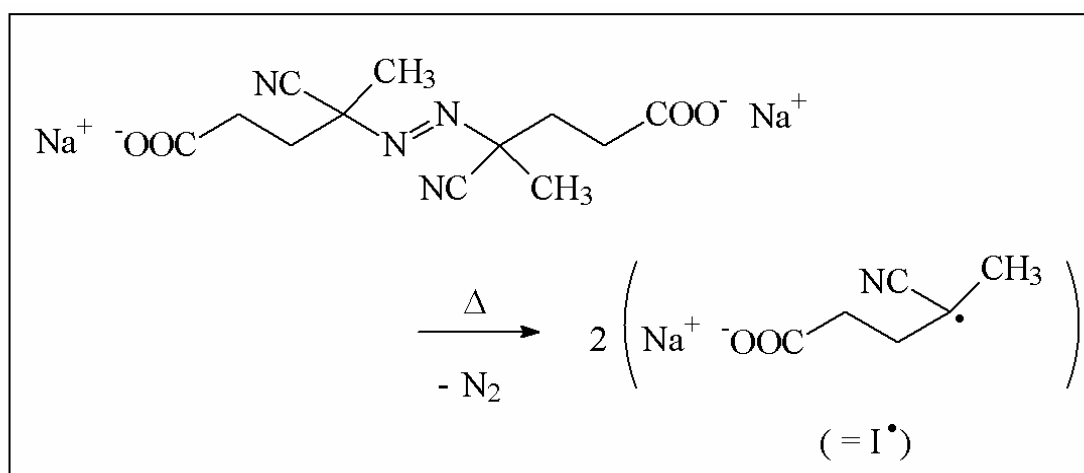
Scheme 2.2-3: Thermal homolysis of the initiator V501.

This step is followed by the addition of a radical I• to a monomer molecule, as proposed on Scheme 2.2-4. Indeed, as the primary radical is an electron-rich radical [26] it prefers to react with an electron-poor monomer, and one can assume a preferential addition of I• on the

maleamic acid monomer. Nevertheless, an initiation step on the DADMA monomer can not be entirely excluded (Scheme 2.2-5).
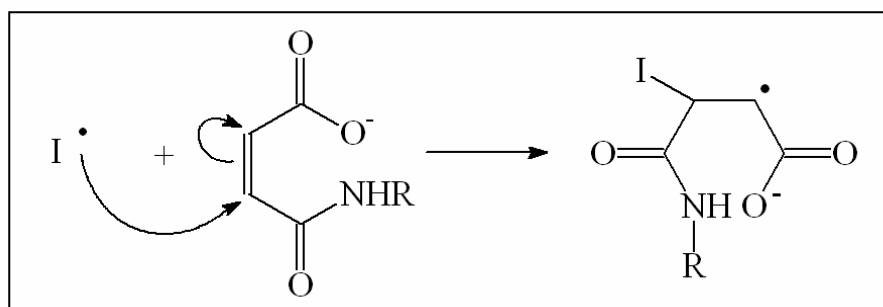
Scheme 2.2-4: Initiation step on a maleamic acid molecule.
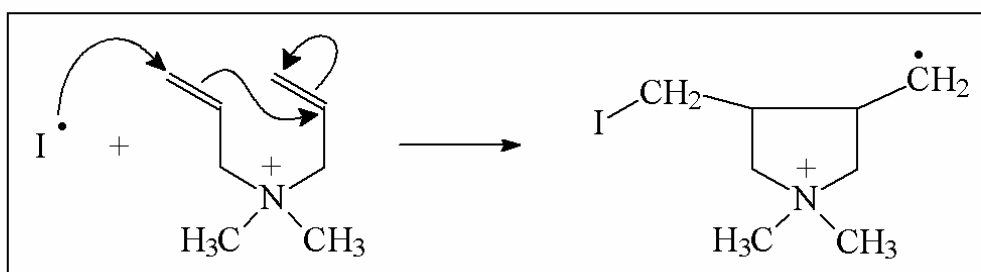
Scheme 2.2-5: Initiation step on a DADMA molecule.

Propagation:

The propagation step consists of the successive addition of a large number of monomer units to the primary active radical molecule.

Due to Coulomb interactions in the pre-formed salt solution (see Chapter 2.2.2.), the maleamic acid radical previously formed will preferentially react with a DADMA molecule (Scheme 2.2-6) for which a cyclopolymerisation mechanism is observed [27]. This adduct with a positively charged terminal monomer unit adds then for analogous reasons to a maleamic acid molecule.

As described in the literature, the resulting alternating copolymerisation of maleic acids and diallylammonium derivatives results in copolymers with alternating cationic and anionic charges [22, 28]. The most evocated reason for the alternating structure of the copolymers is an assumed high polarity difference between the monomers used [29-31].

Still, others explanations are proposed, according to which the alternating structure is mainly explained by the Coulombic attractions between the oppositely charged monomers [32, 33].

In the present case, the alternating incorporation of the amine and acid monomers may be attributed to the formation of ions pairs in solution [34], rather than to a combination of electron-rich and electron-poor monomers, as it is the case for the classic example of the alternating copolymer of styrene and maleic anhydride.

In any case, the propagation of the polymer chains, following an alternating copolymerisation process, can be depicted as follows in the Schemes 2.2.6 and 2.2.7:
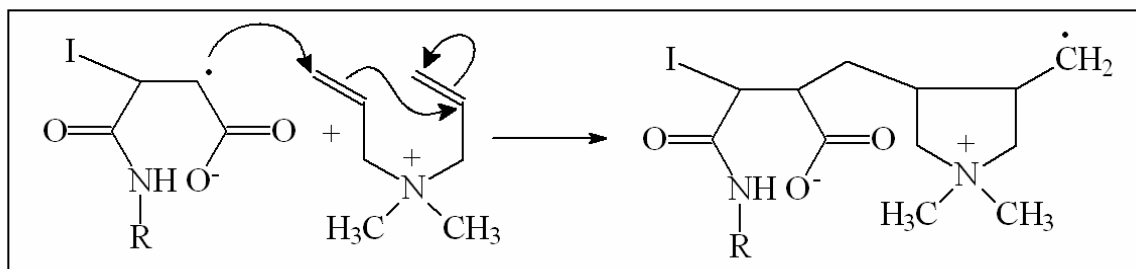
Scheme 2.2-6: Addition of a DADMA molecule on a maleamic acid radical.
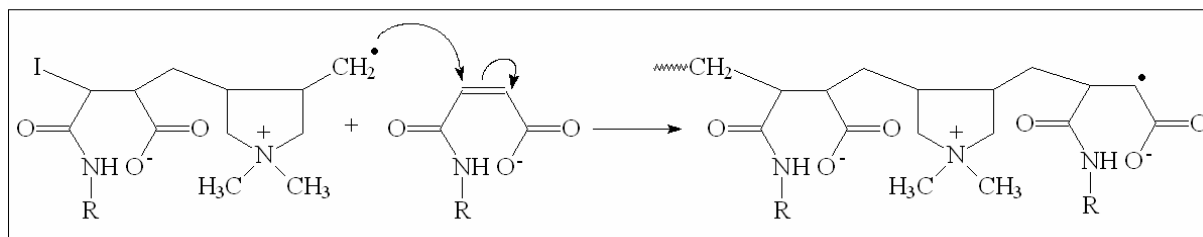
Scheme 2.2-7: Propagation of a polymer chain.

Termination:

The final step of the radical polymerisation is the irreversible termination of the growing polymer radicals, leading to the so-called "dead" polymer.

This step can take place by several possible mechanisms:

- by combination, e.g., coupling of two growing polymer chains;

- by disproportionation, i.e. a radical transfer from a growing chain to another one (by transfer of a hydrogen atom typically);

- by coupling of a growing chain with a primary radical from the initiator;

- by transfer of a radical to another molecule; etc.

The two most common pathways for termination are combination and disproportionation of the growing radicals.

Concerning the homopolymerisation of DADMAC, no disproportionation occurs, and only termination by combination is observed [35]. Moreover, due to the electrostatic interactions, one can assume that the termination of the copolymerisation studied will principally occur as depicted on Scheme 2.2-8, by a combination between an anionic radical and a cationic radical.
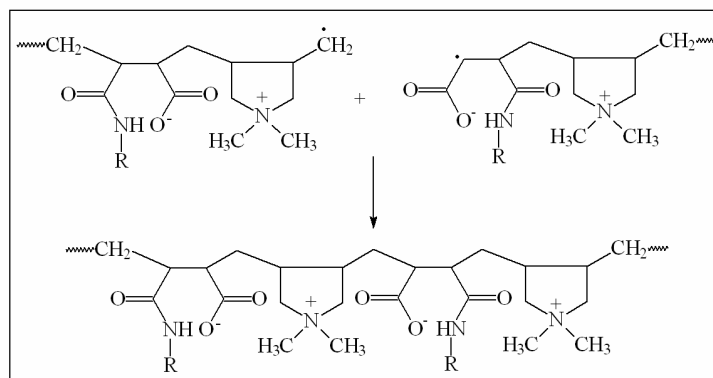
Scheme 2.2-8: Termination by combination.

The following Table 2.2.2 shows the different structures of the polymers synthesized according to the procedure described.

Table 2.2-2: Idealized chemical structure of the polymers synthesized.

| Poly-(N,N'-diallyl-N,N'-dimethylammonium-alt-maleamic carboxylate): **PalH** | Poly-(N,N'-diallyl-N,N'-dimethylammonium-alt-N-butylmaleamic carboxylate): **PalBu** |
| Poly-(N,N'-diallyl-N,N'-dimethylammonium-alt-N-octylmaleamic carboxylate): **PalOc** | Poly-(N,N'-diallyl-N,N'-dimethylammonium-alt-N-phenylmaleamic carboxylate): **PalPh** |

2.2.4. Characterization of the polymers

As reported in Chapter 5.4.2., elemental analysis and ^{1}H-NMR spectroscopy results are in good agreement with the expected molecular structures. Nevertheless, the NMR spectra provided only limited information about the structure of the polymers because of the low signal resolution, the overlap of several broad signal, as well as the limited solubility of the polymers.

Viscosity measurements were also performed. The reduced viscosity of a non-charged polymer can be investigated in salt-free water. However, polyelectrolytes present in water a strong increase of the reduced viscosity at low polymer concentration, due to the so called "polyelectrolyte-effect", observed for the first time by TROMMSDORF [36] and STAUDINGER [37] with poly(methacrylic acid). It was recently proved [38, 39] that the polyelectrolyte effect is mainly due to the increase of intermolecular forces with decreasing concentration, and a rod-coil transition [40, 41] as the main reason as still described in many textbooks of polymer science can be excluded.

Moreover, this effect can be avoid by screening the charges of the polyelectrolytes by adding a salt to the system. Therefore, the viscosity measurements were done in a 0.5M NaCl solution, and the results for the polymers PalH, PalBu and PalPh are summarized in Figure 2.2-3.
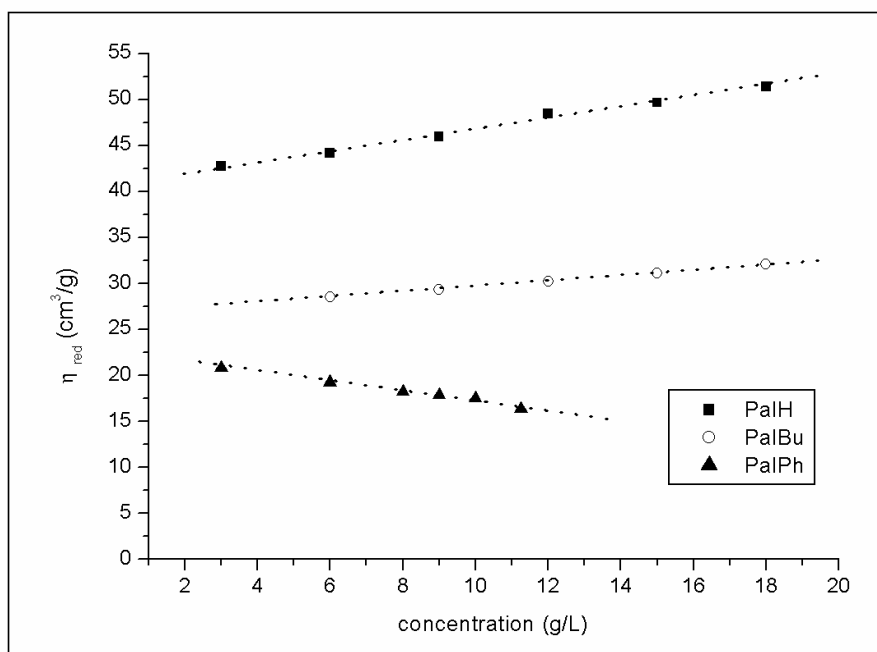
Figure 2.2-3: Reduced viscosity of the polyampholytes in a 0.5M NaCl solution as a function of the polymer concentration.

One observes that the state in solution of the polymers PalH and PalBu can be improved by the addition of salt in the system and the viscosity curves show a normal increase of the viscosity with increasing concentration.

Concerning the polymer PalPh, a normal viscosity behaviour was not found in spite of the addition of NaCl. The decrease of the reduced viscosity with increasing concentration can be explained by a poor solubility of the macromolecule in the solvent used [42]. In poor solvents, aggregation (e.g., stacking between the phenyl groups) of the macromolecules can be assumed [42, 43], and the system is close to the precipitation point [43, 44].

To obtain the molar mass of the polymers synthesized, the KUHN-MARK-HOUWINK equation can be used [24, 27, 45]:

$$[\eta] = K \, M^a$$

where $[\eta]$ represents the intrinsic viscosity of the polymer solution. The constants K and a are characteristic for a given polymer-solution at a given temperature in a given solvent.

However, for the new polyampholytes studied, the constants K and a of the KUHN-MARK-HOUWINK equation are not available.

Nevertheless, in order to obtain an approximation on the molar mass, the constants of the PDADMAC polymer were used (K= 1.12×10^{-4} dL/g; a= 0.82; 1M NaCl; 25°C).

Due to the fact that only the polyampholyte PalH, which does not bear hydrophobic groups, can be dissolved in a salt-solution without aggregation, the molar mass can be calculated only for this polymer.

Thus, with an intrinsic viscosity of $[\eta]$= 40.9 cm^3/g for the polymer PalH, an approximate molar mass of 22,000 g/mol can be derived.

As the polymers were synthesized under the same conditions, one can suggest a similar molar mass for the different polyampholytes.

In addition, the weight average molar masses of the polyampholytes were determined by using the sedimentation velocity method in the analytical ultracentrifuge. The distribution of the weight molar masses resulting from the ultracentrifugation measurements are given in Appendix 2 (Figure A2-1 to A2-4), and the results are reported in Table 2.2-3. The data show for each polymer the presence of two or three main fractions in the molar mass distribution.

Table 2.2-3: Weight average molar masses of the polyampholytes obtained from analytical ultracentrifugation measurements.

	Molar masses (M_w, g/mol)					
	Fraction A	% A	Fraction B	% B	Fraction C	% C
PalH	7,889	23%	18,502	75%	85,898	2%
PalBu	4,599	25%	12,188	63%	49,169	12%
PalOc	8,900	65%	19,381	28%	45,116	7%
PalPh	7,917	38%	21,151	62%		

The ultracentrifuge results for polymers PalH, PalBu and PalPh, confirm with the assumption of a viscosity weight average molar mass of about 20,000 g/mol.

For the polymer PalOc, the first fraction A, with a smaller apparent molar mass (around 9,000 g/mol), represents the higher percentage in the total molar mass of the polymer, showing that the polymer has a smaller apparent molar mass as the one expected. This result could be explained by stronger hydrophobic interactions in the system blocking the propagation of the polymer chains during the polymerisation or by solubility reasons.

2.3.   References

[1] Morishima Y., Prog. Polym. Sci. 15 (1990) 949.

[2] Webber S.E., Chem. Rev. 90 (1990) 1469.

[3] Nagata I., Morawetz H., Macromolecules 14 (1981) 87.

[4] Perrin P., Lafuma F., J. Colloid Interface Sci. 197 (1998) 317.

[5] Sarrazin-Cartalas A., Iliopoulos I., Audeberg R., Olsson U., Langmuir 10 (1994) 1421.

[6] Rulison C.J., Lochhead R.Y., Polym. Prepr., ACS Polym. Chem. 33 (2) (1992) 280.

[7] Dublin P., Strauss U.P., J. Phys. Chem. 71 (1967) 2757.

[8] Dublin P., Strauss U.P., J. Phys. Chem. 77 (1973) 1427.

[9] Wang T.K., Iliopoulos I., Audebert R., Polym. Bull. 20 (1988) 577.

[10] Anghel D.F., Alderson V., Winnik F.M., Mizusaki M., Morishima Y., Polymer 39 (14) (1998) 3035.

[11] Garces F.O., Sivadasan K., Somasundaran P., Turro N.J., Macromolecules 27 (1994) 272.

[12] Moharram M.A., Rabie S.M., El-Gendy H.M., J. Applied Polymer Science 85 (2002) 1619.

[13] Katchalsky A., Spitnik P.J., Polym. Sci. 2 (1947) 432.

[14] Philipp B., Koetz J., Dautzenberg H., Dawydoff W., Linow K.J., *In Applied Polymer Analysis and Characterization*, vol. 2. Ed by John Mitchell, Jr. Carl Hanser Verlag, 1992, p.281.

[15] Dautzenberg H., Jaeger W., Koetz J., Philipp B., Seidel C., Stscherbina D., *Polyelectrolytes*, Carl Hanser Verlag, Munich, 1994, p.133.

[16] Nagasawa M., Holtzer A., J. Am. Chem. Soc. 86 (4) (1964) 531.

[17] Fenyo J.C., Beaumais J., Selegny E., J. Polym. Sci. 12 (11) (1974) 2659.

[18] Colombani D., Prog. Polym. Sci. 22 (1997) 1649.

[19] Moad G., Solomon D.H., *The Chemistry of Free Radical Polymerisation*, Pergamon, Oxford, 1995.

[20] Hahn M., Jaeger W., Schmolke R., Behnisch J., Acta Polym. 41 (1990) 107.

[21] Jaeger W., Hahn M., Lieske A., Zimmermann A., Macromol. Symp. 111 (1996) 95.

[22] Hahn M., Koetz J., Philipp B., K.J. Linow, J. Acta Polym. 40 (1989) 36.

[23] Coleman L.E., Bork J.F., Dunn H., J. Org. Chem. 24 (1) (1959) 135.

[24] Thünemann A.F., Sander K., Jaeger W., Dimova R. Langmuir 18 (2002) 5099.

[25] Sander K., *Synthese und Characterisierung neuartiger Polyampholyte und deren Wechselwirkungen mit Tenside*, Mensch & Buch Verlag, 2002.

[26] Giese B., Angew. Chem. 8 (1989) 993.

[27] Butler G.B., *Cyclopolymerisation and Cylocopolymerisation,* Marcel Dekker Inc., New York, 1992.

[28] Kudaibergenov S., Jaeger W., Laschewsky A., Adv. Polym. Sci. 201 (2006) 1.

[29] Mayo F.R., Walling C., Chem. Rev. 46 (1950) 191.

[30] Ham G.E., *Copolymerisation*, Wiley, New York, 1964.

[31] Elias H.G., *Makromoleküle*, Hüthig & Wepf Verlag, Basel, 1975.

[32] Salamone J.C., Watterson A.C., Hsu T.D., Tsai C.C., Mahmud M.U., Wisniewski A.W., Israel S.C., J. Polym. Sci., Part C: Polym. Symp. 64 (1978) 229.

[33] Salamone J.C., Raheja M.K., Anwaruddin Q., Watterson A.C, J. Polym. Sci., Part C: Polym. Lett. 23 (1985) 655.

[34] Rullens F., Devillers M., Laschewsky A., Macromol. Chem. Phys. 205 (2004) 1155.

[35] Hahn M., Jaeger W., Angew. Makromol. Chem. 198 (1992) 165.

[36] Trommsdorf E., Dissertation, Universität Freiburg, 1931.

[37] Staudinger H., *Die hochmolekuleren organischen Verbindungen Kautschuk und Cellulose*, Springer Verlag, Berlin, 1932.

[38] Antonietti M., Briel A., Förster S., J. Chem. Phys. 105 (17) (1996) 7795.

[39] Antonietti M., Briel A., Förster S., Macromolecules 30 (1997) 2700.

[40] Fuoss R.M., Strauss U.P., J. Polym. Sci. 3 (1948) 246.

[41] Fuoss R.M., Strauss U.P., J. Polym. Sci. 3 (1948) 603.

[42] Schaumburg H., *Polymere*, *Werkstoffe und Bauelemente der Elektrotechnik 6*, B.G. Teubner Stuttgart, 1997, p.49.

[43] Kulicke W.M., Clasen C., *Viscosimetry of Polymers and Polyelectrolytes*, Springer Verlag, Berlin, 2004, p.51.

[44] Koetz J., *Untersuchung zur Bildung von Symplexfällungen*, Dissertation, Teltow-Seehof, 1986, p.40.

[45] Arndt K.F., Müller G., *Polymercharakterisierung*, Hanser, München, 1996.

3.   POLYELECTROLYTE-MODIFIED MICROEMULSIONS

In recent years, interest has been turned to the incorporation of non charged or charged polymers in microemulsions and on their influence on the phase behaviour and the structure of the microemulsion. In general, different types of polymers, soluble in water or oil or both media, can be incorporated into multicomponent microemulsions without macroscopic phase separation [2-6].

When the polymer is soluble only in the dispersed phase, the molar mass and the type of polymer can strongly affect the properties of the resulting polymer-modified microemulsions. When the molar mass of the polymer is low in comparison to the droplet size, the polymer can be directly incorporated into the individual droplets. On the other hand, when the molar mass increases, the polymer can induce a cluster formation [1].

Moreover, the type of polymer has also to be taken into account since the surfactant head groups can interact with the functional groups of the polymer.

The incorporation of oppositely charged polyelectrolytes into water-in-oil microemulsion droplets, without a macroscopic phase separation, is of special interest for increasing the surfactant film-stability. Such polymer-modified microemulsions can be used thus as a new, more rigid template for the nanoparticle formation.

In the following chapter, different types of polyelectrolytes, bearing or not hydrophobic groups, are incorporated in diverse microemulsion systems. Their influence on the phase behaviour of the systems is investigated by means of conductivity, differential scanning calorimetry, viscosity measurements and/or Cryo-SEM microscopy to determine the perturbations of the droplet structure and intermicellar interactions when the water soluble polymers are solubilized in the system.

3.1. Hydrophobically modified poly(sodium acrylates) in a CTAB-based microemulsion

3.1.1. Microemulsion phase diagrams

The phase diagrams are determined optically by titrating the oil-alcohol/surfactant mixture with water or the corresponding aqueous polyelectrolyte solution, and the detailed procedure is given in Chapter 5.4.

The system investigated consists of a toluene-pentanol mixture 1:1 (volume ratio) as oil component, and of the cationic cetyltrimethylammonium bromide (CTAB) as surfactant.

The phase diagram of the quaternary system CTAB/toluene-pentanol (1:1)/water shows an optically clear area in the oil corner, which can be related to the formation of a water in oil microemulsion (L_2 phase, or inverse swollen micelles) (Figure 3.1-1).
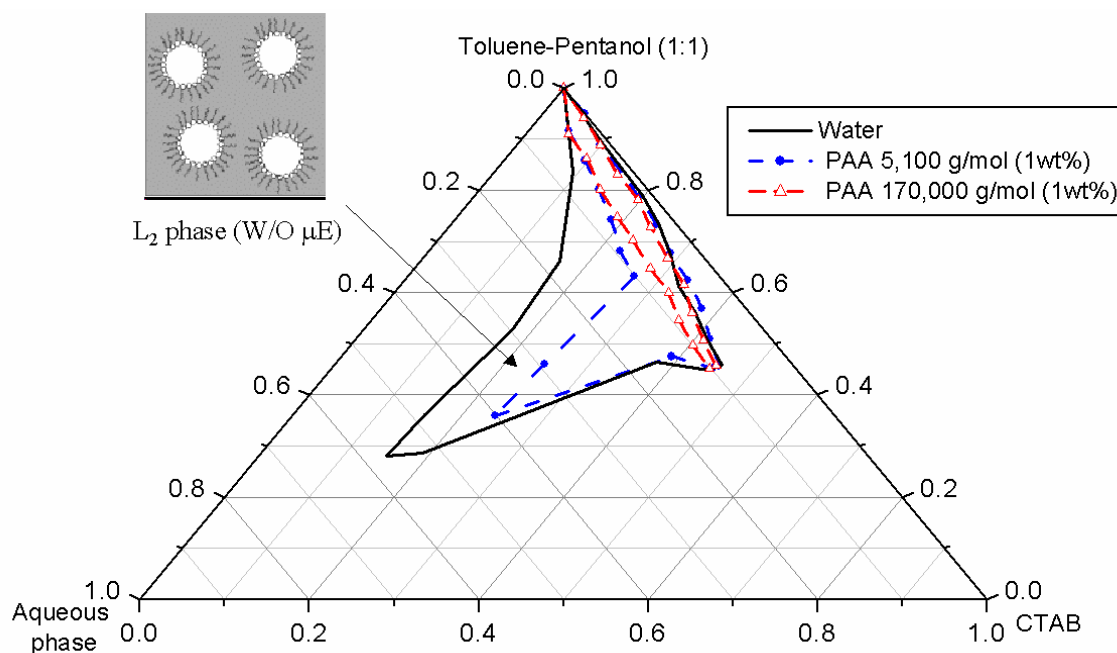
Figure 3.1-1: L_2 phase of the CTAB/toluene-pentanol (1:1)/water system depending on the added poly(acrylate).

When water is substituted by a 1% by weight PAA-solution (M_w=5,100 g/mol), a reduction of the initial inverse microemulsion area is observed (see Figure 3.1-1). First of all, the decrease of the L_2 phase can be related to aggregation phenomena between the surfactant molecules and the oppositely charged polyelectrolyte. Under conditions where the isotropic phase still exists, interactions between the surfactant head groups and the polyelectrolyte lead to a

modification of the properties of the surfactant film, such as the bending elasticity and the spontaneous curvature.

Moreover, the area of the L_2-phase is much more decreased when poly(sodium acrylate) of higher molecular weight (M_w=170,000 g/mol) is added. Only a narrow isotropic area is observed even for a modified system at a polymer concentration of 1% by weight. In this case the polymer can not be longer incorporated in the individual droplets, leading to the formation of clusters and finally to a macroscopic phase separation [1].

Thus, when the attractive interactions between the surfactant molecules and the polymer become to strong, phenomena of phase separation can be observed, especially in the case of PAA [7]. Consequently, for a better compatibility of the polyanion, the hydrophobicity of the PAA (M_w=5,100 g/mol) was increased by incorporating hydrophobic side chains (see Chapter 2.1.).

In comparison to the PAA system, hydrophobically modified poly(sodium acrylates) are added in the previous system. First of all, it has to be mentioned that the modified polyelectrolytes can be incorporated into the CTAB-based microemulsion droplets, too (Figure 3.1-2). At 3% or 10% of polymer modification (samples noted respectively PA3C4 and PA10C4) no significant change of the L_2 phase occurs in comparison to the unmodified PAA. However, when the degree of hydrophobicity of the polymer increases to 20% (polymer named PA20C4), the inverse microemulsion area really diminishes, and the prolongation of the isotropic phase in direction to the water corner almost disappears.
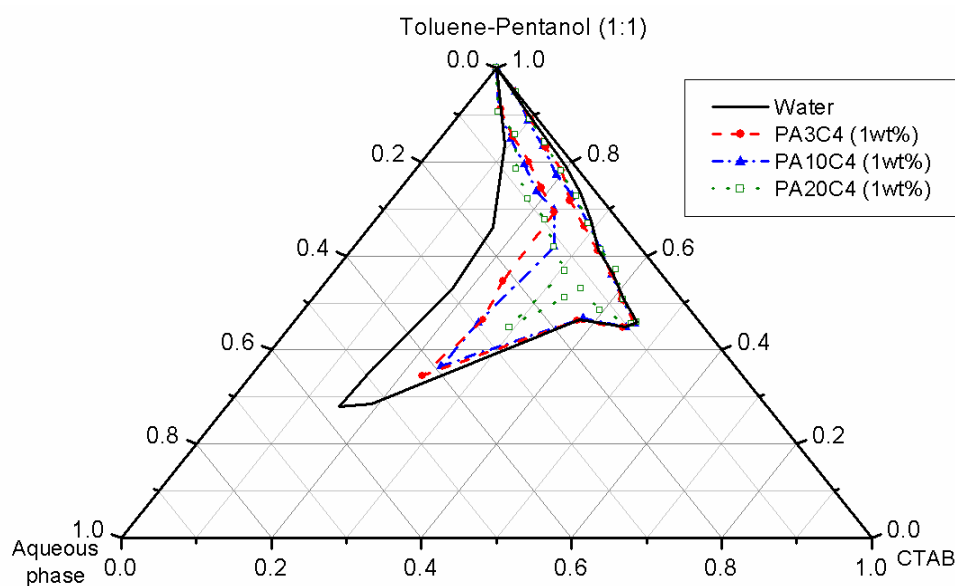
Figure 3.1-2: L_2 phase of the CTAB/toluene-pentanol (1:1)/water system depending on the hydrophobicity of the polyelectrolyte added.

In general, it has to be stated here that phenomena of phase separation are predominantly observed when the molar mass and/or the hydrophobicity of the PAA is increased.

How can be understood this phase behaviour?

Binding of an oppositely charged surfactant to a polyelectrolyte will lead to a reduced charge of the resulting complex, thereby lowering its hydrophilicity and the inter-polymer repulsion, and with increasing binding precipitation can be observed. Moreover, by incorporating hydrophobic side chains into the polyelectrolyte the decreasing electrostatic part of interactions can be overcompensated by an additional hydrophobic effect. Under such conditions the restrictions for the formation of a microemulsion are no longer fulfilled, and an attractive phase separation due to a surfactant-polyelectrolyte complex formation is observed.

3.1.2. L$_2$-phase characterization

3.1.2.1. Conductivity measurements

Conductometry is a useful technique to obtain information on micellar interactions and to access any structural changes occurring in a system [8-12].

The L$_2$ phase, this means an oil-continuous microemulsion with spherical water droplets, can be well characterized by conductivity measurements. Due to the low conductivity of the oil phase, phenomena of percolation of the water droplets (dynamic processes of temporary cluster formation [13-17]) can be related to an increase of the conductivity. Moreover, the presence of additives (polymers) can also affect the process of percolation and therefore the conductance in the system, by influencing the surfactant film of the microemulsion.

To check the influence of the anionic polymers on the exchange-process between the microemulsion droplets, electrical conductivity measurements are carried out by starting from a surfactant/oil ratio ω=40/60, and by adding water (or the aqueous polymer solution) along the dilution line.

As to be seen in Figure 3.1-3, the conductivity first increases upon water addition in the system and reaches a maximum. This jump in the conductivity is a characteristic feature of a w/o microemulsion and indicates the percolation of charges through the droplets.
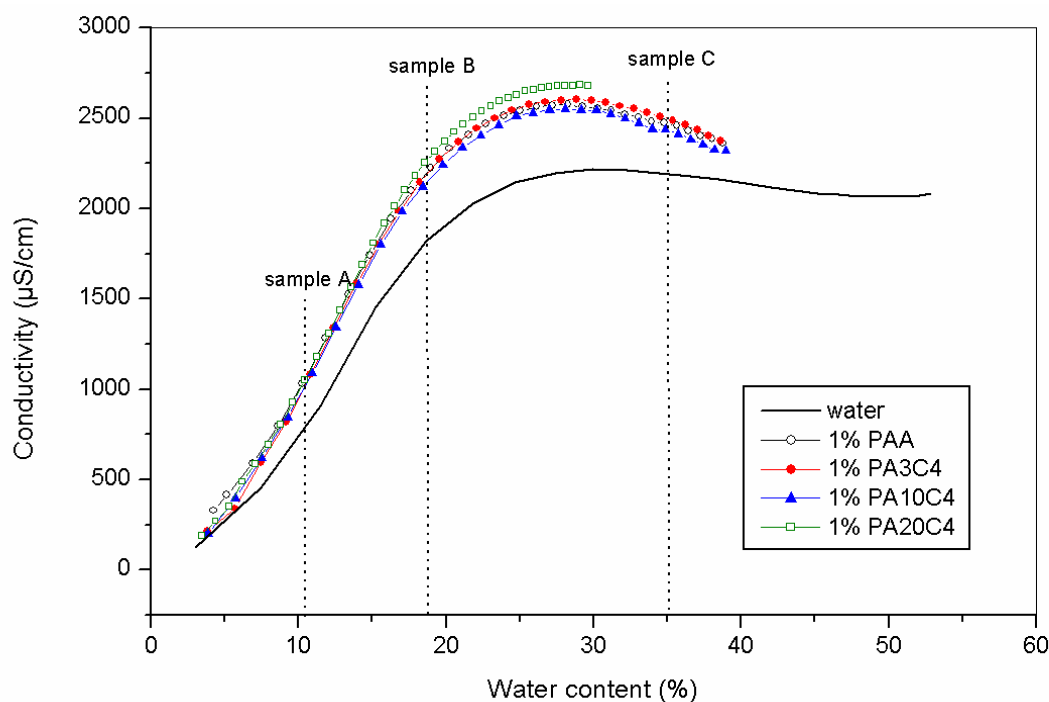
Figure 3.1-3: Conductivity measurements results at ω=40/60, by titration with 1 wt% aqueous polymer solutions.

It has to be noted that in the system studied the percolation boundary can not be determined because percolation occurs immediately even at low water content.

In presence of the polyanions, the conductivity is increased as expected and reaches a maximum at lower water concentration in comparison to the water-based system. Then, at higher water content (above 30% by weight) the conductivity of the PAA modified systems decreases. This behaviour indicates a weakening of the droplet exchanges induced by the polyelectrolytes and can be explained by an increase of the viscosity inside the water-in-oil droplets.

However, no significant changes can be observed by incorporating hydrophobic side chains.

3.1.2.2. Rheological measurements

For a more comprehensive discussion, the conductivity measurements are accompanied by rheological measurements.

Three isotropic mixtures, samples A, B and C (Table 3.1-1), have been studied in much more detail by means of shear experiments. It has to be noted that the sample C does not exist for the modified-microemulsion with the polymer PA20C4.

Table 3.1-1: Composition of samples A to C.

Sample	CTAB/Oil/Water (wt ratio)	CTAB/Oil (wt ratio)
A	36/54/10	40/60
B	32.6/48.9/18.5	40/60
C	25.9/38.9/35.2	40/60

Both systems, i.e. the non-modified and polyelectrolyte-modified CTAB microemulsions show a Newtonian flow behaviour (see Appendix 3, Figure A3-1).

First of all, one can conclude from the experimental data that the shear viscosity increases with increasing water content (Figure 3.1-4) due to the increasing droplet size and/or droplet-droplet interactions.

Moreover, by incorporating 1 wt % PAA into the microemulsion no significant changes in the shear viscosity can be observed. However, the microemulsions with the hydrophobically modified PAA-derivatives show a higher viscosity at higher water contents (sample B and C).
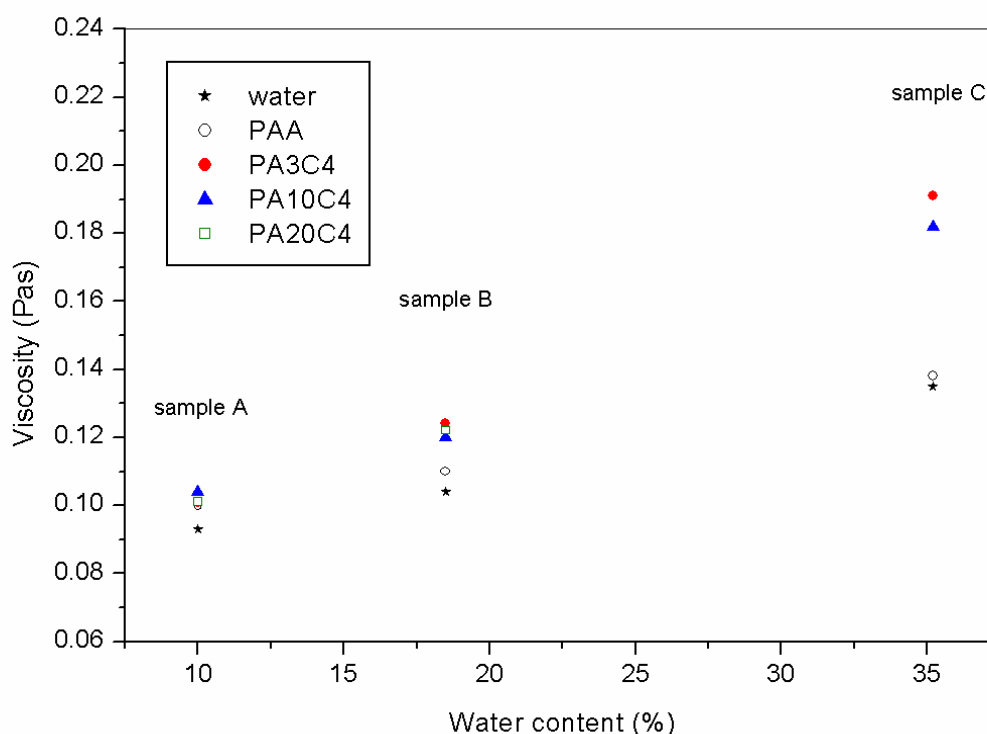
Figure 3.1-4: Evolution of the shear viscosity of the different polyelectrolyte-modified microemulsions (polymer concentration 1 wt %) depending on the water content.

3.1.2.3. Calorimetric measurements

Differential Scanning Calorimetry, DSC, is an useful method to obtain information about the melting behaviour of water in aqueous systems and is sensitive to the presence of adjacent interfaces. In dependence on the melting point, one can distinguish free or bulk water (melting point: around 0°C), from interfacial water (melting point: around -10°C), and bound water (melting point: below -10°C) [18, 19]. In addition, it is well known that in presence of polyelectrolytes, the bulk water peak can be shifted up to lower temperatures.

Micro-DSC measurements are performed on the isotropic phase of the system CTAB/toluene-pentanol/water, following again the dilution line with ω= 40/60 and the heating curves of the non modified CTAB microemulsion are given in the Appendix 3, Figure A3-2.
At low water content (sample A) the main peak with a peak top at −3.82°C can be related to the interfacial water of the system, and the shoulder at about -1°C to bulk-like water. By increasing the water content, the interfacial water peak is shifted to lower values and the bulk water peak increases.

In presence of polyelectrolytes (Figure 3.1-5), the bulk water peak for the samples A and B disappears. Only for higher water contents (sample C), the bulk water peak and interfacial water peak coexist. However, at point C, in presence of polyelectrolytes, the interfacial water peak becomes larger in relation to the bulk water peak. One can suppose that more water is incorporated into the interfacial region.
Regarding the melting enthalpies, it can be mentioned that all the water in the inverse microemulsion droplets can freeze under the experimental conditions given here.
Nevertheless, whatever the polyelectrolyte added, the DSC results were the same and so they do not permit to differentiate the interactions between CTAB and the modified or non-modified polymers.
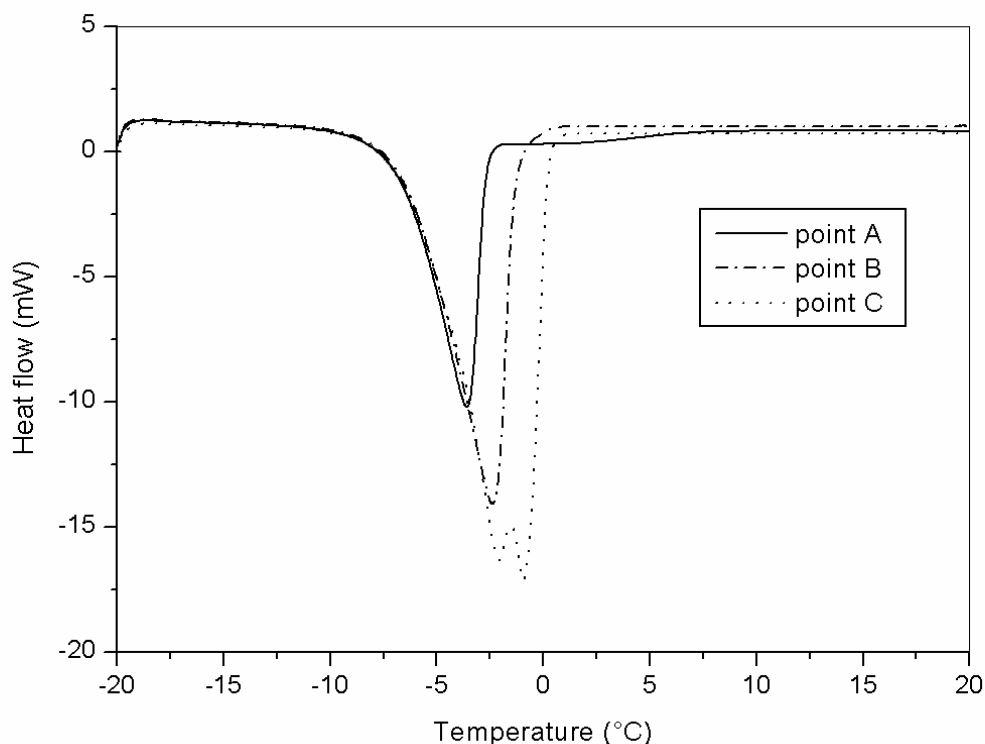
Figure 3.1-5: DSC heating curves of the CTAB/toluene-pentanol (1:1)/1 wt % PA10C4 inverse microemulsions at different composition.

3.1.2.4. Potentiometric titration with a surfactant selective electrode

To study the interactions between the different anionic polyelectrolytes and the cationic surfactant in diluted systems, a surfactant selective electrode can be used. Polymer-surfactant interactions in diluted solutions seem to be important to understand the phenomena in microemulsion droplets. Compared to the uncharged polymer, the formation of surfactant-polyelectrolyte complexes is conceptually more straightforward since there are well-defined binding sites on the polyelectrolytes. Moreover, the properties of the polyelectrolytes are of obvious importance for the interactions with surfactants. These factors include chemical composition, linear charge density, location of the charges and flexibility of the polymers [20].

A number of methods have been employed to study the interactions between polyelectrolytes and surfactants in solution such as surface tension, electrical conductivity, viscosity, electrophoresis and so on [21]. Surfactant selective electrodes have been developed and lead to great progress [22, 23]. The binding isotherms permit to extract association constants and cooperativity parameters.

The typical emf responses in aqueous surfactant solutions, in absence and presence of polymer are shown in Figure 3.1-6, where emf is plotted against the logarithm of the total surfactant concentration ($c_{s,t}$).
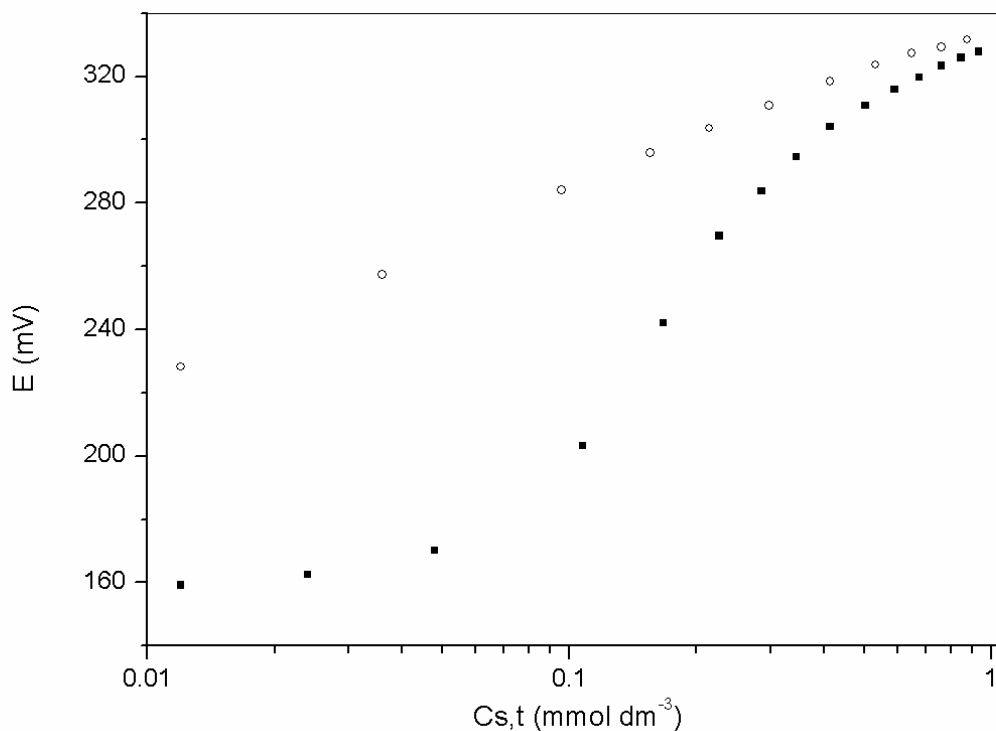
Figure 3.1-6: Potentiogram. Polymer ionic group concentration: (○) 0 mM (reference); (■) 0.2 mM of non-modified PAA.

A Nernstian response of the electrode can be found in the polymer-free solution by titrating continuously with a concentrated surfactant solution, i.e. the slope is nearly 59 mV/decade. In presence of the non-modified PAA (M_w = 5,100 g/mol) the deviation from the ideal response allows the calculation of the amount of bound surfactant ($c_{s,b}$) and the equilibrium concentration ($c_{s,f}$). A binding isotherm can be constructed by plotting $n = \Delta c/c_p$ versus $\log(c_{s,f})$, where $\Delta c = c_{s,t} - c_{s,f}$ is the difference between the total ($c_{s,t}$) and equilibrium concentration, with c_p being the total polymer concentration; n represents the degree of binding (mol of bound surfactant/mol of carboxyl ion) [24].

Figure 3.1-7 demonstrates the binding isotherm of CTAB to PAA, as well as the binding isotherms of CTAB to the hydrophobically modified polymers.

55
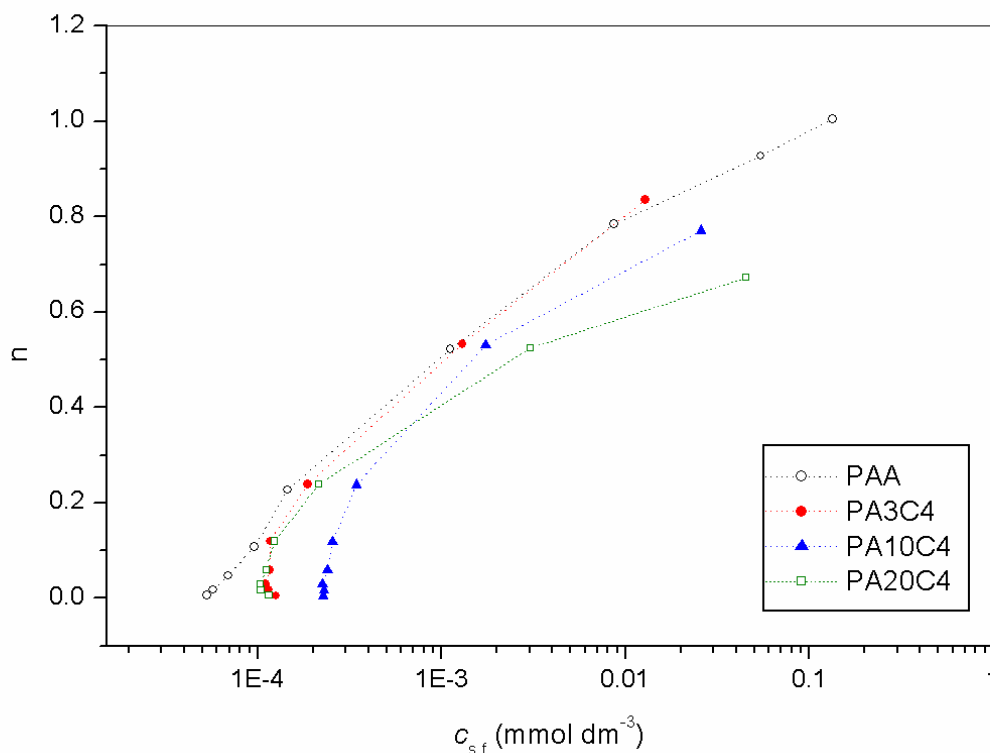
Figure 3.1-7: Binding isotherms of CTAB to the different polyelectrolytes.

Taking into account that the affinity of the surfactant for the polymer chain is increased when the polymer bears hydrophobic side chains, stronger cooperative interactions can be assumed. The CAC (critical aggregation concentration) of the surfactant in such a system is expected to be lower than the corresponding one of the unmodified poly(sodium acrylate) system [25, 26].

The experimental results show that the binding starts at a relatively small equilibrium surfactant concentration, around 5×10^{-5} mmol/dm^3 for the PAA. When the degree of hydrophobicity is increased to 3% or 10%, a decrease of the affinity of the surfactant for the oppositely charged polymers is observed. However, a further increase of the degree of hydrophobicity to 20%, leads to a decrease of the CAC again.

These results can be explained by the fact that polyelectrolyte-surfactant complexes are stabilized mainly by electrostatic interactions [27]. As shown in the previous potentiometric titration with a pH-electrode (Chapter 2.1.2.), the acidity of the polymer decreases with increasing hydrophobicity, and thus the electrostatic interactions between the surfactant and this polymer.

However, hydrophobic interactions between the surfactant alkyl tail and the polymer appears to play a secondary role due to the small length of the alkyl side chains. Only at a higher degree of hydrophobicity, hydrophobic interactions become predominant.

The binding isotherms were also analysed using the theoretical treatment for cooperative binding with nearest-neighbour interactions [28-30]. This treatment considers only two equilibriums:

$$(EE) + S \overset{K}{\leftrightarrow} (OE) \qquad\qquad (1)$$

$$(OE) + S \overset{Ku}{\leftrightarrow} (OO) \qquad\qquad (2)$$

where E represents an empty polymer binding site, O an occupied binding site, and S the free surfactant. K and Ku are the equilibrium constants, and u is the cooperativity parameter. Equilibrium (2) represents the binding of a free surfactant to a site adjacent to an occupied site. Cooperative polymer-surfactant interactions may be described by the Satake and Yang's equation [29]:

$$n = (1/2)\{1 + (s - 1)/[(1 - s)^2 + 4s/u]^{1/2}\} \qquad (3)$$

$$(c_{s,f})_{0,5} = (Ku)^{-1} \qquad\qquad (4)$$

where $(c_{s,f})_{0,5}$ is the equilibrium concentration of the free surfactant at the half bound point ($n=0.5$), and s corresponds to $Kuc_{s,f}$. The binding constants Ku are summarized in Table 3.1-2.

Table 3.1-2: Ku-values for the binding of CTAB to the different polyelectrolytes.

Polymer	Ku (dm^3/mmol)
PAA	898
PA3C4	771
PA10C4	577
PA20C4	328

Table 3.1-2 shows that the increase of the hydrophobicity from PAA to PA20C4 results in a decrease of the cooperativity of the binding process. This statement is in agreement to those reported for other hydrophobic modified polymers, i.e. poly(maleic acid-co-alkyl vinyl ether) [31-33] or poly(sodium acrylate) modified with C_{12}- and C_{18}-alkylamide chains [25], where the charged groups are located close to the polymer backbone and are well separated from the hydrophobic groups.

The cooperativity in PAA binding CTAB arises because a surfactant tends to bind at a site adjacent to a site which has already bound a surfactant. Indeed the hydrophobic interactions

between the alkyl chains of the two bound surfactants provide a free energy gain in comparison to the binding to an isolate site. Concerning the modified polyelectrolytes, microdomains are likely to exist. The binding of a surfactant to a microdomain will be anticooperative, as entropy will tend to favour the binding of an oncoming surfactant to an empty microdomain rather than to one containing a surfactant [31].

3.1.3. Conclusion

The previous investigations have revealed that an optically clear region of the phase diagram in the CTAB/toluene-pentanol (1:1)/water system still exists after the incorporation of the anionic polyelectrolyte PAA, or the hydrophobically modified derivatives. In general, the polymers induce a reduction of the isotropic phase. This effect can be enlarged by increasing the degree of hydrophobicity of the polymer and/or the molar mass of the polymer. The L_2 phase of the CTAB/toluene-pentanol (1:1)/aqueous polymer system is characterized by a low viscosity and a Newtonian flow behaviour. Other interesting features of the polymer-modified inverse microemulsions are their high conductivity due to a percolation, and the disappearance of the bulk-like water at low water content. At higher water content, bulk water and interfacial water coexist. However, in presence of polyelectrolytes the amount of interfacial water can be increased. From these experimental results, one can conclude that the polyelectrolytes are incorporated into the individual inverse micelles, attached at the interface at the surfactant film.

To study the polymer-surfactant interactions in more detail potentiometric measurements in diluted systems were realized. Titration in presence of a surfactant selective electrode shows that the cooperativity of the binding process between the polyelectrolyte and the oppositely charged surfactant molecules is decreased with increasing the degree of hydrophobicity of the polymer. However, this effect can be related to the formation of microdomains, and therefore to a lowering of the hydrophilicity of the polyelectrolyte.

Taking this knowledge into account, it becomes plausible that the incorporation of the hydrophobically modified polyelectrolytes into the L_2-phase is much more complicated due to the precipitation of more hydrophobic polyelectrolyte-surfactant complexes with microdomains.

3.2. Poly(ethyleneimine) in a SDS-based microemulsion

3.2.1. Microemulsion phase diagrams

In a first step, different inverse microemulsions are investigated as "nanocontainer" for the branched poly(ethyleneimine). The oil component is a toluene-pentanol mixture (1:1) (volume ratio). Three different types of surfactant, i.e. the cationic cetyltrimethylammonium bromide (CTAB), the anionic sodium dodecylsulfate (SDS) and the zwitterionic sulfobetaine (SB), are used to form microemulsions. It is then checked if the L_1 and L_2 phases previously formed still exist when water is substituted by aqueous solutions of PEI.

As reported in Chapter 3.1.1., the phase diagram of the quaternary system CTAB/toluene-pentanol (1:1)/water shows at room temperature a L_2 phase in the oil corner. The incorporation of 1 wt% PEI in this system leads to a significant reduction of the initial microemulsion area (see Appendix 4, Figure A4-1). An increase of the polymer concentration up to 20 wt% does not influence further the microemulsion area. One can assume that the polymer can not be easily incorporated into the individual droplets due to repulsive electrostatic forces between the polymer and the surfactant, which leads finally to a macroscopic phase separation at higher water concentrations [1].

The same effect is observed when PEI solutions are incorporated into the SB/toluene-pentanol (1:1)/water system. Again, the L_2 phase is decreased dramatically (see Appendix 4, Figure A4-2).

The partial phase diagram of the quaternary system SDS/toluene-pentanol (1:1)/water shows at T = 22°C an optically clear area in the oil corner, which can be related to the formation of a water-in-oil microemulsion (L_2 phase) (Figure 3.2-1). In the water corner of the diagram, a second optically clear area corresponds to an oil-in-water microemulsion (L_1 phase). The L_2 phase is examined by Cryo-SEM, and the micrograph in Figure 3.2-2 reveals individual droplets of water as expected.

When water is substituted by a 1 wt% PEI-solution, only a small reduction of the initial microemulsion area is observed. Moreover, it can be noticed that at a polymer concentration ≥5 wt%, the L_2 phase is shifted towards the surfactant corner. With a concentrated polyelectrolyte solution of 10 wt %, an inverse microemulsion can still be formed, but the

area of the L_2 phase is slightly reduced. The addition of 10 wt% PEI-solution in the system decreases the maximum of water solubilization from 36.3% to 27.8%.
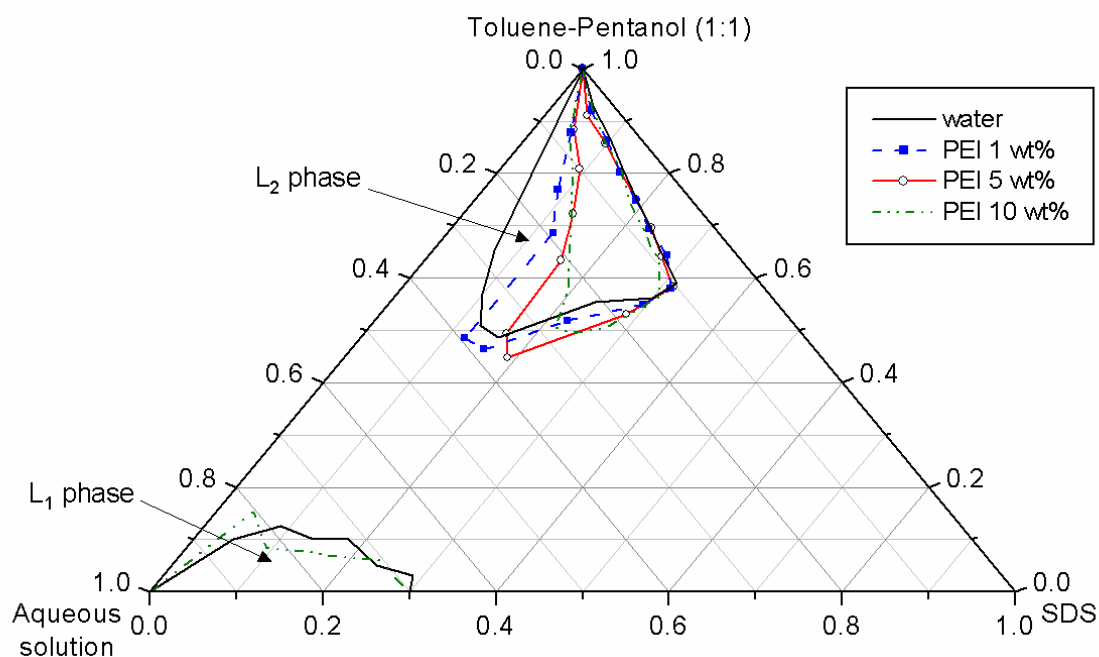
Figure 3.2-1: Partial phase diagrams at 22°C of the SDS/toluene-pentanol (1:1)/water system in presence of different PEI concentrations.
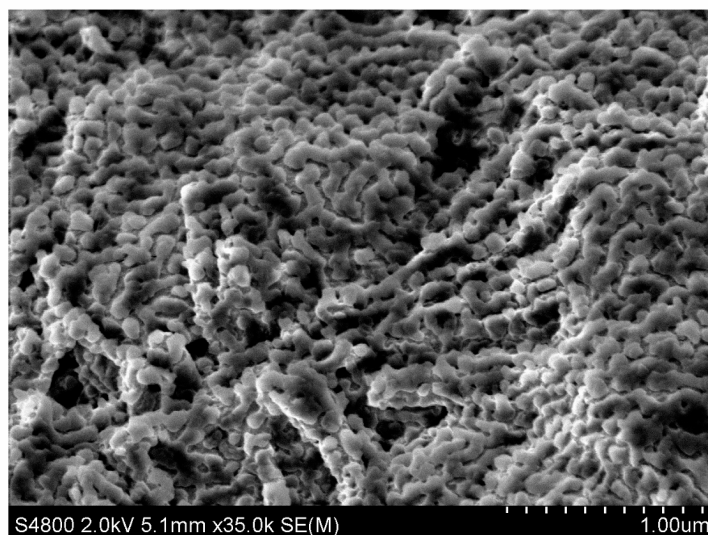
Figure 3.2-2: Cryo-SEM micrograph of the L_2 phase of the SDS/toluene-pentanol (1:1)/water system.

Surprisingly, at a polymer concentration of 20 wt%, an isotropic phase channel has been found that connects the toluene-pentanol corner with the water corner of the phase diagram (Figure 3.2-3).
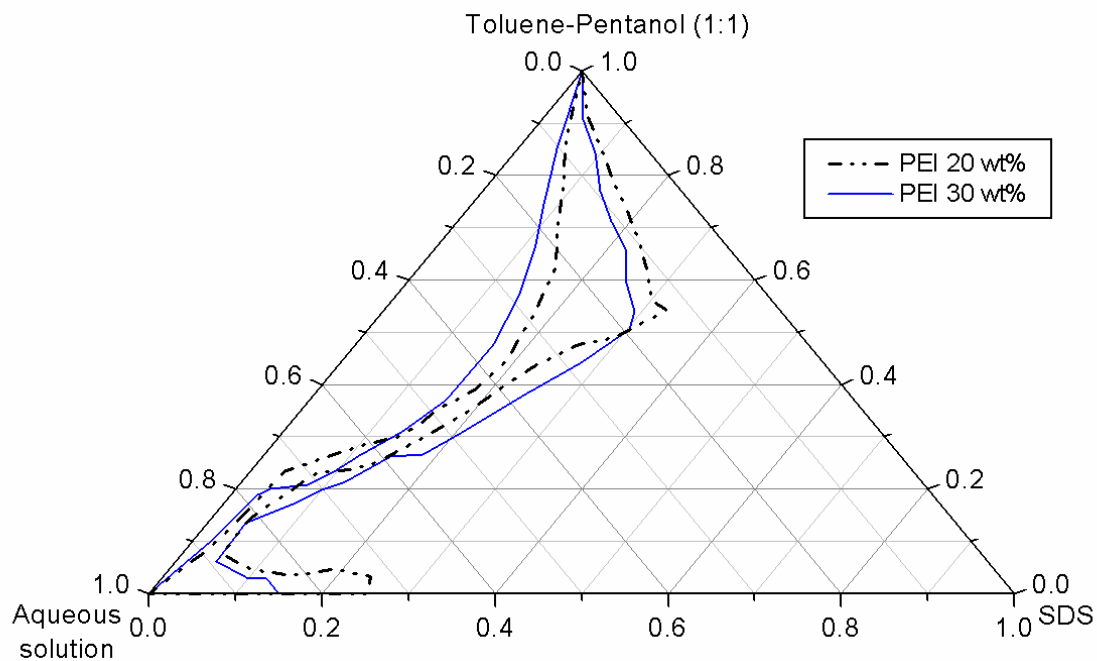
Figure 3.2-3: Partial phase diagrams at 22°C of the system SDS/toluene-pentanol (1:1)/PEI at 20 and 30 wt% in water.

In the large majority of ternary and quaternary systems, the regions of the L_1-phase and the L_2-phase are well separated in the phase diagram [34, 35]. But, in some cases, as reported for the present study, a connection between these both regions, i.e., a common isotropic phase connecting the water corner and the oil corner, can exist [36, 37].

Starting from the L_2 phase, the formation of the phase channel can be explained by an increase of the water solubilization capacity of the inverse swollen micelles, combined by a change of the spontaneous curvature of the surfactant film to zero. Indeed, several theoretical [38-41] and experimental [42, 43] studies have shown that the individual structure of a surfactant dispersion, that means a droplet or sponge-like-one, is mainly determined by the surfactant film bending elasticity.

The isotropic phase formed in the system studied occurs at a surfactant/oil ratio of 33/67 and is in some parts narrow.

The Cryo-SEM micrograph (Figure 3.2-4) reveals the sponge structure of the bicontinuous phase in the channel between the L_1 and the L_2 phases.
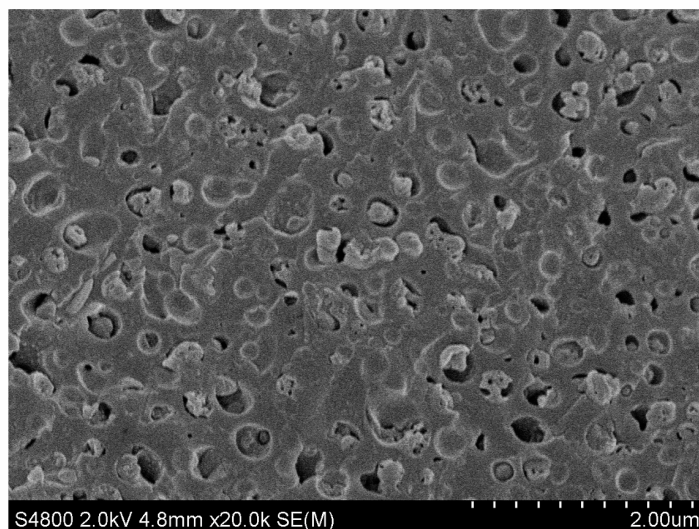
Figure 3.2-4: Cryo-SEM micrograph of the bicontinuous phase with 30 wt% polymer in water.

If the polymer concentration is further increased, one can observe an enlargement of the phase channel as well as a strong reduction of the L_1 phase in the water corner. This can be explained by an increase of the hydrophobicity of the interfacial layer due to polyelectrolyte-surfactant interactions, when the PEI concentration in water is increased.

3.2.2. Influence of the temperature

When the temperature of the unmodified system SDS/toluene-pentanol/water is increased from 22°C to 30°C, no significant change of the microemulsion area can be observed. A further increase of the temperature to 40°C induces a slight widening of the L_2 phase (see Appendix 5, Figure A5-1). Indeed, the temperature has generally no effect on the stability of anionic surfactant films.

However, this behaviour is drastically changed in presence of the polymer. When pure water is replaced by 10 wt% of PEI, an increase of the temperature from 22°C to 30°C induces a significant enlargement of the L_2 phase and the maximum of water solubilization is shifted from 27.8 % to 57.6 % at a constant surfactant/oil ratio, as shown in Figure 3.2-5. A further increase of the temperature to 40°C leads only to a small widening of the L_2 microemulsion area, but does not further influence the maximum of solubilization. Besides, the increase of the temperature does not induce any significant changes on the area of the L_1 phase.
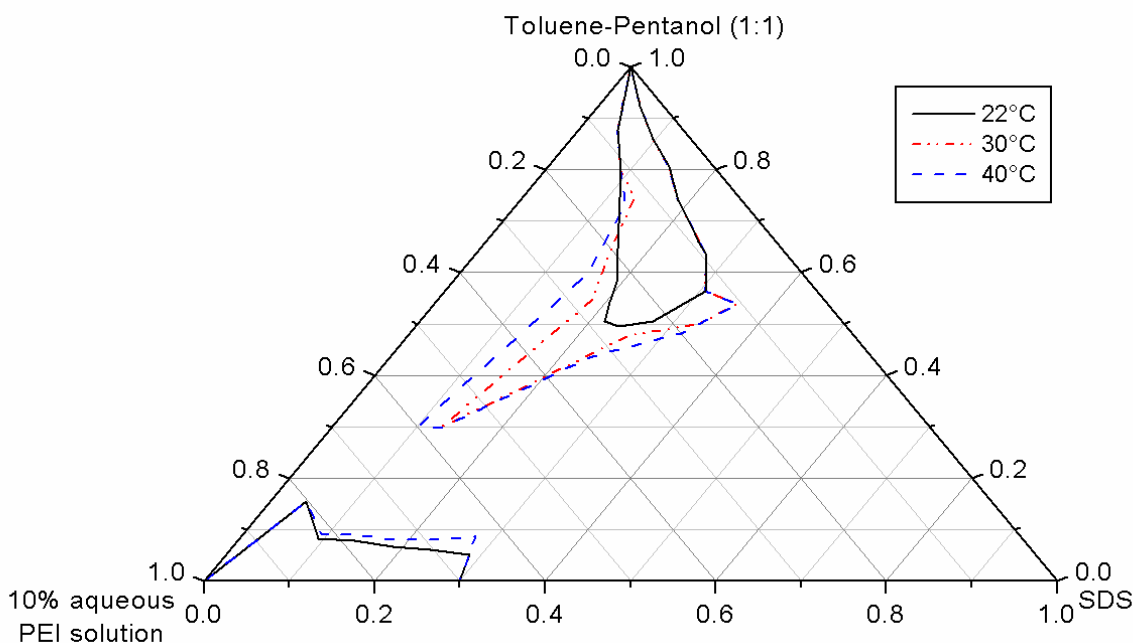
Figure 3.2-5: Influence of the temperature on the partial phase diagram of the system SDS/toluene-pentanol (1:1)/PEI 10 wt% in water.

Thus, an increase in temperature leads to an enhancement of the solubilization capacity in inverse microemulsions modified with PEI and to a phase transition from the w/o microemulsion to a sponge-like phase.

3.2.3. L$_2$-phase characterization

3.2.3.1. Rheological characterization

The viscosity of a surfactant based mixture is a typical indicator for the structure of the corresponding system. Therefore, the shear viscosity is measured along a water dilution line (given as a solid line in Appendix 6, Figure A6-1) in the bicontinuous channel of the system SDS/toluene-pentanol/PEI 20 wt% in water. It has to be noted that the surfactant/oil ratio ω is kept constant along this line ($\omega = 33/67$).

Four samples (compositions are given in Table 3.2-1) are investigated along this dilution line by means of viscosity measurements.

Table 3.2-1: Composition of samples A to D.

Sample	SDS/Oil/Aq. phase (wt ratio)	SDS/Oil (wt ratio)
A	23.1/46.9/30	33/67
B	19.8/40.2/40	33/67
C	16.5/33.5/50	33/67
D	13.2/26.8/60	33/67

The shear viscosities are given in Figure 3.2-6 as a function of the shear rate.

Points A and B show a Newtonian flow behaviour with relatively low viscosity in the range of 33 to 55 mPas, which can be related to a L_2 phase. Indeed, such low viscosities are typically observed for microemulsions, consisting of individual spherical droplets [44, 45]. Furthermore, the increase of the shear viscosity from A to B with increasing water content can be related to the enlarged droplet size and/or droplet-droplet interactions, as well as to the increasing polymer concentration in the aqueous phase.
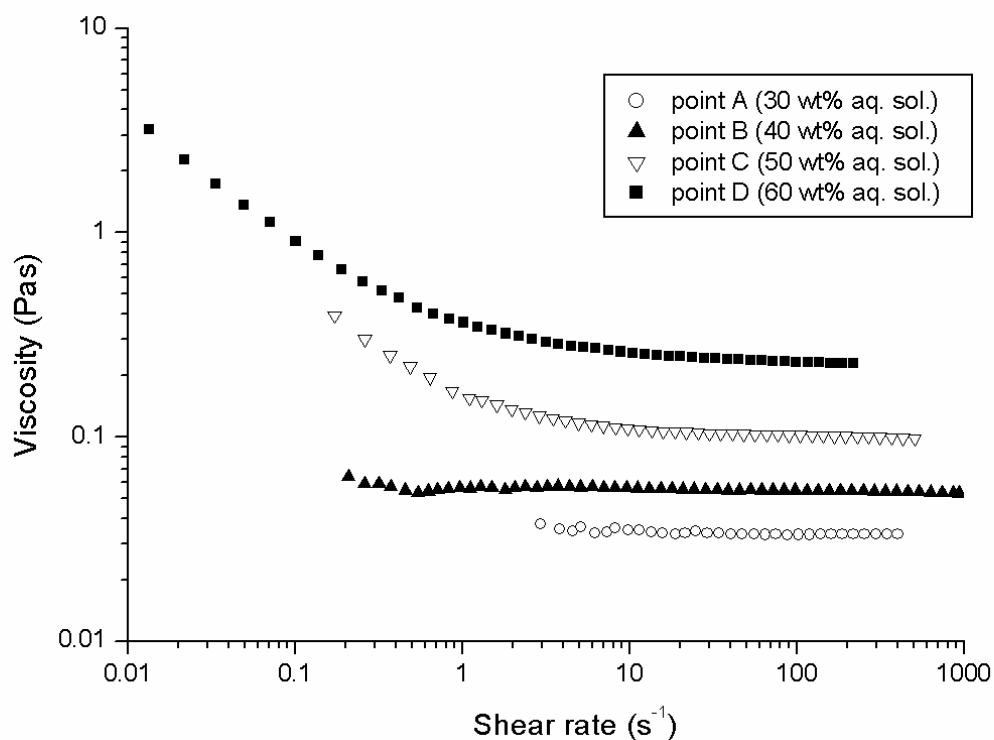
Figure 3.2-6: Evolution of the shear viscosities as a function of the shear rate, at 22°C along the dilution line ω = 33/67, for the system SDS/toluene-pentanol (1:1)/PEI 20 wt% in solution.

When more water is solubilized in the microemulsion (points C and D), a shear-thinning effect is observed: the viscosity first decreases with increasing shear rate until it arises a constant value at a shear rate > 2 s^{-1}. Moreover, the viscosity in the plateau range is increased from A to D. The transition from a Newtonian to the non-Newtonian flow behaviour can be related to a phase transition from the L_2 phase to a sponge-like phase [46, 47].

3.2.3.2. Conductivity measurements

As shown in Chapter 3.1.2., the presence of polymers can affect the process of percolation and therefore the conductance in the system, by influencing the surfactant film of the microemulsion.

Thus, the influence of the branched-PEI on the exchange-process between the microemulsion droplets, i.e. on the percolation phenomenon, has been examined by means of conductivity measurements.

Electrical conductivity measurements are carried out by starting from different surfactant/oil ratios ω, and by adding water (or the aqueous polymer solution) along the dilution line.

Results obtained at 22°C for ω= 20/80 with different concentrations of polymer, are illustrated in Figure 3.2-7. It is noticeable that the addition of 1 wt% of polymer solution does not induce any changes in the conductivity. However, at higher polymer concentration, the conductivity strongly drops and the percolation phenomenon disappears for the polymer-modified microemulsions. It must be noted that the same results are observed for ω= 10/90; 15/85; and 25/75.

The disappearance of the percolation phenomena in presence of a high concentrated PEI-solution, suggests that the polymer reduces the rate of exchange of material between two colliding droplets as well as the attractions between the droplets [14-17, 48-50]. This means that the addition of branched-PEI into the system changes the droplet-droplet interactions from attractive to repulsive. Similar trends have been previously observed by Suarez et al. [51] in microemulsion composed of AOT/alcohol/water/decane in presence of several water soluble polymers.
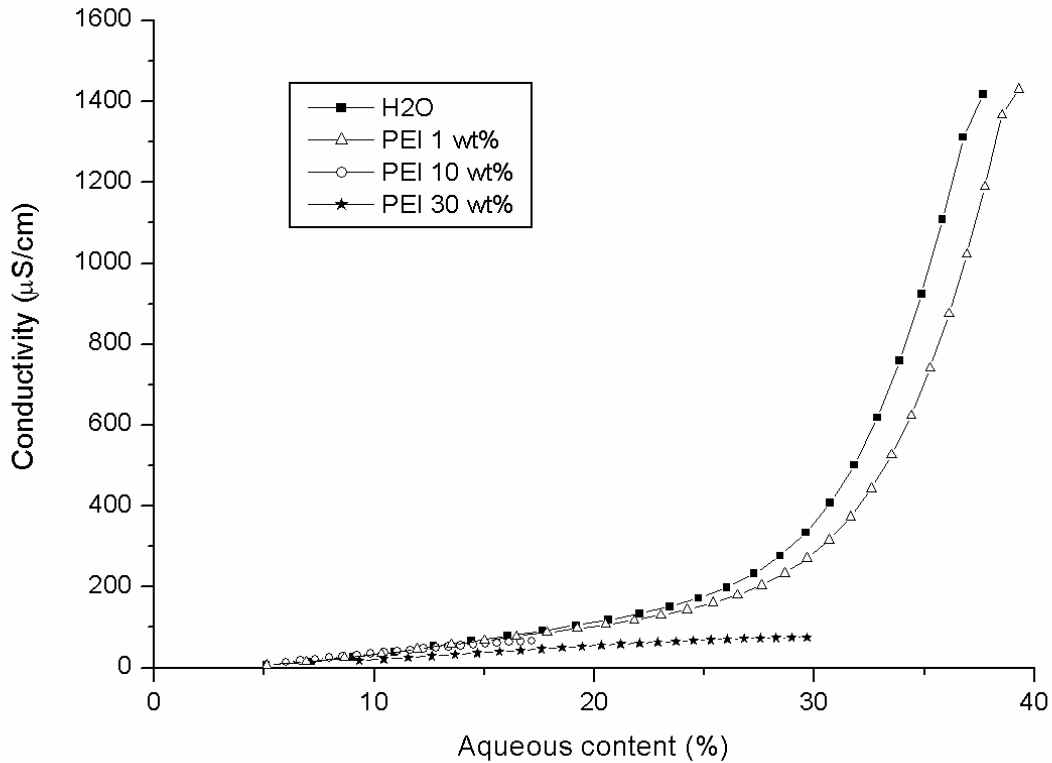
Figure 3.2-7: Evolution of the conductivity at 22°C along the dilution line ω = 20/80, for different concentrations of polymer, as a function of the aqueous phase content.

In a second set of experiment, conductivity measurements are carried out at 22°C along the same line used for the viscosity measurements (ω = 33/67, see Appendix 6), by adding an aqueous polymer solution of 30 wt%.

The conductivity is given in Figure 3.2-8 as a function of the percentage of added aqueous phase. The conductivity first increases upon water addition. The moderate slope in the conductivity can be related to a weak percolation of charges through the droplets in the L_2 phase; phenomenon which was found to be much stronger for the unmodified system (see Appendix 7, Figure A7-1). Moreover, at about 40 % of aqueous solution added, a transition to a pseudo-plateau at approximately 600 μS/cm is observed, which can be related to the transition from an aqueous system of dispersed micellar aggregates to a bicontinuous structure [45, 52]. A further increase of the aqueous content (> 60 %) leads to a second steeper jump in the conductivity, indicating an evident structural change in the system: one goes from a bicontinuous structure to an oil-in-water microemulsion [52-54]. These results are consistent with that found via the rheological measurements where points C and D belong to the bicontinuous transition phase between the L_2 and L_1 phases.
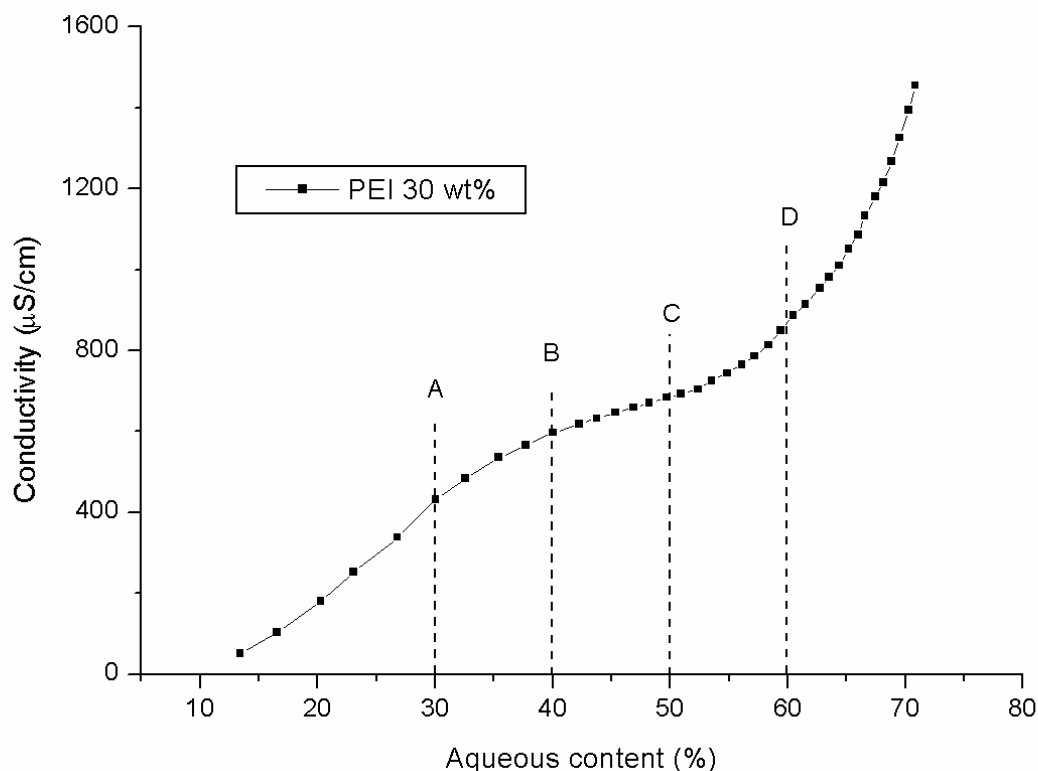
Figure 3.2-8: Evolution of the conductivity at 22°C along the dilution line ω = 33/67, as a function of the aqueous phase content and for a polymer concentration of 30 wt%.

3.2.3.3. DSC measurements

Micro-DSC measurements are performed on the isotropic phase of the system SDS/toluene-pentanol/PEI 20 wt% in water, following again the dilution line with ω= 33/67 (see Appendix 6). The melt enthalpies are listed in Table 3.2-2.

Table 3.2-2: Micro-DSC results of the system SDS/toluene-pentanol/PEI 20 wt% in water along the dilution line ω = 33/67.

Sample	Aqueous phase concentration (wt %)	Bulk water		Interfacial water	
		Peak top (°C)	Melt Enthalpy (J/g)	Peak top (°C)	Melt Enthalpy (J/g)
A	30	0.1	20.0	-7.1	253.2
B	40	—	—	-7.2	235.2
C	50	-3.8	45.1	-6.9 / -9.0	177.9
D	60	-2.7	127.2	-9.1	85.8

From the enthalpy of about 226 J/g, one can calculate that approximately 70% of the water incorporated into the system can be detected.

The DSC results allow to follow the structural transition from a water-in-oil microemulsion to a bicontinuous phase.

Point A reveals two main water peaks: a small bulk-water peak at 0°C and a large interfacial-water peak around −7.1°C. The increase of water content (point B) in the droplets is accompanied by the disappearance of the bulk-water peak, and only the interfacial water can be detected. If the water content is further increased, a free-water peak appears at around −3.8°C (point C), and the amount of interfacial-water starts to decrease. At point D, the free-water peak (at around −2.7°C) further increases and the interfacial-water further decreases. The micro-DSC results can be reasonably explained by the formation of a sponge-like phase in the channel between the L_2 and the L_1 phases, where water is no longer completely restricted at an interface and free water can in addition be detected.

3.2.4. Conclusion

The addition of the water soluble branched-PEI induces important changes in the phase behaviour of the SDS/toluene-pentanol/water system. The droplet phases (L_1 and L_2) found in absence of polymer, still exist when pure water is replaced by aqueous solutions of PEI, but their extent is strongly influenced by the polymer concentration, the surfactant/oil ratio and the temperature.

One of the most important effect of the polymer PEI is to increase the efficiency of the surfactant. At higher concentration (> 20 wt%), the polymer enhances the maximum of solubilization of water in the inverse microemulsions by stabilizing the surfactant film of larger swollen droplets. This effect can also be induced at lower polymer concentrations by increasing the temperature from 22°C to 40°C.

At higher temperature, the degree of disorder is increased and an association of the polymer to the interfacial region is much more favoured. Hence, an increase of deformability of the film is obtained and the branched poly(ethyleneimine) can thus help to form an isotropic channel, even at lower polymer concentration.

It can also be argued that the presence of the polymer decreases the interdroplet interactions as well as the fluidity of the surfactant film [55], and thereby makes the formulation in general more stable towards temperature [56].

Another important finding is that the polymer, at higher concentration, modifies the effective hydrophilicity of SDS by changing the sign of the spontaneous curvature of the surfactant film. The addition of PEI to a given SDS/toluene-pentanol/water mixture induces indeed the formation of a sponge-like phase and an inversion of the microemulsion type from an oil-in-water to a water-in-oil.

The L_2 phase of the SDS/toluene-pentanol/aqueous polymer system is characterized by a low viscosity and a Newtonian flow behaviour. In comparison, the bicontinuous channel shows higher viscosity values, and a shear-thinning behaviour.

Moreover, it was demonstrated that the polymer strongly affects the exchange between the microemulsion droplets in the L_2 phase of the modified-system. The percolation behaviour, present in the unmodified system, completely disappears when the polymer concentration increases, which suggests that the polymer changes the droplet-droplet interactions from attractive to repulsive in the SDS system.

Detailed conductivity measurements were also performed along a dilution line in the isotropic channel, which permit to follow the structural transitions occurring in the system. In the first part of the microemulsion area, the L_2 phase was characterised by a moderate increase of the conductivity due to the weak percolation of the droplets. The percolation is indeed hindered due to the polymer-surfactant film interactions and the moderate increase of the conductivity can be explained by the more bound counterions and/or the reduced droplet-droplet interactions. At higher water content, a pseudo-plateau in the conductivity reveals the transition from an aqueous system of dispersed micellar aggregates to a bicontinuous structure. The following steep jump of the conductivity can be related to a second evident structural change in the system: a phase transition from a bicontinuous structure to an oil-in-water microemulsion.

Finally, the DSC measurements allow to follow the changes of the water properties in the system, from interfacial-water in the L_2 phase to free-water in the sponge phase by measuring the melting point and the melting enthalpies at different water content inside the isotropic channel.

One can therefore conclude that the incorporation of water soluble polymer into water-in-oil microemulsion droplets is of special interest to increase the surfactant film stability and to influence the properties of the microemulsion system.

3.3. Hydrophobically modified polyampholytes in a SDS-based microemulsion

3.3.1. Comparison between the polymers PalH and PalBu

3.3.1.1. Microemulsion phase diagrams

Different inverse microemulsions are investigated as "nanocontainer" for the polyampholytes. The oil component is a toluene-pentanol mixture with a 1:1 volume ratio. 2 different types of surfactants, i.e. the cationic CTAB, and the anionic SDS were used for the preparation of microemulsions. It is then checked if the microemulsion phases previously formed still exist when water is substituted by aqueous solutions of polyelectrolyte.

The incorporation of 1 wt% PalH into the quaternary system CTAB/toluene-pentanol (1:1)/water induces a significant reduction of the initial microemulsion area (see Appendix 8, Figure A8-1). An increase of the polymer concentration up to 5 wt% leads to the quasi disappearance of the L_2 phase area. One can assume that the polymer can not be easily incorporated into the individual droplets due to repulsive electrostatic forces between the cationic part of the polymer and the surfactant head group [1].

The same effect is observed when PalBu solutions are incorporated into the CTAB system. Again, the L_2 phase is decreased in presence of the polymer (see Appendix 8, Figure A8-2). However, one can observe that the reduction of the microemulsion area is not so pronounced as for the polymer PalH. In this case, the incorporation of the polymer bearing hydrophobic groups is favoured by hydrophob-hydrophob interactions between the polymer chains and the surfactant tails.

When water is substituted by a 1 wt% PalH-solution in the quaternary system SDS/toluene-pentanol (1:1)/water at 22°C, a slight reduction of the initial inverse microemulsion area is observed (Figure 3.3-1). However, at a polymer concentration of 5 wt%, the L_2 phase is slightly increased. For 10 wt% polymer, the L_2 phase is significantly enlarged and the maximum of water solubilization is shifted from 36.3% to 42.2% at a constant surfactant concentration.
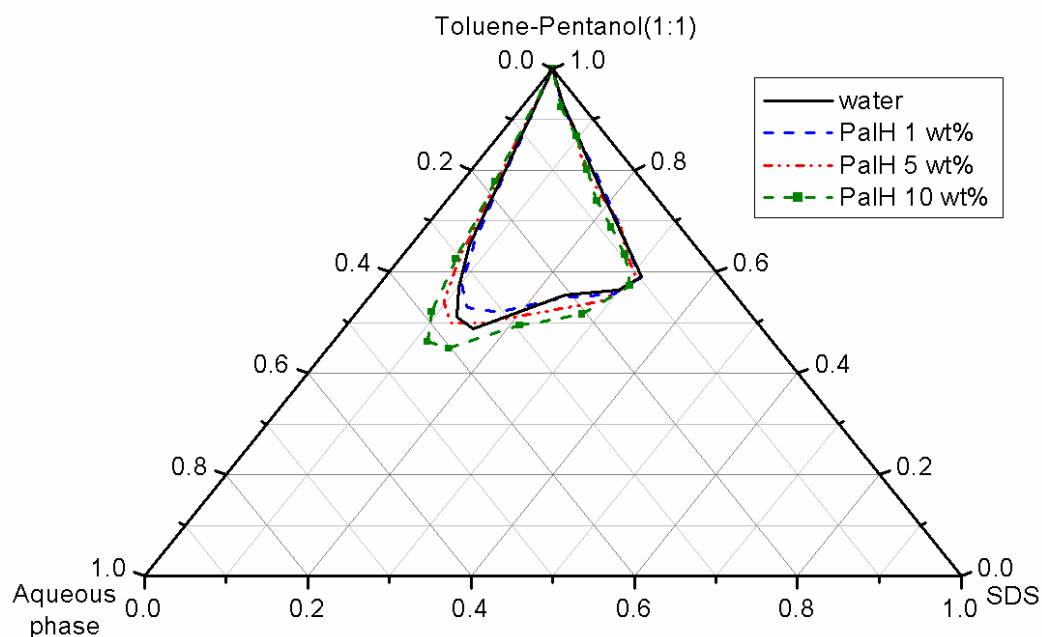
Figure 3.3-1: L$_2$ phase at 22°C of the SDS/toluene-pentanol (1:1)/water system in presence of different PalH concentrations.

When the polymer PalH is replaced by PalBu (Figure 3.3-2) at a polymer concentration $\geq$ 5 wt%, an extension of the L$_2$ phase is observed. At 10 wt% polymer solution, the maximum of water solubilization in the oil continuous microemulsion is shifted to 41.5% at a constant surfactant concentration.
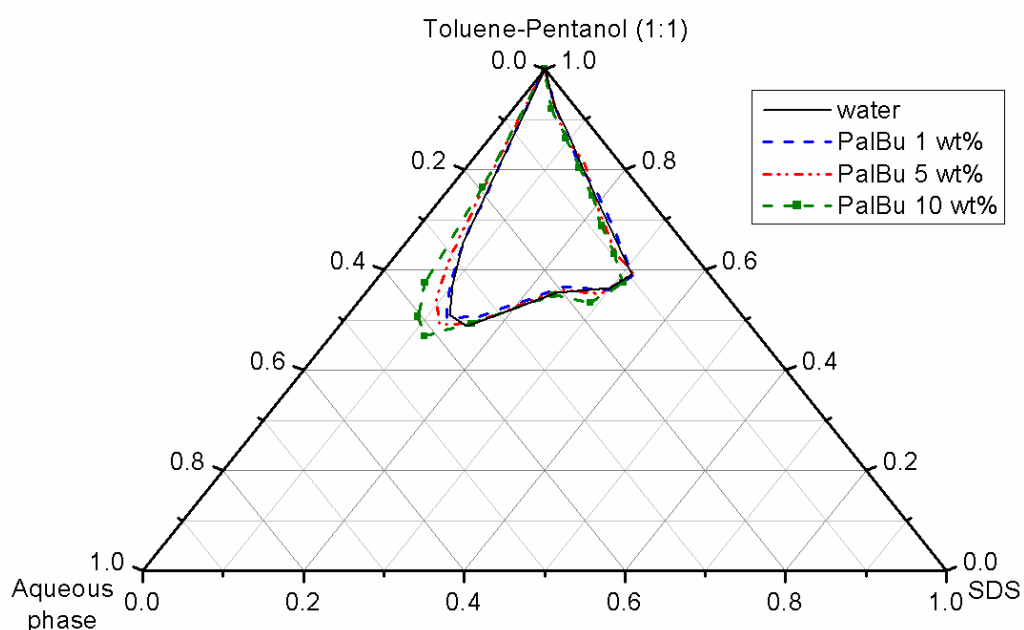
Figure 3.3-2: L$_2$ phase at 22°C of the SDS/toluene-pentanol (1:1)/water system in presence of different PalBu concentrations.

For both polymer-modified microemulsions, the increase of the water solubilization capacity can be related to an increase of the bending elasticity of the interfacial film due to weak Coulombic interactions between the cationic functional groups of the polyampholyte and the anionic head groups of the surfactant.

3.3.1.2. Influence of the temperature

As already outlined in Chapter 3.2.2 the unmodified system SDS/toluene-pentanol/water is not changed by increasing the temperature from 22°C to 40°C.

When water is substituted by a 1 wt% polymer solution no significant changes are observed.

With the incorporation of the polyelectrolyte PalH into the microemulsion, the effect of the temperature becomes more significant. Indeed, for 5 wt% polymer, it is noticeable that the L_2 phase is extended towards the water corner when the temperature increases (see Appendix 9, Figure A9-1). Noteworthy, at 40°C and for a polymer concentration of 10 wt% (Figure A9-2), it becomes possible to extend the microemulsion until 46.1% of aqueous solution, content which represents an increase of 9.8% compared to the unmodified system.

Concerning the PalBu-modified microemulsion, the isotropic phase range is also affected by an increase of temperature. At 40°C with a polymer concentration of 5 wt%, the part of incorporated water is already at 44.6% (Appendix 9, Figure A9-3).

When the PalBu concentration is increased to 10 wt%, the maximum of solubilization reaches 46.7% at 30°C (Figure A9-4), that means 10.4% more than for the unmodified system.

Surprisingly, at 40°C and at a polymer concentration of 10 wt%, the polymer PalBu induces the formation of a phase channel between the oil and water corners of the diagram (Figure 3.3-3). Starting from the L_2 phase, the formation of the phase channel can be explained as previously by an increase of the water solubilization capacity of the inverse swollen micelles, combined by a change of the spontaneous curvature of the surfactant film to zero.
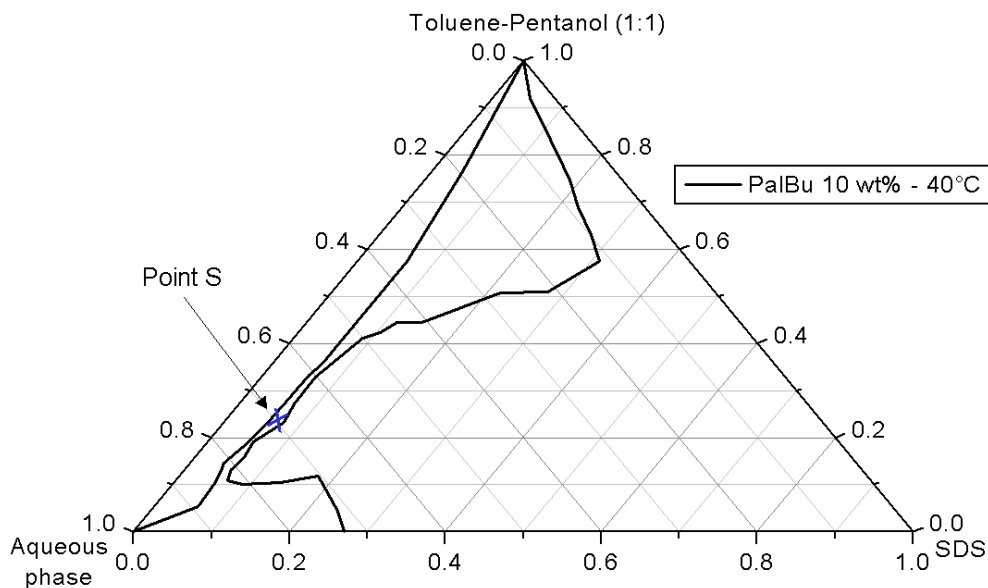
Figure 3.3-3: Partial phase diagram at 40°C of the system SDS/toluene-pentanol (1:1)/PalBu 10 wt% in water.

The Cryo-SEM micrograph in Figure 3.3-4 reveals at point S (marked in Figure 3.3-3) the bicontinuous structure of the studied microemulsion in the channel between the L_1 and the L_2 phases. The differences with the micrograph of the unmodified L_2 phase (Chapter 3.2.1, Figure 3.2-2) are notable.

Similar results were already observed by our group by adding poly(N-vinyl-2-pyrrolidone) [57] or poly(ethylene glycol) [51] to the SDS/xylene-pentanol/water system, or by Bellocq by adding poly(ethylene glycol) into the AOT/isooctane/water system [3].
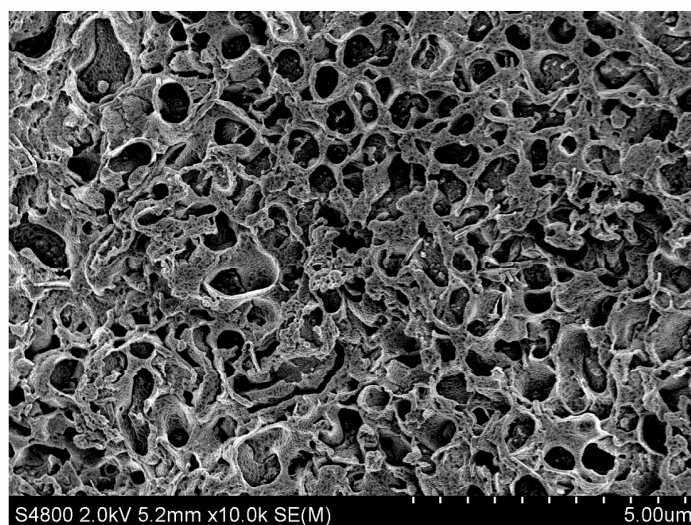
Figure 3.3-4: Cryo-SEM micrograph at point S of the bicontinuous channel in the system SDS/toluene-pentanol (1:1)/PalBu 10 wt% in water.

3.3.1.3. Conductivity measurements

As seen previously in Appendix 7, Figure A7-1, the conductivity of the unmodified system remains first constant when water is added. A further increase of the water content is accompanied by a steep increase of the conductivity. This jump in the conductivity is characteristic for the percolation of charges through the droplets (dynamic processes of temporary cluster formation).

A boundary of percolation can thus be determined for the system SDS/toluene-pentanol/water as a function of the mixture composition (Figure 3.3-5). The shift of the percolation boundary is then investigated in presence of the two copolymers PalH and PalBu, at 1 wt% and 10 wt% (see conductivity results in Appendix 10, Figure A10-1 and A10-2).
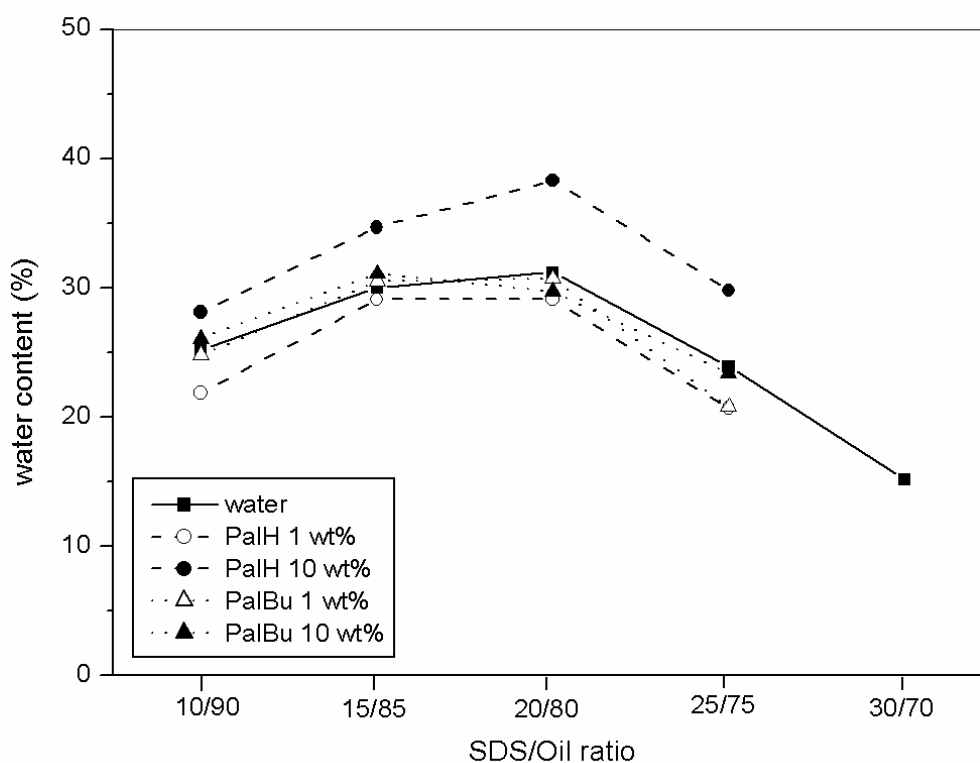
Figure 3.3-5: Boundary of percolation for the system SDS/toluene-pentanol (1:1)/water depending on the polymer added and its concentration.

First of all, it has to be mentioned that the percolation still exists in presence of polyelectrolytes. Furthermore, the polymer PalBu does not affect the percolation phenomena between the microemulsion droplets and no change or shift can be (within the experimental error) noticed even if the concentration of PalBu is increased to 10 wt%.

When the 1 wt% PalH solution is incorporated into the system, no significant change can be observed. However, if the concentration is increased to 10 wt%, the results show a shift of the percolation boundary to higher water contents. For the SDS/oil ratio 20/80, a maximum shift of 7% can be measured in comparison to the unmodified system. Moreover, one can also observe a diminution of the conductivity value in the PalH-modified system.

3.3.1.4. Rheological investigations

For a more comprehensive discussion, the conductivity measurements are accompanied by rheological measurements. These can provide information about the interactions of the microemulsion surfactant film with the polyelectrolytes. 4 isotropic mixtures, samples A, B, C and D (see Table 3.3-1) have been studied in much more detail by means of shear experiments.

Table 3.3-1: Composition for samples A-D

Sample	SDS/Oil/Water [a] (wt ratio)	Water/SDS (wt ratio, R_w)
A	10/80/10	1
B	15/70/15	1
C	20/60/20	1
D	15/55/30	2

[a] Or aqueous polyampholyte solution.

All systems investigated, i.e. the unmodified and polyelectrolyte-modified microemulsions show a Newtonian flow behaviour.

The rheological data show for the unmodified system that the shear viscosity increases from B to D (Figure 3.3-6). However, the weight ratio R_w (water/surfactant) is increased from B→D, and the surfactant concentration is constant. Therefore, the shear viscosity increase with increasing water content can be related to the increasing droplet size and/or droplet-droplet interactions.

At the points A, B and C, the ratio R_w is constant (see Table 3.3-1), but the aqueous solution content is increased in the order: A→B→C. Under these conditions, one can expect a constant droplet size but increasing droplet number. The experimental data (Figure 3.3-6) show for the unmodified system that the shear viscosity is twice as large at higher water content. This can

be explained by a simple concentration effect (i.e., increase of the number of microemulsion droplets with an approximately uniform size).
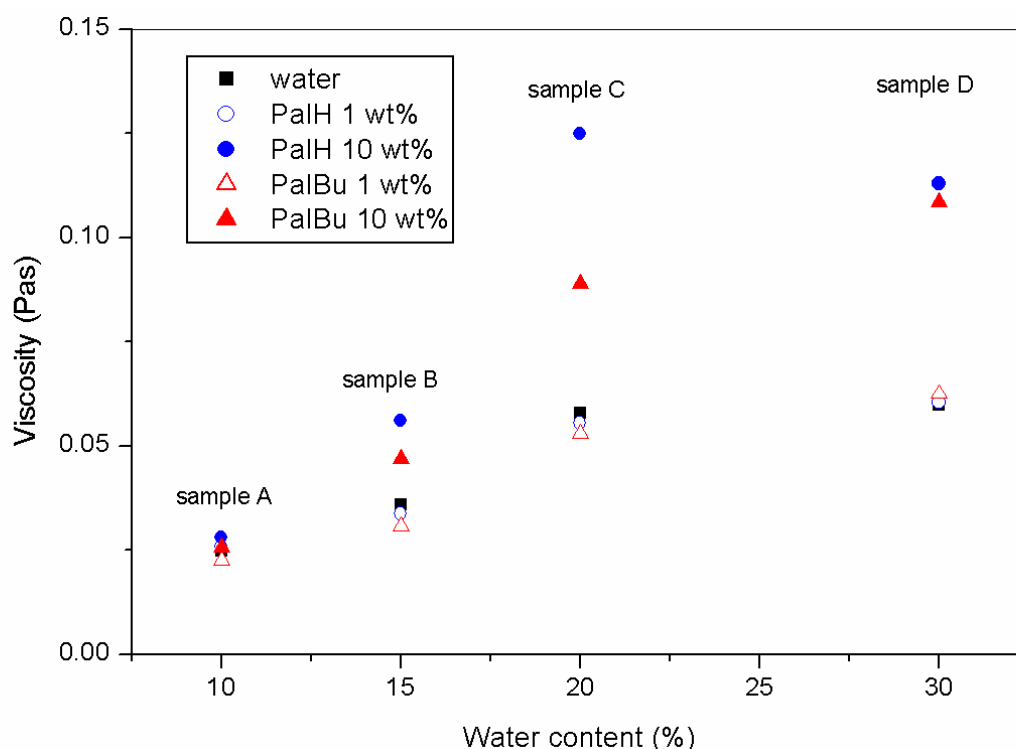
Figure 3.3-6: Evolution of the shear viscosities of the different polyelectrolyte modified microemulsions as a function of the water content.

When 1 wt% of polymer is incorporated into the microemulsion, no change of the shear viscosity is observed, whatever the polymer added. But, at a polymer concentration of 10 wt% a significant increase of the shear viscosity has to be mentioned for samples B, C and D. For instance, sample C with 10 wt% PalH shows a viscosity twice as high as the sample without polymer.

At higher polymer concentrations, one can assume that the polymer interacts with the surfactant film, which leads to an increase of the droplet-droplet interactions and hence to an increase of the shear viscosity.

3.3.1.5. Conclusion

The investigations have revealed that an optically clear region of the phase diagram in the SDS/toluene-pentanol (1:1)/water system still exists after the incorporation of the polyampholytes PalH and PalBu. In general, the copolymers induce an extension of the

isotropic phase in direction of the water corner, effect enforced by increasing the concentration of the polymer. This can be explained by a change in the bending elasticity of the interfacial film induced by Coulombic interactions between the functional groups of the polyelectrolyte and the surfactant head groups.

The copolymers added have a quite similar effect on the L_2 phase at room temperature (22°C), but a different behaviour at higher temperature. The incorporation of small hydrophobic side chains (butyl groups) along the copolymer backbone involves the formation of a bicontinuous channel when the temperature arises 40°C. Assumingly, PalBu, as hydrophobically modified copolymer, tends to form microdomains at room temperature [58] and these microdomains disappear at higher temperature. In this case, in addition to the electrostatic interactions between the surfactant head group and the polymer, hydrophobic interactions between the surfactant tail and the hydrophobic side chains have to be taken into account. These additional hydrophobic-hydrophobic interactions affect the surfactant film stability and increase the solubilization capacity of the microemulsion droplets, which is then combined with a change of the spontaneous curvature of the surfactant film to zero, followed by the formation of a bicontinuous phase channel.

One feature of the W/O microemulsion droplets is their low viscosity and Newtonian flow behaviour. The increase of the shear viscosity as a function of the polymer concentration confirms well the assumption of polyelectrolyte-stuffed inverse microemulsion droplets. Moreover, the polymer PalH induces a stronger increase of the viscosity of the mixture in comparison to PalBu. This can be explained by the fact that the polymer PalBu, involved in the formation of microdomains at room temperature, does not interact so strongly with the surfactant film as PalH.

Another interesting feature of the SDS/toluene-pentanol (1:1)/water inverse microemulsion is its high conductivity due to percolation phenomena. The percolation still exists in presence of polyelectrolytes. It is also notable that the polymer PalH at a concentration of 10 wt% delays the percolation of the droplets and diminishes the maximal value of the conductivity. This can be explained by a modification of the interfacial film due to the presence of the polymer and by an increase of the repulsion between the droplets. However, the polymer PalBu does not affect the percolation, which can be explained again by the formation of microdomains.

3.3.2. PalOc-modified microemulsions

3.3.2.1. Microemulsion phase diagrams

The system investigated is composed of a toluene-pentanol mixture (1:1) as oil component (volume ratio), and of the anionic SDS as surfactant. It is then examined if the L_2 phase formed in the unmodified system still exists when water is substituted by aqueous solutions of PalOc.

The comparison between the polymers PalBu and PalOc will permit to examine, in microemulsion, the effect induced by the presence of longer hydrophobic groups on the polymer chains.

The incorporation of 1 wt% PalOc into the quaternary system SDS/toluene-pentanol (1:1)/water induces no significant change of the initial microemulsion area (see Figure 3.3-7). In the same way, when the polymer concentration is further increased up to 10 wt% almost no modification of the initial inverse microemulsion area is observed.

Figure 3.3-7: L_2 phase at 22°C of the SDS/toluene-pentanol (1:1)/water system in presence of different PalOc concentrations.

Thus, in presence of PalOc, bearing longer hydrophobic groups, no extension of the microemulsion area can be observed, as it was the case for the polymer PalBu.

These experimental results can be explained by the fact that the self-aggregation of the polymer PalOc is higher as the one of PalBu, due to stronger intra and inter-molecular hydrophob-hydrophob interactions between the polymer chains. Therefore, one can suppose that the polymer PalOc forms preferentially aggregates with microdomains in the bulk water part of the microemulsion droplets, and does almost not interact with the interface.

3.3.2.2. Influence of the temperature

As already demonstrated in Chapter 3.2.2. the unmodified SDS/toluene-pentanol/water system is not changed by increasing the temperature from 22°C to 40°C.

Concerning the PalOc-modified microemulsion, the isotropic phase range is not affected by the increase of temperature. At a polymer concentration of 10 wt% no significant change of the L_2 phase is observed when the temperature increases from 22°C to 40°C (see Appendix 11, Figure A11-1).

Again, one can conclude that the polymer does not strongly interact with the interface and is present in the microemulsion droplets in the form of aggregates, even if the temperature is increased.

3.3.2.3. Conductivity measurements

As formerly observed, conductometry is a useful technique to access any structural changes occurring in a system [8-12].

Therefore, to verify the incorporation of the polymer PalOc in the L_2 phase, conductivity measurements are performed. Indeed, the presence of the polymer should affect the process of percolation and therefore the conductance in the modified-system.

First of all, it has to be mentioned that the percolation still exists in presence of the polyampholyte PalOc (see Appendix 11, Figure A11-2 and A11-3).

Furthermore, the polymer does not affect the percolation boundary as no shift can be (within the experimental error) noticed even if the concentration of PalOc is increased to 10 wt% (Appendix 11, Figure A11-3).

However, one can observe a strong decrease of the conductivity maximum value especially when the polymer concentration is increased (Appendix 11, Figure A11-3). The polymer does influence the rate of exchange between the microemulsion droplets, presumably by a concentration effect, which confirms the incorporation the polyelectrolyte PalOc in the inverse microemulsion droplets.

3.3.3. PalPh-modified microemulsions

3.3.3.1. Microemulsion phase diagrams

The incorporation of 1 wt% PalPh into the quaternary system CTAB/toluene-pentanol (1:1)/water induces a significant reduction of the initial microemulsion area (see Appendix 12, Figure A12-1). An increase of the polymer concentration up to 5 wt% leads to a further decrease of the L_2 phase area. One can again assume that the polymer can not be easily incorporated in the individual droplets due to repulsive electrostatic forces between the cationic part of the polymer and the surfactant head group [1].

When water is substituted by a 5 wt% PalPh-solution in the quaternary system SDS/toluene-pentanol (1:1)/water at 22°C, a slight increase of the initial inverse microemulsion area is observed (Figure 3.3-8). At a polymer concentration of 10 wt%, no further change of the L_2 phase can be observed.

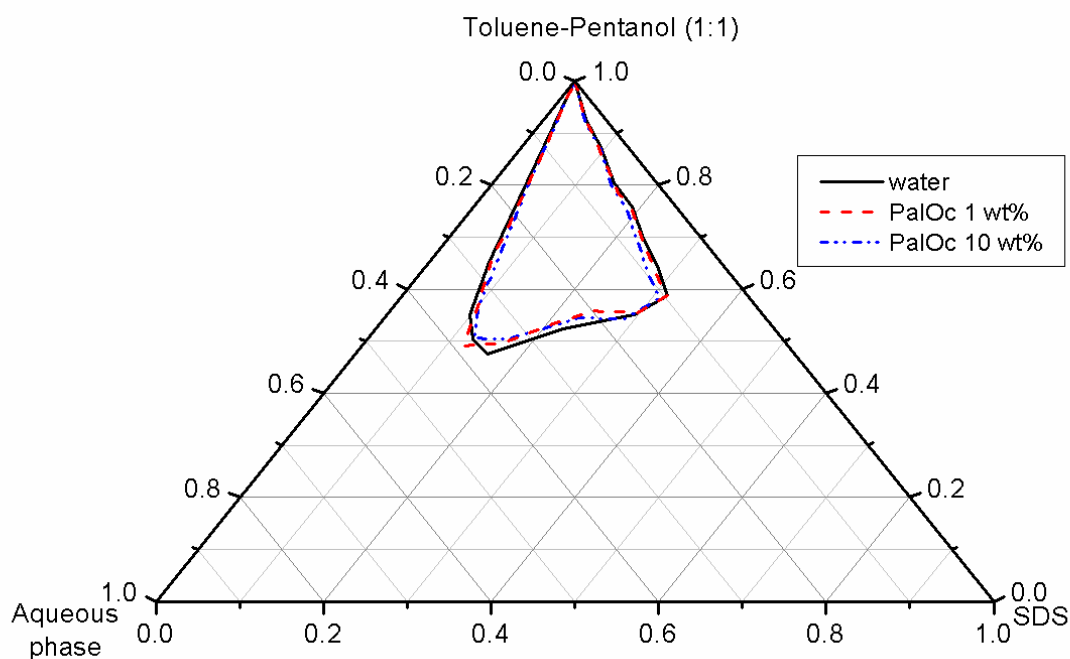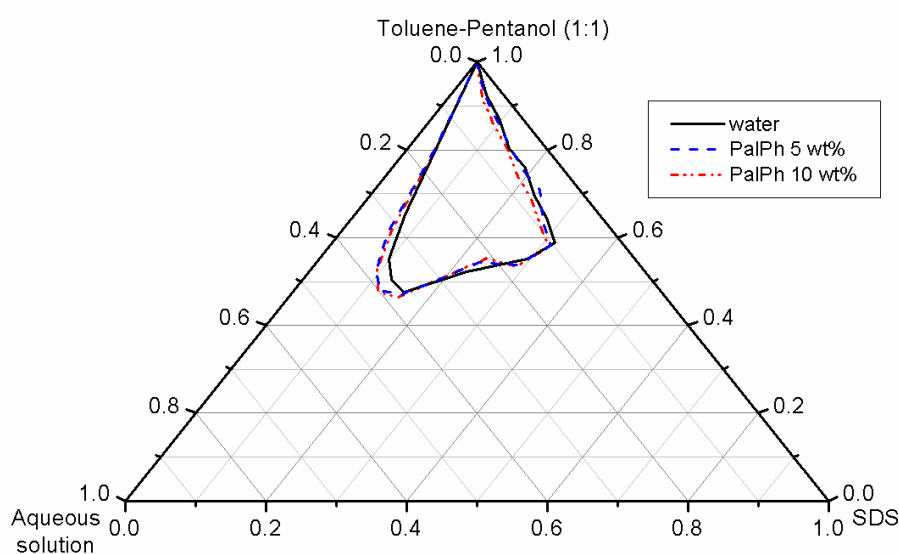*Figure 3-8*: L_2 phase at 22°C of the SDS/toluene-pentanol (1:1)/water system in presence of different PalPh concentrations.

3.3.2.2. Conductivity measurements

To verify the incorporation of the polymer PalPh in the inverse microemulsion droplets, conductivity measurements are performed on the system SDS/toluene-pentanol (1:1)/PalPh 5 wt% in water.

First of all, one can conclude from Figure 3.3-9 that the percolation phenomenon still exists in presence of the polyelectrolyte, and that the percolation boundary is again not affected by the incorporation of the polyelectrolyte as no shift can be (within the experimental error) observed.
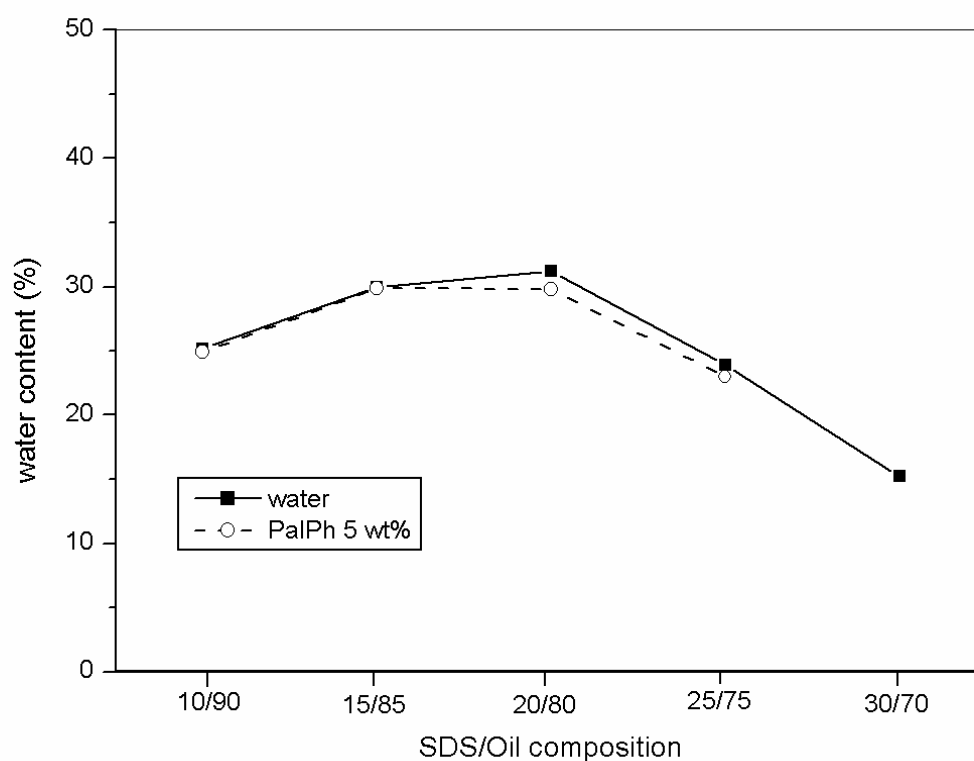
Figure 3.3-9: Comparison of the percolation boundary of the unmodified system SDS/toluene-pentanol (1:1)/water and the 5 wt% PalPh-modified system.

However, one can remark that the conductance is strongly affected in presence of the polymer, and the conductivity maximum value strongly increases in the PalPh-modified microemulsion droplets (see Appendix A12, Figure A12-2). One can then conclude from the experimental results that the polymer is incorporated into the inverse microemulsion droplets.

3.4. References

[1] Meier W., Langmuir 12 (1996) 1188.

[2] Lang J., J. Phys. Chem. 100 (1996) 5156.

[3] Bellocq A.M., Langmuir 14 (1998) 3730.

[4] Bagger-Jorgensen H., Olsson U., Iliopoulos I., Mortensen K., Langmuir 13 (1997) 5820.

[5] Lianos P., Phys. Chem. 100 (1996) 5155.

[6] Plucinski P., Reitmeir J., Coll. Surf. A 122 (1997) 75.

[7] Koetz J., Brühl I., Kosmella S., Reich J., Tiersch B., J. Coll. Interf. Sci. 186 (1997) 141.

[8] Krishnan K., Burghardt W.R., Lodge T.P., Bates F.S., Langmuir 18 (2002) 9676.

[9] Meier W., Eicke H.F., Current Opinion in Colloid Interface Sci. 1 (1996) 279.

[10] Alvarez E., Garcia-Rio L., Mejuto J.C., Navaza J.M., J. Chem. Eng. Data 43 (1998) 123.

[11] Cametti C., Bordi F., Colloid Polym. Sci. 276 (1998) 1044.

[12] Paul B.K., Mitra R.K., J. Colloid Interface Sci. 288 (2005) 261.

[13] Jada A., Lang J., Zana R., J. Phys. Chem. 93 (1989) 10.

[14] Eicke H.F., Borkovec M., Dasgupta B., J. Phys. Chem. 93 (1989) 314.

[15] Boned C., Peyrelasse J., Saidi Z., Phys. Rev. E 47 (1993) 468.

[16] Feldman Y., Korlovich N., Nir L., Garti N., Phys. rev. E 51 (1995) 378.

[17] Schubel D., Colloid Polym. Sci. 276 (1998) 743.

[18] Senatra D., Gabrielli G., Guarini G.T., Europhys. Lett. 2 (6) (1986) 455.

[19] Garti N., *Thermal behavior of dispersed systems,* Surfactant Science Series vol. 93, Marcel Dekker Inc., New York Basel, 2001.

[20] Koetz J., Kosmella S., Beitz T., Prog. Polym Sci. 26 (8) (2001) 1199.

[21] Liu J., Takisawa N., Kodama H., Shirahama K., Langmuir 14 (1998) 4489.

[22] Hayakawa K., Santerre J.P., Kwak J.C.T., Macromolecules 16 (1983) 1642.

[23] Liu J., Takisawa N., Shirahama K., J. Phys. Chem. 101 (1997) 7520.

[24] Kosmella S., Koetz J., Shirahama K., Liu J., J. Phys. Chem. 102 (1998) 6459.

[25] Magny B., Iliopoulos I., Zana R., Audeberg R., Langmuir 10 (1994) 3180.

[26] Shimizu T., Seki M., Kwak J.C.T., Coll. Surf. 20 (1986) 289.

[27] Goddard E.D., Hannan R.B., J. Coll. Interf. Sci. 55 (1) (1976) 73.

[28] Zimm B.H., Bragg J.K., J. Chem. Phys. 31 (1959) 526.

[29] Satake I., Yang J.T., Biopolymers 15 (11) (1976) 2263.

[30] Schwarz G., Eur. J. Biochem. 12 (1970) 442.

[31] Benrraou M., Zana R., Varoqui R., Pefferkorn E., J. Phys. Chem. 96 (1992) 1468.

[32] Anthony O., Zana R., Langmuir 12 (1996) 1967.

[33] Anthony O., Zana R., Langmuir 12 (1996) 3590.

[34] Söderman O., Walderhaug H., Lindman B., J. Phys. Chem. 89 (1985) 1795.

[35] Shah O., *Micelles, Microemuslions and Monolayers*, Science and Technology, Marcel Dekker Inc., New York Basel, 1998.

[36] Fontell K., Khan A., Lindström B., Maciejewska D., Puang-Ngern S., Colloid Polym. Sci. 269 (1991) 727.

[37] Jahn W., Strey R., J. Phys. Chem. 92 (1988) 2294.

[38] De Gennes P.G., Taupin C., J. Phys. Chem. 86 (1982) 2294.

[39] Huse D., Liebler S., J. Phys. (Paris) 49 (1988) 605.

[40] Andelman D., Cates M.E., Roux D., Safran S.A., J. Phys. Chem. 87 (1987) 7229.

[41] Wennestroem H., Olsson U., Langmuir 9 (1993) 365.

[42] Porte G., Appell J., Bassereau P., Marignan J., J. Phys. (Paris) 50 (1989) 1335.

[43] Hervé P., Roux D., Bellocq A.M., Nallet F., Gulik-Krzywicki T., J. Phys. II 3 (1993) 1255.

[44] Quemada D., Langevin D., J. Theor. Appl. Mechanics Special Issue, 201 (1985).

[45] Gradzielski M., Valiente M., Hoffmann H., Egelhaaf S., J. Colloid Interface Sci. 205 (1998) 149.

[46] Beitz T., Koetz J., Wolf G., Kleinpeter E., Friberg S.E., J. Colloid Int. Sci. 240 (2001) 581.

[47] Krishnan K., Burghardt W.R., Lodge T.P., Bates F.S., Langmuir 18 (2002) 9676.

[48] Jada A., Lang J., Zana R., J. Phys. Chem. 93 (1989) 10.

[49] Cazabat A.M., Chatenay D., Langevin D., Meunier J., Faraday Discuss. Chem. Soc. 76 (1982) 291.

[50] Safran S., Webman I., Grest G.S., Phys. Rev. A 32 (1985) 506.

[51] Suarez M.J., Levy H., Lang J., J. Phys. Chem. 97 (1993) 9808.

[52] Koetz J., Andres S., Kosmella S., Tiersch B., Composite Interfaces 13 (4-6) (2006) 461.

[53] Carnali J.O., Lindman B., Söderman O., Walderhaug H., Langmuir 2 (1986) 51.

[54] Carnali J.O., Ceglie A., Lindman B., Shinoda K., Langmuir 2 (1986) 417.

[55] Mehta S.K., Sharma S., J. Colloid Interface Sci. 296 (2006) 690.

[56] Paul B.K., Mitra R.K., J. Colloid Interface Sci. 295 (2006) 230.

[57] Koetz J., Beitz T., Kosmella S., Tiersch B., Proceedings CESIO 5th World Surfactant Congress Firenze (Italy) vol. 1 (2000) 499-506.

[58] Strauss U.P., Chiao Y., Macromolecules 19 (1986) 355.

4. NANOPARTICLE FORMATION IN PRESENCE OF POLYELECTROLYTES

4.1. Hydrophobically modified poly(acrylates)

The reduction and stabilization of gold colloids by adding hydrophobically modified anionic polyelectrolytes are investigated in much more details in diluted aqueous solutions. The polymers used are derivatives of poly(acrylates) (see Chapter 2.1.). The aim of the study is to show the influence of the degree of substitution on the reduction and stabilization behaviour. However, this opens a way to come to effectively stabilized gold nanoparticles in non-polar solvents.

First of all, the polymers are added at room temperature and the reduction process is investigated over a longer time period (up to 8 days). In comparison, the reduction process is realized at higher temperature, i.e., 100 °C (see protocols in Chapter 5.5.1.).

4.1.1. Formation of gold nanoparticles

After adding the various polymer solutions to the metal precursor, the aqueous solutions are characterized by means of UV-vis spectroscopy to study the direct formation of the gold nanoparticles, which absorb, in dependence on their particle size, between 500 and 600 nm. Figure A13-1 in Appendix 13 shows, e.g., the time dependent absorption spectra of the tetrachloroaureate solution in presence of PA3C4 for the procedure at room temperature. The first absorption peak can be detected after a few hours demonstrating that the reduction process is quite slow at room temperature.

Tables 4.1-1 and 4.1-2 show the results for the gold nanoparticle formation depending on the different polyelectrolytes added, and the procedure employed for the synthesis. Notable features given here are the colour of the solution, the UV-vis absorption maximum, and the particle size determined by dynamic light scattering. Depending on the particle size and the degree of agglomeration, gold nanoparticles can present a wide range of colour from red to blue. For example, monodisperse small gold nanoparticles with a particle size of 18 nm exhibit a red colour. A change of the colour to purple or blue indicates the formation of larger particles and/or aggregation phenomena.

Table 4.1-1. Features of gold nanoparticles obtained by reduction with various polyelectrolytes at room temperature.

			Particle size (nm)
Polymer	λ_{max}[b] (nm)	Colour	DLS [a]
PAA	533	red-pink	19
PA3C4	535	pink	24.5
PA10C4	550-600	purple-blue	130
PA20C4	529	pink	25.5

[a] average value of the main fraction (>95%) obtained by automatic peak analysis by number.

[b] UV-vis absorption wavelength.

Table 4.1-2. Features of gold nanoparticles obtained by reduction with various polyelectrolytes at 100°C.

			Particle size (nm)
Polymer	λ_{max}[b] (nm)	Colour	DLS [a]
PAA	533	purple-pink	37.5
PA3C4	532	purple	18
PA10C4	527	pink	18
PA20C4	528	red-pink	18

[a] average value of the main fraction (100%) obtained by automatic peak analysis by number.

[b] UV-vis absorption wavelength.

In addition, the particles are studied by means of electrophoretic light scattering to measure the electrokinetic potential (zeta potential) at the particle surface. The particles reveal a negative zeta potential of about -30 to -50 mV, according to the polymer used for the reduction. Indeed, the zeta potential depends on the degree of hydrophobicity of the polyanion added. It has to be noted that the lowest value of -50mV is observed for the non modified PAA, as to be expected. One can conclude that the surface charge of the particles is dominated by the adsorption layer of the polymer. This means that the nanoparticles produced are stabilized due to the adsorption of the polyelectrolyte layer.

4.1.1.1. Reduction process realized at room temperature

In the case of the unmodified PAA a red coloured solution is obtained, which is stable over several months. Dynamic light scattering measurements and TEM micrographs (see Table 4.1-1 and Figure 4.1-1) confirm that gold nanoparticles with an average particle size of

19 nm are formed. In this case, the polyelectrolyte adsorbed at the particle surface, stabilizes the nanoparticles against flocculation due to electrostatic repulsion forces. However, in addition to spherical nanoparticles, normally observed by using a fast sodium borohydride reduction, triangular and cylindrical structures are observed (Figure 4.1-1, b). Because of the adsorption of the anionic polyelectrolyte onto the nanoparticles, the morphology of the particles seems to be influenced in a characteristic way. These results suggest a polymer-controlled crystallization during the primary crystallization as well as the superstructure formation process [1, 2].

Figure 4.1-1: Electron micrographs (a and b) and size distribution (DLS) of gold nanoparticles produced at room temperature with PAA.

At low degree of substitution by hydrophobic side chains (PA3C4), the individual nanoparticles start to aggregate, and the colour of the sample changes to pink. Electron micrographs show particle aggregates in the order of about 120 nm, consisting of individual much smaller primary nanoparticles (ca. 20 nm in size), which correlates very well with the mean particle size of 24.5 nm determined by DLS (Table 4.1-1). This behaviour can be explained predominantly by hydrophob-hydrophob interactions, which lead to a partial

aggregation of the individual particles. When the degree of hydrophobicity of the polymer is increased to 10%, a purple-blue coloured dispersion is obtained. The tendency to form aggregates is enhanced and much larger aggregates of about 130 nm are detected by means of dynamic light scattering and transmission electron microscopy.

A further increase of the number of hydrophobic side chains induces the formation of smaller nanoparticles. However, the mean particle size (25.5nm) is somewhat larger in comparison to the unmodified PAA, and the size distribution, too, as to be seen by dynamic light scattering (see Table 4.1-1 and Figure 4.1-2). This increase of the mean particle size correlates with the fusion to some larger tri- or multi-angular gold nanoparticles (compare EM micrograph in Figure 4.1-2, b). The colour of the dispersion is pink again. The particles seem to be once again better stabilized against collision and this behaviour can be explained by an additional steric stabilization effect. Nevertheless, this steric stabilization does not prevent an increase of the polydispersity in comparison to the unmodified PAA.
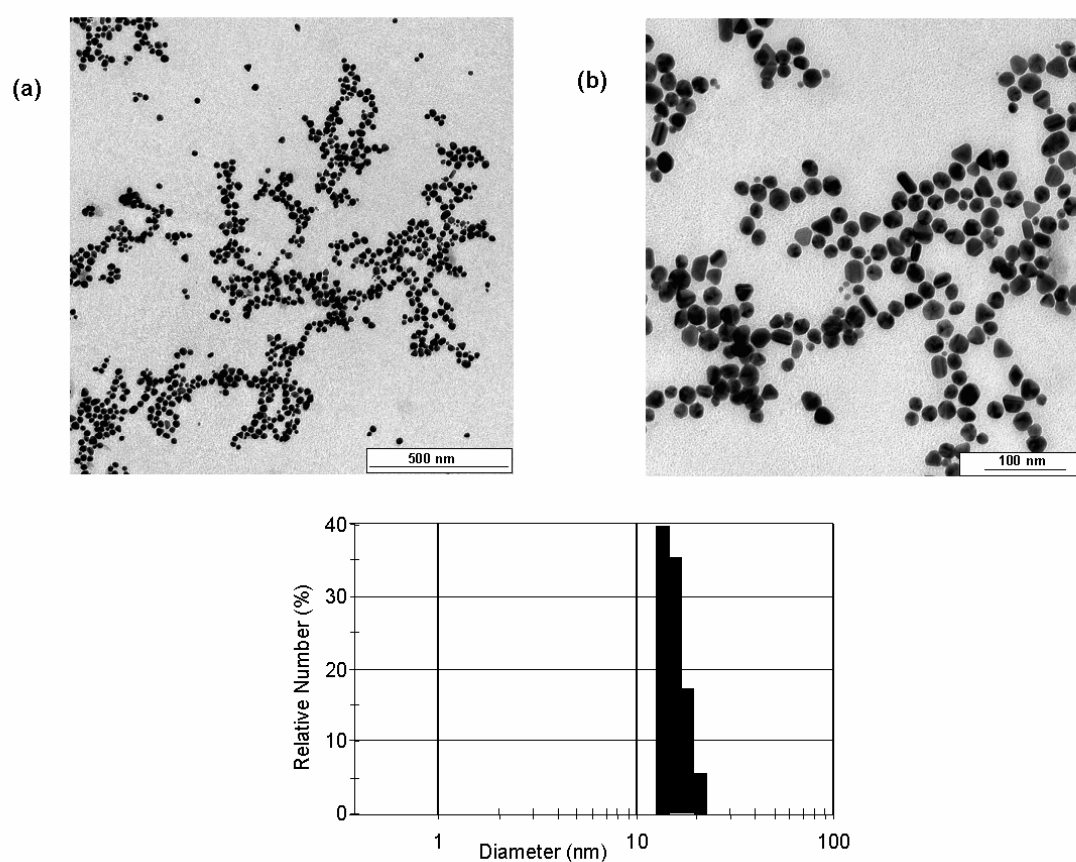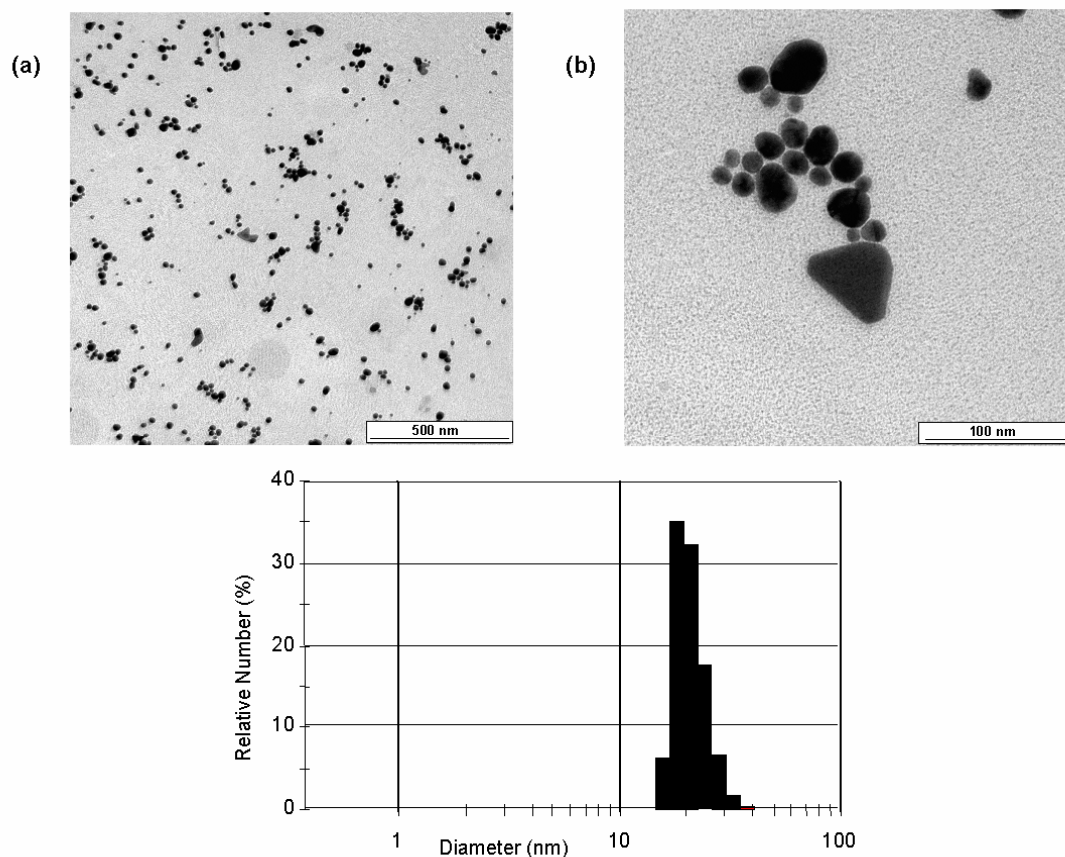

Figure 4.1-2: Electron micrographs (a and b) and size distribution (DLS) of gold nanoparticles produced at room temperature with PA20C4.

It has to be mentioned here that a later heating of the polyelectrolyte-gold dispersions up to 100°C does not change the particle size of the gold nanoparticles, and consequently no colour change can be observed.

4.1.1.2. Reduction process realized at 100°C

By using the unmodified PAA, a purple-pink colour is obtained already after 20 minutes at reflux. The mean particle diameter measured by DLS is 37.5 nm (Table 4.1-2) with a somewhat larger particle distribution (see Figure 4.1-3). In good agreement, the TEM micrograph shows particle aggregate structures between 30 and 50 nm.

When the reaction mixture is heated for a longer time, coagulation occurs (blue colour and precipitation).
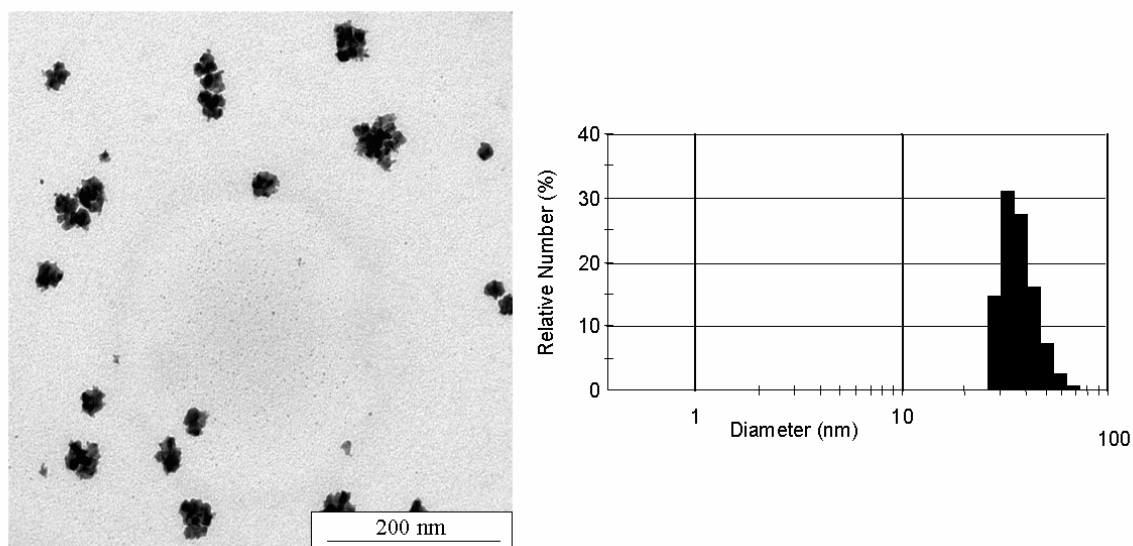
Figure 4.1-3: Electron micrograph and size distribution (DLS) of gold nanoparticles produced at 100°C with PAA.

By using the hydrophobically modified polymers (degree of substitution ≥ 10%), red-pink coloured solutions containing nanoparticles with an average particle size of 18 nm (Table 4.1-2) can be obtained, and visualised by TEM (Figure 4.1-4). Moreover, the nanoparticles formed are stable at 100°C for a longer time and the polydispersity of the nanoparticles formed decreases as visualised on Figure 4.1-4.

It seems to be of interest to note that all the particles obtained are spherical, whatever the polymer used, in contrast to the synthesis at room temperature.
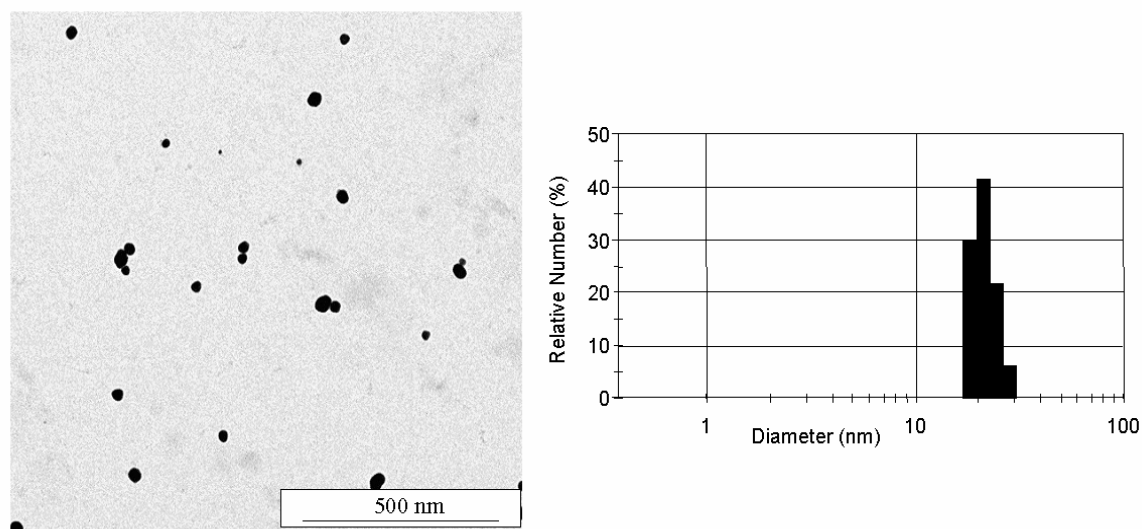
Figure 4.1-4: Electron micrograph and size distribution (DLS) of gold nanoparticles produced at 100°C with PA10C4.

Additional measurements carried out at a higher polymer concentration (polymer:metal = 10:1) show bigger particle dimensions. This means, the particles tend to aggregate at higher polymer concentrations.

4.1.2. Conclusion

It has been confirmed that hydrophobically modified polyelectrolytes can act as both reducing and stabilizing agent for the formation of gold nanoparticles.
One advantage of the method used here is that the reduction can be realized in water at room temperature very slowly or much faster by heating up the system to 100°C. In both cases gold nanoparticles of colloidal dimensions can be produced. However, the size and shape of the individual nanoparticles mainly depends on the polyanion added, and the temperature procedure used.

For the synthesis at room temperature, in presence of polyacrylates a tendency to form triangular or rod-like nanoparticles has to be mentioned. When hydrophobic side chains are incorporated into the polymer chain, the stability of the primary gold nanoparticles can be strongly influenced. In general, the colloidal stability is decreased and aggregation phenomena are observed. However, the most unstable situation is observed at a degree of substitution of 10%. This means at higher degrees of substitution ($\geq$ 20%) the hydrophobic

stabilization effect becomes dominant. This behaviour can be understood with regard to the different types of stabilization which have to be taken into account here. When the degree of substitution is low, at about 3%, the hydrophob-hydrophob interactions can lead to a weak aggregation, in comparison to effects observed by using associating polymers. When the degree of hydrophobic side chains is increased, up to 10%, the flocculation tendency is increased furthermore. However, at about 20% of substitution, the particles are stabilized again due to an additional steric repulsion in combination to the electrostatic repulsion effect. Taken into account that polyelectrolytes with both ionic and hydrophobic groups are well known to form local micelles in water [3-5], the additional steric repulsion can be understood on the basis of the formation of microdomains at the particle surface, as schematised in Figure 4.1-5.
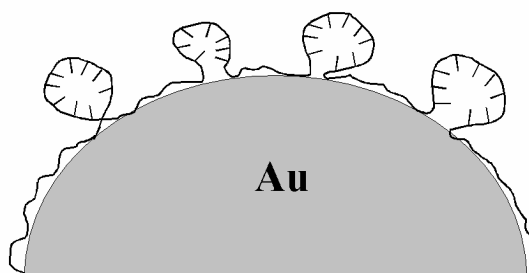
Figure 4.1-5: Model proposed for the formation of hydrophobic microdomains at the surface of the gold nanoparticles.

When the reduction process is realized much more quickly at 100°C, a tendency to form spherical particles is observed, whatever the polymers used. Moreover, the degree of hydrophobic modification of the polymer is of real interest for the stability of the particles. It was observed that with higher degree of substitution ($\geq$ 10%) more stable nanoparticles were formed, due to the combination of an electrostatic with a steric stabilization effect. The quite different temperature dependent flocculation behaviour can be explained by two different types of steric stabilization. In the case of the hydrophobic side chain modified PAA, an entropic repulsion, characterized by a lower flocculation temperature, leads to aggregation phenomena at room temperature, but not yet at 100°C. When PAA is used, an enthalpic repulsion, characterized by an upper flocculation temperature, leads to aggregation phenomena at 100°C, but not yet at room temperature.

Basing on this knowledge it becomes possible to tune first of all the size and shape of the primary nanoparticles by varying the degree of hydrophobic side chains of the polyacrylates as well as the temperature.

4.2. Branched poly(ethyleneimine)

As presented in Chapter 1.4.5., it was recently shown that polyelectrolytes can act as both reducing and stabilizing agents for the formation of gold nanoparticles. Indeed, stable gold particles have successfully been obtained in aqueous systems with linear poly(ethyleneimine) [6], branched poly(ethyleneimine) [7, 8], with polyacrylates [9] (see also Chapter 4.1.) or with pluronics (copolymers with PEO-PPO-PEO blocks) [10], where the polymers can act as reducing agents.

In the following part, the reduction and stabilization of gold colloids by adding commercially available branched poly(ethyleneimine) is investigated for the first time in a microemulsion template phase in comparison to an aqueous solution.

4.2.1. Formation of gold nanoparticles

4.2.1.1. Nanoparticle formation in aqueous phase

First of all, the process of nanoparticle formation is investigated, in the absence of any other reducing agents, in aqueous polymer solution (see protocol of reaction in Chapter 5.5.2.). The compositions of the samples used for the study are summarized in Table 4.2-1.

Table 4.2-1. Compositions and features of the samples A to E, in aqueous phase.

Sample	c_{PEI} (wt%)	c_{HAuCl4} (mmol/L)	r^a	t^b (min)	Colour^c	λ_{max}^d (nm)	D^e (nm)
A	1	2	1:1	30	Red	534	18.9
B	5	2	1:1	20	Strong red	531	19.3
C	10	2	1:1	20	Strong red	529	20.9
D	1	2	1:10	3	Strong red	525	9.1
E	1	20	1:5	2	Brown	/	1300

[a] Mass ratio between the polymer solution and the hydrogen tetrachloroaureate solution.

[b] Time of reaction at 100°C.

[c] Colour of the solution after reaction.

[d] UV-vis absorption wavelength in water.

[e] Mean diameter of the particle calculated by DLS, average value of the main fraction (>99%) obtained by automatic peak analysis by number.

Three different samples A, B and C (see Table 4.2-1) are used in order to check the effect of the PEI-concentration on the reduction process while the metal precursor concentration is kept constant (2 mmol/L) as well as the mass ratio between both solutions (1:1). In comparison, two other mixtures are prepared, where the mass ratio between the polyelectrolyte solution and the metal precursor solution is changed (sample D), as well as the HAuCl$_4$ concentration (sample E).

After adding the PEI solution to the aqueous solution of HAuCl$_4$, the mixture is heated in an oil bath to 100°C. The reaction is stopped then by cooling down the mixture, and the gold particles formed are characterized. Notable features of the nanoparticles obtained are listed in Table 4.2-1: the time of reaction, the colour of the solution, the UV-vis absorption maximum, and the particle size determined by dynamic light scattering.

For samples A to C, red solutions are obtained, which are stable over several months. Dynamic light scattering measurements show that independently of the polymer concentration, gold nanoparticles with an average size of 20 ± 1 nm are formed.
A decrease of the mass ratio between the PEI and HAuCl$_4$ solutions to 1:10, induces the formation of smaller nanoparticles with an average particle size of 9.1 nm as to be seen in Table 4.2-1 for sample D. The colour of the dispersion is red and the UV-vis absorption maximum decreases, confirming the formation of smaller gold nanoparticles. The TEM micrographs (Figure 4.2-1) show nanoparticles of 7.1 ± 2.3 nm, which is in agreement with the average diameter determined by dynamic light scattering.

In addition, sample D is studied by means of electrophoretic light scattering to measure the electrokinetic potential (zeta potential) at the particle surface. The particles reveal a positive zeta potential of $+30 \pm 3$ mV. One can conclude that the surface charge of the particles is dominated by the adsorption layer of the cationic polymer. This confirms that the nanoparticles produced are stabilized by the adsorption of a polyelectrolyte layer.

Finally, it has to be noted that the reaction time necessary for the formation of the gold particles was significantly reduced from 30 min to 3 min by changing the mass ratio between the polymer and the HAuCl$_4$ solutions.
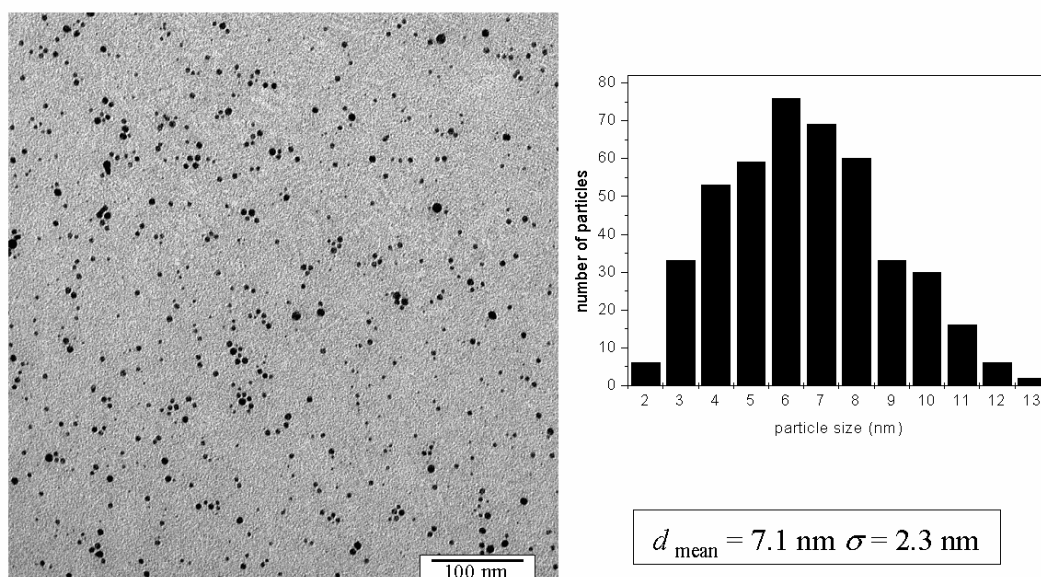
$d_{mean} = 7.1$ nm $\sigma = 2.3$ nm

Figure 4.2-1: Electron micrograph and size distribution (from TEM) of gold nanoparticles produced in aqueous phase from sample D.

A further increase of the metal precursor concentration leads to the aggregation of the gold particles, only a few seconds after their formation. The colour of sample E is brown, and the aggregate size measured by DLS about 1300 nm.

In aqueous solutions, it is noticeable that the reducing polyelectrolyte, which is adsorbed at the particle surface, effectively stabilizes the nanoparticles against aggregation due to electrosterical repulsion forces.

It seems to be also of interest to note that all particles obtained are spherical.

4.2.1.2. Nanoparticle formation in PEI-modified microemulsions

Polyelectrolyte-modified microemulsions are attractive for the nanoparticle formation due to their special features (see Chapter 1.3.4). Indeed, the incorporation of polymers into the L_2 phase can affect the nanoparticle formation process as follows:

- increase of the film stability of the droplets due to polyelectrolyte-surfactant interactions.
- control of the nanoparticle growth process due to polyelectrolyte-nanoparticle interactions.
- stabilization of the nanoparticles formed due to electrosteric stabilization generated by the polyelectrolyte.

In the following part, the interest is focused on the effect of the branched polyelectrolyte PEI concerning the formation of Au nanoparticles in microemulsion in comparison to the diluted aqueous system, in absence of any other reducing agent (see protocol in Chapter 5.5.2.).

Two adequate microemulsions containing respectively PEI and HAuCl$_4$ are mixed together. Due to the spontaneous collision of the microemulsion droplets both components enter in contact, but do not react with each other until the mixture is heated up to 100°C. The mixture is then cooled down, and the colour effect is noticed.

The formation of nanoparticles is investigated at the specific microemulsion composition (SDS/oil/aqueous polymer solution) = (24/56/20). Different polyelectrolyte and metal precursor concentrations are used (samples F and G given in Table 4.2-2).

From the TEM micrographs, the diameters of approximately 200 particles are used to calculate the average particle size (mean diameter, d), and the standard size deviation (σ) of the nanoparticles produced.

Table 4.2-2. Compositions and features of the samples F and G, in microemulsion.

Sample	c $_{PEI}$ (wt%)	c $_{HAuCl4}$ (mmol/L)	r [a]	t [b] (min)	$d_{1\ mean}$ [c] (nm)	σ_1 [d] (nm)	$d_{2\ mean}$ [e] (nm)	σ_2 [f] (nm)
F	1	20	1:20	3	9.4	4.7	/	/
G	5	10	1:5	6	10.6	3.7	8.6	3.5

[a] Mass ratio between the polymer solution and the hydrogen tetrachloroaureate solution.

[b] Time of reaction at 100°C.

[c] Mean diameter of the particle calculated from TEM micrographs in microemulsion.

[d] Standard deviation of the mean particle diameter in microemulsion.

[e] Mean diameter of the particle calculated from TEM micrographs after redispersion in water.

[f] Standard deviation of the mean particle diameter after redispersion in water.

TEM micrographs taken directly from the microemulsion reveal that the nanoparticles formed for sample F (see Figure 4.2-2, a) are spherical, with a size of 9.4 ± 4.7 nm (Table 4.2-2).
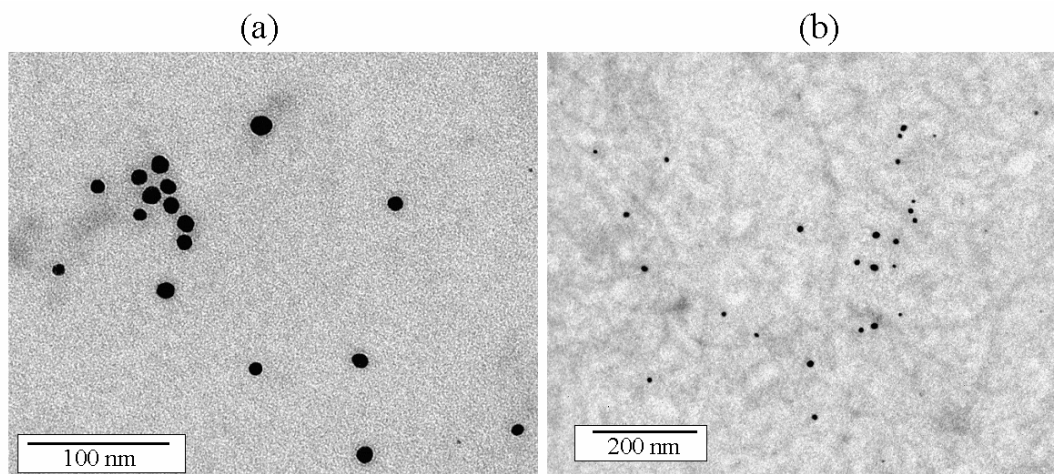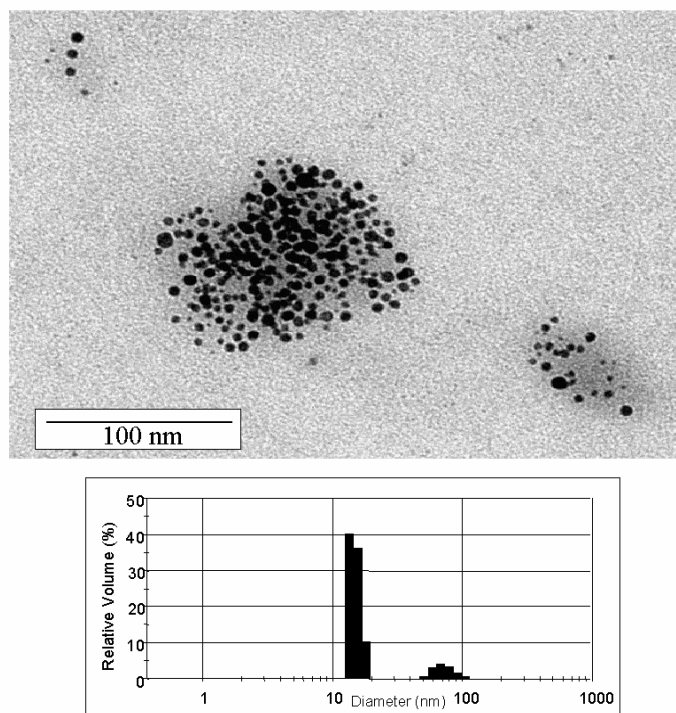
Figure 4.2-2: Electron micrographs of gold nanoparticles in microemulsion for (a) sample F and (b) sample G.

Also, for sample G, spherical gold nanoparticles with average size of 10.6 ± 3.7 nm can be observed (Figure 4.2-2, b). UV-vis measurements of the microemulsions show again a typical absorption peak at 529 nm. One can conclude from the experimental results that the polyelectrolyte PEI can act as reducing and stabilizing agent not only in aqueous phases but also in much more complex systems, e.g., in w/o microemulsion droplets.

In a second step, the microemulsions containing the Au nanoparticles are dried in a vacuum oven at 30°C to remove the solvents. The crystalline powders obtained are then redispersed in water and the resultant solutions are characterized by dynamic light scattering in combination with transmission electron microscopy.

For sample F, nanoparticles of 15 and 80 nm are detected by dynamic light scattering after solvent evaporation and redispersion in water.

The TEM micrograph in Figure 4.2-3 shows particle aggregates consisting of individual, much smaller, primary particles in agreement with the DLS measurements. In this case, one can assume that the polymer concentration is not high enough to prevent an aggregation of the primary formed particles during the drying process.

Figure 4.2-3: Electron micrograph and DLS results of gold nanoparticles of sample F after solvent evaporation and redispersion in water.

When the polymer concentration is increased, the primary particles can be stabilized much better against aggregation as to be seen on the TEM micrograph of sample G (Figure 4.2-4), and spherical gold particles of 8.6 ± 3.5 nm can be redispersed in water.
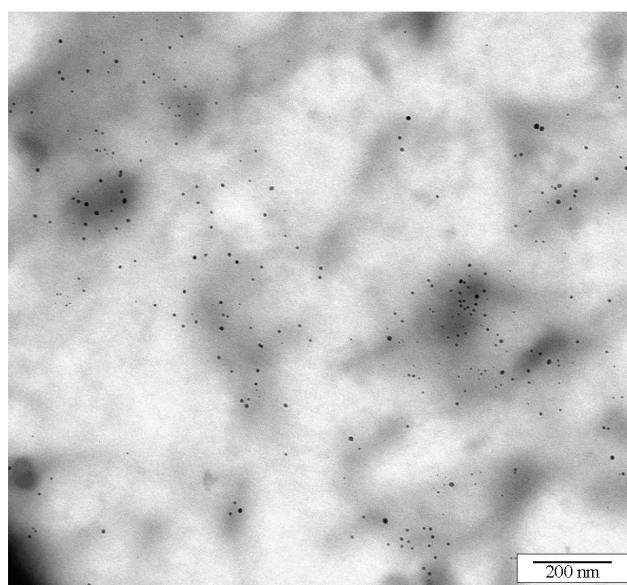
Figure 4.2-4: Electron micrograph of gold nanoparticles of sample G after solvent evaporation and redispersion in water.

It has here to be stated that the particle size of the gold particles can not be decreased furthermore by using the microemulsion template phase.

4.2.1.3. Conclusion

It has been demonstrated that branched poly(ethyleneimine) can act as both reducing and stabilizing agent for the formation of gold nanoparticles.
The advantage of the method used here is that the reduction can be realized by heating up the solution to 100°C in water or in a microemulsion template phase. In both cases, spherical gold nanoparticles of colloidal dimensions below 10 nm can be produced.
For the synthesis in aqueous solution, small gold nanoparticles of 20 nm are obtained and stabilized due to the adsorption of the polyelectrolyte layer on the particle surface, as demonstrating by the zeta potential measurements. A decrease of the mass ratio between the PEI and $HAuCl_4$ solutions induces the formation of smaller nanoparticles with a mean diameter of 7.1 nm $\pm$ 2.3 nm in a significant shorter reaction time (3 min).

In a second step, our investigations have revealed that an optically clear region of the phase diagram in the SDS/toluene-pentanol (1:1)/water system still exists after the incorporation of PEI. In general, the polymer induces a reduction of the area of the isotropic phase. Moreover, concentrated polymer solutions up to 10 wt % can be incorporated in the microemulsion droplets.
The SDS-based microemulsion was successfully used for the Au nanoparticle formation and small particles of 9.4 $\pm$ 4.7 nm were produced inside the droplets. Again the polymer acts as a reducing agent, avoiding the introduction of another salt in the microemulsion, which could destabilizes it. It has to be stated here that the reduction of $HAuCl_4$ in the SDS/xylene-pentanol/water microemulsion by using strong reducing agents (like $NaBH_4$) leads to the formation of large gold aggregates sedimentating immediately.
After solvent evaporation, the particles previously produced can be redispersed in water without a change of their size obtained in the microemulsion, which represents a real advantage. At higher polymer concentrations, aggregation phenomena, occurring during the drying-process, are prevented, and gold nanoparticles of 8.6 $\pm$ 3.5 nm are recovered. The polymer adsorbed at the particle surface can indeed stabilize the particles due to electrosterical stabilization, and prevent their aggregation.
However, the size of the individual nanoparticles could not be drastically influenced by the method used. In both cases, the same particle size range was obtained. One can suppose that

the branched polymer already acts as a "template" during the nucleation process and the formation of the nanoparticles in water as well as in microemulsion. As a consequence, an additional template effect of the microemulsion was not observed.

However, one can assume that the particle dimensions are tuned by varying the molecular parameters (e.g. molar mass and degree of branching) of the PEI used, and further experiments should be focused on these modifications.

4.2.2. Formation of barium sulphate nanoparticles

In the present part, an attempt is made to recover $BaSO_4$ nanoparticles produced in a polyelectrolyte-modified microemulsion consisting of SDS/toluene-pentanol/PEI 20 wt% in water.

Two adequate microemulsions containing respectively $BaCl_2$ and Na_2SO_4 are mixed together (see protocol in Chapter 5.6.), and the process of $BaSO_4$ nanoparticles formation is induced. The formation of nanoparticles is investigated at two different microemulsion compositions listed in Table 4.2-3. Point X belongs to the L_2 phase (inverse microemulsion droplets) of the system, whereas point Y belongs to the bicontinuous channel of the system studied (see Chapter 3.2.).

Table 4.2-3. Composition at point X and Y.

Point	SDS/Oil/PEI (wt %)	Type of microemulsion
X	20/60/20	Water-in-oil
Y	13.2/26.8/60	Bicontinuous

The optically clear resulting solutions are then dried, and the crystalline powders obtained are redispersed in water. The size and shape of the nanoparticles produced are investigated by means of DLS measurements and TEM microscopy.

At point X, small nanoparticles of 17 nm in combination with larger aggregates about 80 nm are measured by DLS. The TEM micrograph in Figure 4.2-5 confirms the previous results and show small quasi-spherical nanoparticles in presence of bigger triangular aggregates.
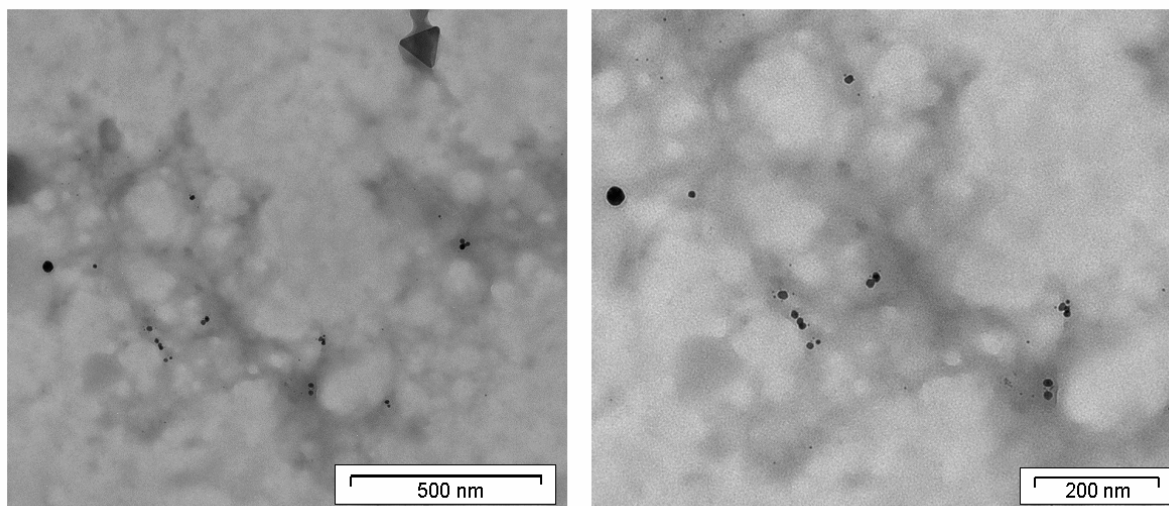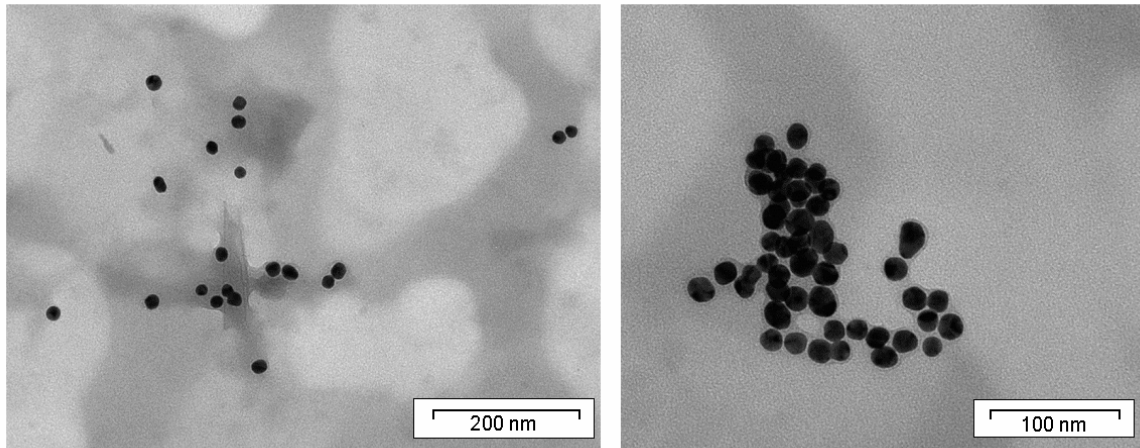
Figure 4.2-5: Electron micrographs of BaSO$_4$ nanoparticles at point X after solvent evaporation and redispersion in water.

In addition, the BaSO$_4$ nanoparticles are studied by means of electrophoretic light scattering to measure the electrokinetic potential (zeta potential) at the particle surface. The particles produced at point X from the polyelectrolyte-modified system reveal a negative zeta potential of about $-$ 60 $\pm$ 4 mV. Hence, the surface charge of the particles is dominated by the adsorption layer of the anionic SDS surfactant. One can conclude that the particles synthesized are stabilized due to electrostatic interactions, but from this experimental results no statement can be made about the adsorption of the polymer.

In the bicontinuous channel, BaSO$_4$ nanoparticles with an average size of 13.6 nm $\pm$ 2.5 nm were detected by DLS. Figure 4.2-6 shows the corresponding EM-micrographs of the dispersion at point Y. From the TEM micrographs, an average particle size of 18.0 nm, and a standard size deviation of 2.5 nm are calculated for the nanoparticles produced, which correlates well with the results obtained by DLS.

The electrokinetic potential at the BaSO$_4$ particle surface is then investigated to obtain more information about the stabilization process in the dispersion.

The particles produced at point Y reveal a negative zeta potential of about $-$ 20 $\pm$ 1 mV. One can here conclude that, in addition to the adsorption of the surfactant layer, the nanoparticles produced are stabilized due to the adsorption of the cationic polymer layer, as to be confirmed by the increase of the zeta potential value.

Figure 4.2-6: Electron micrographs of BaSO$_4$ nanoparticles at point Y after solvent evaporation and redispersion in water.

Finally, one can again suppose that the branched polymer acts as a "template" during the nucleation process, which permits the formation of small BaSO$_4$ particles even in the bicontinuous phase. In this particular case, the template effect of the microemulsion is no more necessary to produce particles on the nanometer scale.

4.3. Hydrophobically modified polyampholytes

4.3.1. Formation of gold nanoparticles

The polyampholytes are studied with regard to their reducing and stabilizing properties for the formation of gold nanoparticles in aqueous system.

For this purpose, PalOc-solutions of different concentration are prepared and mixed in the absence of any other reducing agents with $HAuCl_4$ precursor solutions as summarized in Table 4.3-1.

Table 4.3-1. Compositions and features of the samples A to C, in aqueous phase.

Sample	c $_{PalOc}$	c $_{HAuCl4}$	r [a]	t [b]	Colour [c]	λ_{max} [d]	D [e]
	(wt%)	(mmol/L)		(min)		(nm)	(nm)
A	1	3	1:1	1min 45s	Red	535	14.3 ± 5.0
B	1	10	1:1	3min 45s	Yellow-gold	/	/
C	5	2	1:1	1min 30s	Brown	/	> 1000

[a] Mass ratio between the polymer solution and the hydrogen tetrachloroaureate solution.

[b] Time of reaction at 100°C.

[c] Colour of the solution after reaction.

[d] UV-vis absorption wavelength in water.

[e] Mean diameter of the particle calculated by DLS, average value of the main fraction (>99%) obtained by automatic peak analysis by number.

After heating at 100°C, the solution is cooled down and the colour effect is noted.

Due to the coloration of the solution, one can first conclude that the polyampholyte PalOc can act alone as reducing agent for the formation of gold particles.

For sample A, a red solution is obtained, which is stable over several months. Dynamic light scattering measurements show that gold nanoparticles with an average size of 14.3 nm are formed. However, the deviation of $\pm$ 5.0 nm shows a light polydispersity of the particles produced.

In addition, the TEM micrographs (Figure 4.3-1) show nanoparticles of 25.5 $\pm$ 11.5 nm, which is in agreement with the average diameter determined by dynamic light scattering.
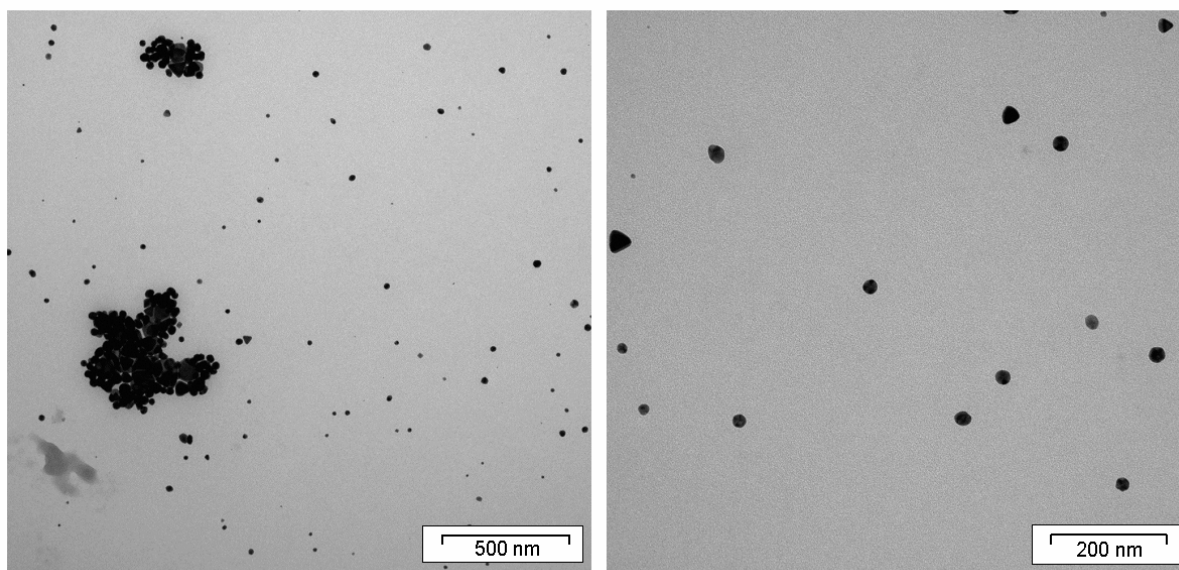
Figure 4.3-1: Electron micrographs of Au nanoparticles for sample A.

Furthermore, sample A is studied by means of electrophoretic light scattering to measure the electrokinetic potential at the particle surface. The particles reveal a positive zeta potential of $+20 \pm 5$ mV. One can assume here that the positively charged part (DADMA monomers) of the copolymer dominates the surface charge of the particles, and one can conclude that the nanoparticles synthesized are stabilized by the adsorption of a polyelectrolyte layer.

Moreover, an increase of the metal precursor concentration leads to an increase of the reaction time and finally to an aggregation and precipitation of the gold particles formed as to be seen in Table 4.3-1. As well, an increase of the polymer concentration leads to the formation of larger aggregates. This result is correlated by the brown colour of the sample after reaction and by an aggregate size superior at 1000 nm measured by DLS.

4.3.2. Formation of barium sulphate nanoparticles

In the following part, the effect of the zwitterionic polyelectrolytes PalH and PalBu, varying in the hydrophobicity, is checked with regard to the formation of $BaSO_4$ nanoparticles in the modified SDS/toluene-pentanol (1:1)/water microemulsions.
For this process, two adequate microemulsions respectively containing $BaCl_2$ and Na_2SO_4 are mixed together (see protocol in Chapter 5.6.). A more detailed description of the $BaSO_4$ particle formation process was previously described in Chapter 1.3.4. [29].

Due to the spontaneous collision of the microemulsions droplets, BaSO$_4$ particles are formed and are directly characterized in solution by dynamic light scattering and after solvent evaporation by transmission electron microscopy. The formation of nanoparticles is investigated for three different microemulsion compositions (points A, B and C; see Table 4.3-2) in the unmodified system as well as in the 10 wt % polyelectrolyte-modified systems.

Table 4.3-2. Composition of the samples A to D.

Sample	SDS/Oil/Water [a] (wt ratio)	Water/SDS (wt ratio, R_w)
A	10/80/10	1
B	15/70/15	1
C	20/60/20	1
D	15/55/30	2

[a] Or aqueous polyampholyte solution.

The dynamic light scattering experimental results reveal that the nanoparticles formed have a very small average size, around 5 nm for points A and B, independent of the system used. For the point C, one can observe smaller BaSO$_4$ particles, around 2 nm in presence of PalH and 3.2 nm in presence of PalBu, in comparison to 3.9 nm observed for the unmodified system (see Table 4.3-3).

Table 4.3-3. Results of dynamic light scattering experiments.

| Samples at point C	Particle size (nm) [a]
Without polymer	
In microemulsion	3.9 (100%)
Redispersed in water	108 (48%) 350 (52%)
10 wt % PalH	
In microemulsion	2.0 (100%)
Redispersed in water	3.9 (94%) 12.2 (6%)
10 wt % PalBu	
In microemulsion	3.2 (100%)
Redispersed in water	3.4 (92%) 10.3 (8%)

[a] Average values obtained by automatic peak analysis by volume.

In a second step, the microemulsions containing the BaSO$_4$ nanoparticles are dried in a vacuum oven at 30°C to remove the solvents. The crystalline powders obtained are then

redispersed in water and the dispersions are characterized again by dynamic light scattering in combination with transmission electron microscopy.

From the unmodified microemulsion, much larger particle aggregates in the order of 100-350 nm are observed. When the samples are filtered with a 200 nm filter, smaller nanoparticles of about 3 nm size can be measured, in addition to bigger aggregates. These results show that the primary particles formed in the microemulsion tend to aggregate during the drying process and are not sufficiently stabilized.

On the other hand, a significant decrease of the particle size can be induced by adding polyelectrolytes to the system. Indeed, in presence of PalH or PalBu, the primary particles do not aggregate during the drying process and small nanoparticles of about 4 nm can be redispersed (Table 4.3-3). In good agreement, the TEM micrographs show small $BaSO_4$ particles with an average particle size of 5 nm, obtained in the PalH-modified system (Figure 4.3-2 (a)) and in the PalBu-modified system (Figure 4.3-2 (b)).
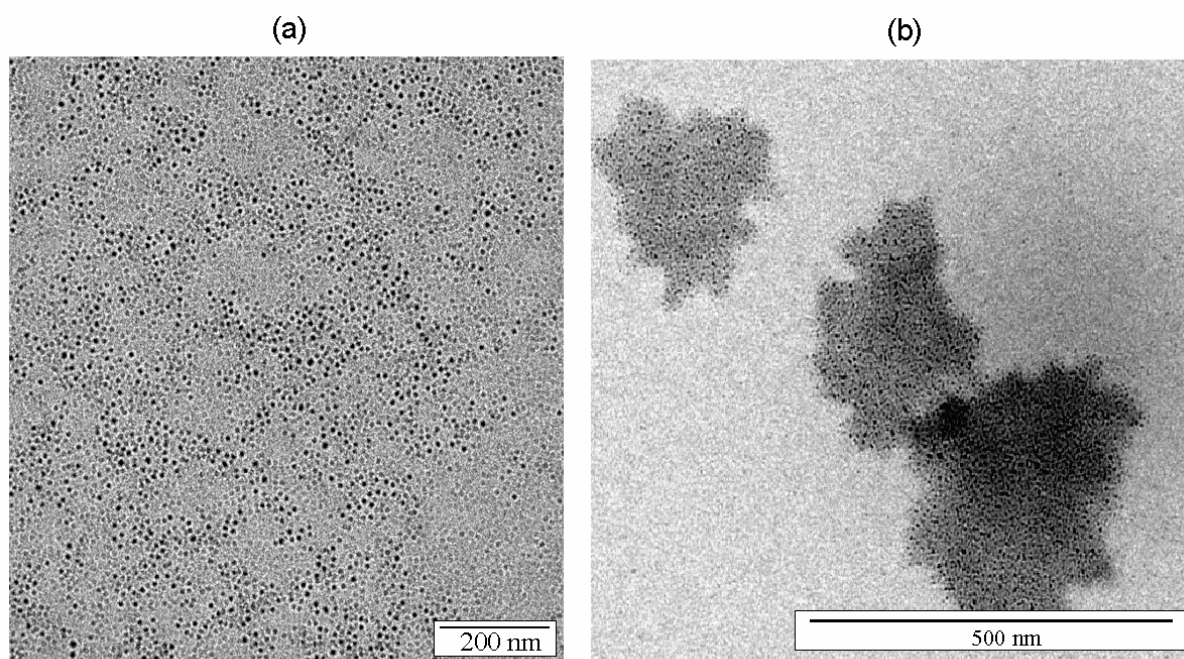
Figure 4.3-2: Electron micrographs of the water redispersed $BaSO_4$ with (a) 10 wt% PalH and (b) 10 wt% PalBu.

In presence of polymers, aggregation phenomena, induced during the drying-process, are well prevented, and monodisperse $BaSO_4$ nanoparticles with an average size of 5 nm are obtained. The copolymers are indeed involved in the nanoparticles formation by increasing the film stability of the microemulsion droplets due to polyelectrolyte-surfactant interactions, and by stabilizing the particles due to electrosteric stabilization, thus preventing their aggregation.

104

However, there is no significant difference between the two polymers studied here with regard to their stabilizing properties.

In addition, the $BaSO_4$ nanoparticles are studied by means of electrophoretic light scattering to measure the electrokinetic potential at the particle surface. The particles obtained from the unmodified system reveal a negative zeta potential of about − 43 mV. Hence, the surface charge of the particles is dominated by the adsorption layer of the anionic surfactant.
The results obtained for the PalH-modified-particles show a higher zeta potential of about − 32 mV. In this case, one can assume that the polymer, adsorbed at the particle surface, decreases the negative potential of the particles surface. Concerning the copolymer PalBu, the same conclusion can be made from an experimental zeta potential of − 37 mV.
This means, the nanoparticles produced are stabilized due to the adsorption of the polyampholyte.

4.4.   References

[1] Limin Q., Cölfen H., Antonietti M., Angew. Chem. Int. Ed 39 (3) (2000) 604.

[2] Shu-Hong Y., Cölfen H., Antonietti M., Adv. Mater. 15 (2) (2003) 133.

[3] Dubin P.L., *Microdomains in polymer solutions*, Plenum Press, New York, 1985.

[4] Laschewski A., Adv. Polym. Sci. 124 (1995) 1.

[5] Koetz J., Kosmella S., Beitz T., Prog. Polym. Sci. 26 (2001) 1199.

[6] Sun X., Dong S., Wang E., Polymer 45 (2004) 2181.

[7] Wang S., Yan J., Chen L., Mater. Lett. 59 (2005) 1383.

[8] Sun X., Dong S., Wang E., J. Colloid Interface Sci. 288 (2005) 301.

[9] Hussain I., Brust M., Papworth A.J., Cooper A.I., Langmuir 19 (2003) 4831.

[10] Sakai T., Alexandridis P., Langmuir 208 (2004) 426.

[11] Wilcoxon J.P., Martin J.E., Parsapour F., Wiedenman B., Kelley D.F., J. Chem. Phys. 108 (21) (1998) 9137.

5.   EXPERIMENTAL PART

5.1.   Analytical methods

^{1}H NMR measurements were carried out using a Bruker AMX-300 spectrometer operating at a proton resonance frequency of 300 MHz. For the characterization of polymers 128 scans were preferred.

IR-spectra were taken from KBr pellets with a Bruker IFS FT-IR spectrometer 66/s.

Elemental analysis was realized by using an EA 1110 (CHNS-O) elemental analyser from CE Instruments.

UV-vis experiments were performed with a Cary 5000 UV-vis NIR spectrophotometer (Varian). Quartz cuvettes with a path length of 1 cm were used.

Transmission electron microscopy (TEM) micrographs of the nanoparticles were recorded on an EM 902 microscope from Zeiss. Samples were prepared by dropping a small amount of the microemulsion, or the redispersed nanoparticle-solutions, on copper grids, dried and examined in the transmission electron microscope at an acceleration voltage of 90 kV.

Cryo-high resolution scanning electron microscopy (Cryo-SEM) micrographs of the microemulsions were examined with a S-4800 microscope from Hitachi. Each sample was cooled by plunging into nitrogen slush at atmospheric pressure. Afterward, the samples were freeze-fractured at -180°C, etched for 60 seconds at -98°C and sputtered with Platinum in the GATAN Alto 2500 Cryo-preparation chamber and then transferred into the Cryo-FE-SEM.

Differential scanning calorimetry (DSC) measurements were carried out with a Setaram Micro-DSC III at a temperature range between −20 and +80°C. The heating and cooling rates were fixed to 0.3 K/min. After cooling, the sample was kept frozen at −20°C for 5h before the heating program started. The differential scanning calorimetric curves were repeated several times.

<u>Principle and theory of DSC [1]</u>:

"Thermal analysis" refers to the group of methods in which some physical properties of a sample are continuously measured as a function of temperature while the sample is subjected to heating or cooling at a controlled rate.

In thermal analysis, measurements of energy changes form the basis of differential scanning calorimetry. The sample (*S*) and the reference (*R*) materials are provided with their own separate furnaces as well as with their own separate temperature sensors. The sample and the reference are maintained at identical temperatures by controlling the rate at which heat is transferred to them (see Figure 5.1-1 (a)).
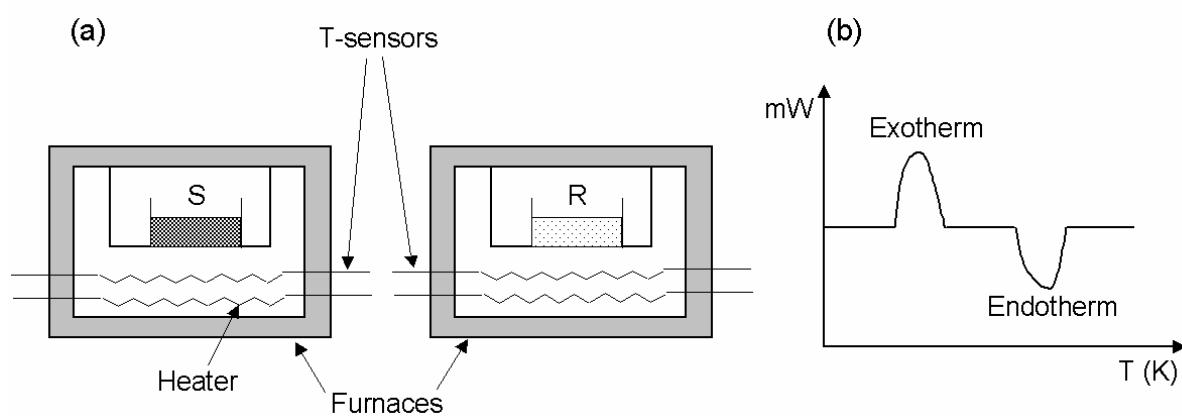
Figure 5.1-1: (a) Instrumental set-up for DSC, S-sample and R-reference.

(b) Typical DSC recording.

DSC experiments measure directly the energy that has to be applied to keep the temperature the same, that energy being the amount of heat that must be supplied during an endothermic process ($\Delta H < 0$), or subtracted during an exothermic process ($\Delta H > 0$). If $\Delta H > 0$, the sample heater is energized and a corresponding signal is obtained; if $\Delta H < 0$, the reference heater is energized in order to compensate for the temperature difference between the furnace of the sample and that of the reference.

Since the energy inputs are proportional to the magnitude of the thermal energies involved in the transition, the records give the calorimetric measurements directly (see Figure 5.1-1 (b)).

Dynamic light scattering (DLS) was used to determine the particle size and particle size distribution of the nanoparticles produced. Measurements were carried out at 25°C at a fixed angle of 173° ("backscattering detection") by using a Nano Zetasizer 3600 (Malvern)

equipped with a He-Ne laser (λ= 633nm; 4 mW) and a digital autocorrelator. For all samples, the results were calculated using the multi-modal distribution mode, and 10 runs of 20 seconds were performed.

The following refractive indices were used: $n^{\text{water}} = 1.33$ and $n^{\text{toluene-pentanol (1:1)}} = 1.449$. The following solvent viscosities were taken (in cP at 25°C): $\mu^{\text{water}} = 0.89$ and $\mu^{\text{toluene-pentanol (1:1)}} = 1.029$. For the measurements, the samples were placed in a glass cuvette.

Principle and theory of DLS [2]:

If a small particle is illuminated by a source of light such as a laser, the particle will scatter the light in all directions. Dynamic light scattering, also known as PCS -Photon Correlation Spectroscopy-, measures the fluctuations of the scattering intensity of particles due to their Brownian motion and correlates them by means of an intensity-time autocorrelator. The correlator compares the scattering intensity at successive small time intervals to derivate the rate at which the intensity is varying. The intensity-time autocorrelation function $g_2(h, t)$ is than calculated as follows:

$$g_2(h,t) = \frac{\langle I(t) \cdot I(t+\tau) \rangle}{\langle I(t) \rangle^2}$$

where h is the magnitude of the scattering vector:

$$h = \frac{4\pi n}{\lambda_0} \sin \frac{\Theta}{2}$$

with n the refractive index of the medium and Θ the scattering angle.

From $g_2(h, t)$, one can derive the correlation function of the electric field $g_1(h, t)$:

$$g_1(h,t) = \sqrt{\frac{g_2(h,t) - \langle I(t) \rangle^2}{\langle I(t) \rangle^2}}$$

Moreover, $g_1(h, t)$ is the Fourier transformation of a space-time correlation function and after mathematical transformation of $g_1(h, t)$, one obtains the relation:

$$g_1(h,t) = Be^{-Dh^2 t}$$

With the assumption of hard spherical particles, the hydrodynamic radius of the scattering object (R_h) can be calculated from the diffusion coefficient (D) according to the Stokes-Einstein equation:

$$D = \frac{kT}{6\pi\eta R_h}$$

with k the Boltzmann constant, η the viscosity of the solvent.

Electrophoretic light scattering was used for detecting the surface charge of the nanoparticles. This technique allows therefore the determination of the zeta potential of the nanoparticles at the effective shear plane between the moveable and non-moveable part of the double layer. Measurements were carried out with a Nano Zetasizer 3600 (Malvern).

Principle and theory of Zeta potential [3]:

The presence of a charge at a particle surface affects the distribution of ions in the surrounding interfacial region, resulting in the formation of the so called electrical double layer close to the surface.

The liquid layer surrounding the particle exists as two parts; an inner region, called the Stern layer, where the ions are strongly bound and an outer, diffuse, region where they are less firmly attached. When a particle moves, ions within the boundary move with it. This boundary is called the surface of hydrodynamic shear or slipping plane and the potential at this boundary is known as the zeta potential (ξ) (see Figure 5.1-2).
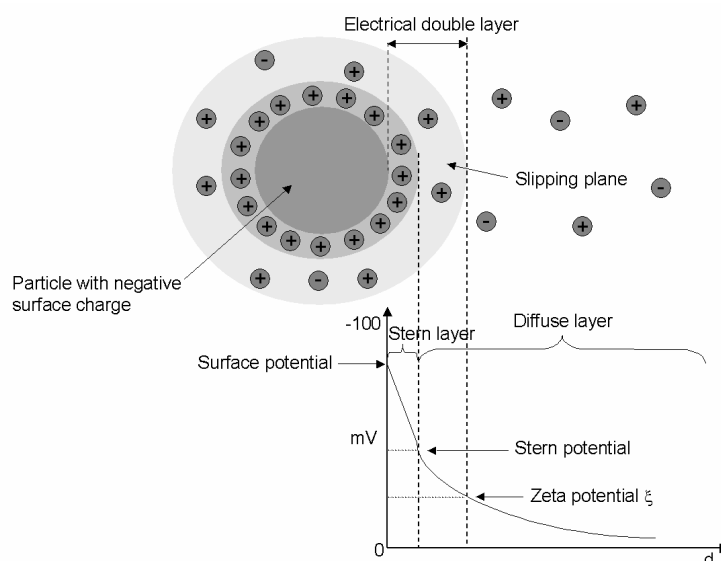
Figure 5.1-2: Representation of the electrical double layer of a negative charged particle.

When an electrical field is applied across an electrolyte, charged particles suspended in the electrolyte are attracted toward the electrode of opposite charge. When equilibrium is reached, the particles move with constant velocity. The velocity of a particle in an electric field is commonly referred to as its electrophoretic mobility (*m*) and is given by the **Henry equation**:

$$m = \frac{2\varepsilon}{3\eta} \xi \cdot f(ka)$$

with ε the dielectric constant, η the viscosity of the medium and *f(ka)* the Henry's function. For particles of smaller dimension in comparison of its electrical double layer *f(ka)* is **1.0**, and is referred to as the **Hückel** approximation. For particles of larger dimension in comparison of its electrical double layer, f(ka) becomes **1.5**, and is referred to as the **Smoluchowski** approximation.

The technique to measure the particle electrophoretic mobility in Malvern's Zetasizer Nano instruments is the Laser Doppler Velocimetry. The receiving optics is focused so as to relay the scattering of particles in the cell. The light scattered at an angle of 17° is combined with the reference beam. This produces a fluctuating intensity signal where the rate of fluctuation is proportional to the speed of the particles.

Conductivity measurements were performed with a LF 2000 micro-processor conductometer from WTW. Electrical conductivity measurements in microemulsion were carried out by starting from different surfactant/oil ratios ω, and by adding water (or the aqueous polymer solution) along the dilution line.

Analytical Ultracentrifugation was used to determine the molecular weights of polymers from evaluation of the sedimentation velocity data. The instrument employed was a Beckman XL-I Analytical Ultracentrifuge with absorbance and interference optics. For evaluation of the raw data, the data evaluation software Sedfit was used.

Rheology measurements were carried out with a dynamic stress rheometer DSR 200 (Rheometrics).

<u>Principle and theory</u> [4]:

Rotation rheometers are available in different geometries. For the rheological characterization of microemulsions, the choice of the rheometer was focused on a concentric cylinder rheometer composed of an outer cup with the radius r_o and an inner cylinder with the radius r_i. The flow of the fluid is confined between the concentric cylinders with the inner cylinder rotating at Ω (SEARLE type) as shown on Figure 5.1-4.
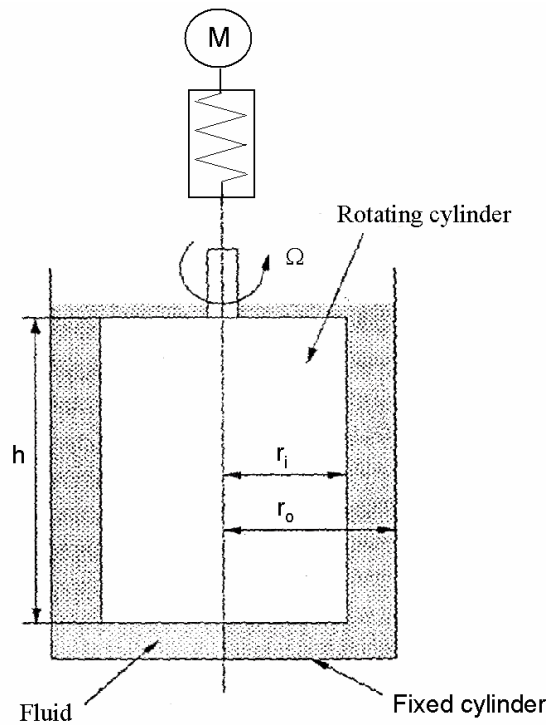

Figure 5.1-4: Schematic representation of a concentric cylinder rheometer (SEARLE type).

Working equations relating the shear stress (τ) to torque measurements (*M*), and the shear rate ($\dot{\gamma}$) to angular velocity (Ω) are given below:

$$\tau = \frac{M}{2\pi r_i r_o h}$$

$$\text{and } \dot{\gamma} = \frac{2r_i r_o}{r_o^2 - r_i^2} \Omega$$

The shear viscosity (η) is then calculated from the relation $\eta = \tau / \dot{\gamma}$ and is expressed as follows:

$$\eta = \frac{\left(r_o^2 - r_i^2\right)}{4\pi h r_o^2 r_i^2} \frac{M}{\Omega}$$

112

Figure 5.1-5 illustrates typical Newtonian, shear-thickening and shear-thinning flow behaviours, which can be found for different systems.
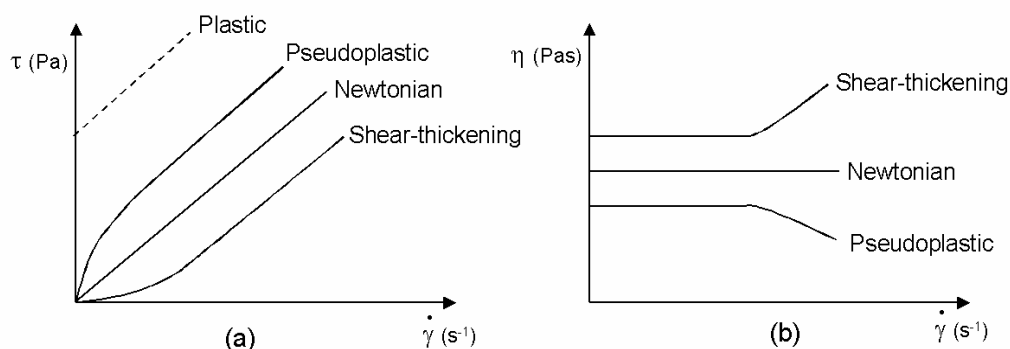
Figure 5.1-5: (a) Flow curves and (b) corresponding shear viscosity curves.

Capillary viscosity measurements, to determine the intrinsic viscosity $[\eta]$ of polymer solutions, were performed with an Ubbelohde capillary (type 53110 /I). Automatic measurements are possible due to a chronometer and a detector system (with photoelectric cells) linked to the viscometer. For each polymer, 15 mL of a 20g/L concentrated polymer solution were inserted in the tank of the capillary. Automatic dilution is possible with a dilution accuracy of 0.05%. The system is permanently maintained at 30°C in a thermostated bath and the polymer solution is homogenized under stirring in the capillary for about 5 min before measurement.

Potentiometric titrations were carried out by using a pH glass electrode. To determine their acidity constants (pK_a^0), the polyanions (salt form) (0.1 wt %) were first changed to their acid form by using an ion exchanger and were then titrated with sodium hydroxide (0.1 N).

A surfactant-selective solid-state membrane electrode was used to determine by means of potentiometry the binding isotherms to CTAB for each poly(acrylic acid). The ionic surfactant specific electrode, with a poly(vinyl chloride) membrane, was purchased from Metrohm Ion analysis. Before use, the surfactant electrode has to be conditioned with the surfactant used for the next potentiometric measurement.
25 mL of the polyelectrolyte solution (0.2 mmol ionic groups pro litre) were titrated with the surfactant solution (30 mM) under stirring. The experiments were carried out at 35°C to work with homogeneous solutions above the CTAB Krafft point. The titration was performed at a speed of 10 mL/hour so that steady-state conditions are realized.

5.2.   Chemicals

Water was purified with the Modulab PureOne water purification system (Continental).

Poly(acrylic acid) sodium salt (PAA) was purchased from Fluka: the average molecular weight given by the producer was 5,100 g/mol. In order to obtain a pure PAA in the acidic form, the commercial sample was purified by ultrafiltration and turned into its acid form with a cation exchanger obtained from Merck.

The branched Poly(ethyleneimine) (PEI) is a commercial product (Polymin P, BASF-Ludwigshafen) with $M_n = 35,000$ g/mol, $M_w = 600,000$ g/mol, demonstrating a broad size distribution, with $M_w/M_n \approx 17$. The highly branched polymer prepared by cationic polymerisation of ethyleneimine, contains primary, secondary, and tertiary amino groups in the approximate ratio 1:2:1. The branching distribution yields presumably spheroid-shaped molecules with an radius of gyration of about 45 nm [5].

Barium chloride ($BaCl_2$), sodium sulphate (Na_2SO_4) and aniline (99+%) were purchased from Merck-VWR.

Methanol (99+%), n-butylamine (99+%), n-octylamine (99+%), 1-methyl-2-pyrrolidone (NMP), dicyclohexylcarbodiimine (CDI), pentanol (99+%), toluene (99+%), sodium hydroxyde (0.1 N), maleic anhydride (99+%), cetyltrimethylammonium bromide (CTAB) (99+%), sodium dodecylsulphate (SDS) (99+%), and 3-(N,N-dimethyldodecylammonio) propanesulphonate [sulphobetaine (SB) 97+%] were obtained from Fluka and were used without further purification.

The metal precursor hydrogen tetrachloroaureate $HAuCl_4$, the sodium borohydride $NaBH_4$, the N,N'-diallyl-N,N'-dimethylammonium chloride (65 wt% in water) and the maleamic acid were purchased from Sigma-Aldrich and used as received.

5.3. Synthesis of hydrophobically modified poly(acrylates)

Procedure:

The PAA (acid form, M_w=5,100 g/mol) is dissolved (for 3 hours) in 1-methyl-2-pyrrolidone (NMP) at 60°C, in a three-neck flask fitted with a condenser, a thermometer, and a magnetic stirrer. Butylamine and N-N'-dicyclohexylcarbodiimide (CDI) (dissolved in NMP) are successively introduced into the PAA solution under vigorous stirring. The temperature is maintained at 60°C and the reaction mixture is stirred for approximately 24 hours in the dark. The system is then cooled down to room temperature, the dicyclohexylurea crystals formed are eliminated by filtration and the polymer is precipitated in its sodium salt form by dropwise addition of a concentrated (40% by volume) NaOH solution. The precipitate is washed by hot (60°C) NMP three times, and three times with cold methanol by vacuum filtration. The crude product is dissolved in water, precipitated in methanol (2 times) and finally freeze-dried.

Note, that the polymers formed are referred as follows: the polymers named PA3C4, PA10C4 and PA20C4 are a PAA respectively modified by 3, 10, or 20% of butylamine along the polymer backbone.

5.4. Synthesis of hydrophobically modified polyampholytes

5.4.1. Monomer synthesis

N-n-butylmaleamic acid.

1 mole of maleic anhydride is dissolved in 100 mL toluene in a three-neck flask fitted with a condenser, and a magnetic stirrer and heated to 80°C. 1 mole n-butylamine in 70 mL toluene is added dropwise to the solution under stirring and the reaction mixture was heated at 80°C for 3 hours. After cooling down the solution, a white precipitate is observed. The product is then filtered off, washed with toluene and twice recrystallized in a methanol-water (1:1) mixture (50g/100 mL). The yield of the reaction is 55%.

^{1}H NMR (300 MHz in DMSO-d$_6$, δ in ppm): 0.9 (t, 3H); 1.3 (sextet, 2H); 1.45 (quintet, 2H); 3.15 (quart, 2H); 6.25 (d, 1H); 6.4 (d, 1H); 9.1(s, 1H).

Elemental analysis. Calculated (C$_8$H$_{13}$NO$_3$): C 56.13%; H 7.65%; N 8.18%. Found: C 55.81%; H 8.21%; N 8.18%.

N-n-octylmaleamic acid.

1 mole of maleic anhydride is dissolved in 100 mL toluene in a three-neck flask fitted with a condenser, and a magnetic stirrer and heated to 80°C. 1 mole n-octylamine in 120 mL toluene is added dropwise to the solution under stirring and the reaction mixture was heated at 80°C for 3 hours. After cooling down the solution, a white precipitate is observed. The product is then filtered off, washed with toluene and twice recrystallized in methanol (60g/100 mL). The yield of the reaction is 86%.

^{1}H NMR (300 MHz in DMSO-d$_6$, δ in ppm): 0.9 (t, 3H); 1.3 (sextet, 10H); 1.45 (quintet, 2H); 3.15 (quart, 2H); 6.25 (d, 1H); 6.4 (d, 1H); 9.15 (s, 1H).

Elemental analysis. Calculated (C$_{12}$H$_{21}$NO$_3$): C 63.41%; H 9.31%; N 6.16%. Found: C 63.16%; H 10.24%; N 6.14%.

N-phenylmaleamic acid.

1 mole of maleic anhydride is dissolved in 100 mL toluene in a three-neck flask fitted with a condenser, and a magnetic stirrer and heated to 80°C. 1 mole aniline in 100 mL toluene

is added dropwise to the solution under stirring and the phenylmaleamic acid precipitates immediately as a light-yellow powder. After complete addition, the reaction mixture was heated at 80°C for 3 hours. After cooling down, the product is filtered off, washed with toluene and twice recrystallized in ethanol (2g/100 mL). The yield of the reaction is 75%.

^{1}H NMR (300 MHz in DMSO-d_6, δ in ppm): 6.3 (d, 1H); 6.45 (d, 1H); 7.1 (t, 1H); 7.35 (t, 2H); 7.65 (d, 2H); 10.4 (s, 1H); 13.15 (s, 1H).

Elemental analysis. Calculated ($C_{10}H9NO_3$): C 62.82%; H 4.75%; N 7.33%. Found: C 62.77%; H 4.88%; N 7.31%.

5.4.2. Polymer synthesis

A free radical polymerisation is carried out with the aqueous solutions of the monomers, at pH 8.5 adjusted by using sodium hydroxide and at 60°C for a period of 16 hours. The reaction is realized in a nitrogen atmosphere and with the 4,4'-azobis-(4-cyano-pentanoic acid) (V501, Wako) as initiator (concentration 0.02 mol/L).

The polymer obtained is then purified by ultrafiltration and freeze-dried.

Poly-(N,N'-dially-N,N'-dimethylammonium-alt-maleamic carboxylate), **PalH**.

Yield of the reaction: 38%.

^{1}H NMR (300 MHz, D_2O, δ in ppm): 1.0–2.9 (8H, -CH-, -CH_2-); 3.0–3.5 (6H, N-CH_3-); 3.6–3.9 (4H, N-CH_2-).

Elemental analysis (in %): Calculated ($C_{12}H_{20}N_2O_3$): C 59.98; H 8.39; N 11.66. Found: C 55.75; H 9.55; N 10.23.

Poly-(N,N'-dially-N,N'-dimethylammonium-alt-N-n-butyl-maleamic carboxylate), **PalBu**.

Yield of the reaction: 40%.

^{1}H NMR (300 MHz, D_2O, δ in ppm): 0.8–4.0 (27H, -CH-, -CH_2-, -CH_3).

Elemental analysis (in %): Calculated ($C_{16}H_{28}N_2O_3$): C 64.84; H 9.52; N 9.45. Found: C 60.20; H 10.62; N 8.71.

Poly-(N,N'-dially-N,N'-dimethylammonium-alt-N-n-octyl-maleamic carboxylate), **PalOc**.

Yield of the reaction: 38.2%.

^{1}H NMR (300 MHz, D$_2$O, δ in ppm): 0.8–4.0 (35H, -CH-, -CH$_2$-, -CH$_3$).

Elemental analysis (in %): Calculated (C$_{20}$H$_{36}$N$_2$O$_3$): C 68.14; H 10.29; N 7.95. Found: C 59.47; H 12.46; N 6.84.

Poly-(N,N'-dially-N,N'-dimethylammonium-alt-N-phenyl-maleamic carboxylate), **PalPh**.

Yield of the reaction: 31.5%.

^{1}H NMR (300 MHz, D$_2$O, δ in ppm): 0.6–3.9 (18H, -CH-, -CH$_2$-, -CH$_3$); 6.9–7.6 (5H, H$_{arom}$).

Elemental analysis (in %): Calculated (C$_{18}$H$_{24}$N$_2$O$_3$): C 68.33; H 7.66; N 8.85. Found: C 62.56 ; H 10.05; N 8.08.

5.5. Microemulsion phase diagrams

The isotropic phase was determined optically by titration of the oil-alcohol/surfactant mixture with water or the corresponding aqueous polymer solution at room temperature (22°C). At first, a mixture of the surfactant, oil, alcohol and water (or the aqueous polymer solution) was stirred or treated in an ultrasonic bath until the system became optically clear. The isotropy of the mixture was optically checked with the help of two crossed TECH SPEC linear polarizing films (Edmund Industry Optik GmbH). The area of the isotropic phase was determined by the dropwise addition of water (or the aqueous polymer solution) to the system. After addition of each drop, the mixture was left in a thermostated bath to guarantee steady-state conditions.

5.6. Formation of gold nanoparticles

5.6.1. Preparation of colloidal gold with poly(acrylates)

Aqueous solutions of polyelectrolyte (1% by weight) were prepared, and stirred 24 hours before use. An aqueous tetrachloroaureate precursor solution (2×10^{-3} M) was also prepared.
Each polymer solution was mixed with the metal precursor solution in a molar ratio of polymer:metal = 3:1 at room temperature. In addition measurements at a polymer:metal ratio 10:1 were carried out, too.
UV-vis spectra were taken immediately after mixing, and from time to time up to 8 days.

In addition, the experiments were carried out under heating conditions. The $HAuCl_4$ solution (2×10^{-3} M) was refluxed for 10 min, and a warm (55-60°C) aqueous solution of polyelectrolyte (molar ratio of polymer:metal = 3:1) was quickly added. Reflux was purchased 15-20 min and the colour effect was noted.

5.6.2. Preparation of colloidal gold with poly(ethyleneimine)

Nanoparticle formation in aqueous solution:

Aqueous solutions of PEI (1, 5 and 10% by weight) were prepared, and stirred 24 hours before use. Aqueous tetrachloroaureate precursor solutions (2, 10 and 20 mM) were also prepared.

The polymer solutions were mixed with the metal precursor solutions in different molar ratio at room temperature. The mixtures were then heated up to 100°C and colour effects were noted.

Nanoparticle formation in microemulsion:

Two adequate microemulsions containing $HAuCl_4$ and PEI respectively, were mixed together. After shaking over 2 minutes, the resulting microemulsion was heated up to 100°C. After cooling down to room temperature, the colour was noted. Afterwards, the mixture was dried in a vacuum oven at 30°C for 48h to remove the solvents (water, toluene and pentanol). The remaining crystalline powder was redispersed in water (0.5 wt %) under ultrasonic treatment and filtered with a 200 nm filter.

5.7. Formation of barium sulphate nanoparticles

Two separately prepared microemulsions containing 10 mmol/L of $BaCl_2$ and 10 mmol/L of Na_2SO_4 respectively, were mixed together. After shaking, $BaSO_4$ nanoparticles were formed spontaneously in the inverse microemulsion droplets. Afterwards the mixture was dried in a vacuum oven at a temperature of 30°C for 48h to remove the solvents (water, toluene and pentanol). The remaining powder was redispersed in water (0.5 wt%) under ultrasonic treatment.

5.8. References

[1] Garti N., *Thermal Behavior of Dispersed systems*, vol. 93, Marcel Dekker, Inc, New York, Basel, 2001.

[2] Hunter R.J., *Foundations of Colloid Science*, vol. I and II, Clarendon Press, Oxford, 1989.

[3] Tadros Th.F., *Solid/Liquid Dispersions*, Academic Press Inc, London, 1987.

[4] Macosko C.W., *Rheology, Principles, Measurements and Applications*, VCH, NY, 1994.

[5] Dautzenberg D., Jaeger W., Koetz J., Philipp B., Seidel Ch., Stscherbina D. *Polyelectrolyte-Formation, Characterization and Application*, Carl Hanser Verlag, NY, 1994.

6.   GENERAL CONCLUSIONS

Hydrophobically modified poly(sodium acrylates) and a new class of hydrophobically modified polyampholytes were synthesized in the present work. On the one hand, the degree of substitution of the polymer was varied from 3 to 20% (hydrophobically modified polyacrylates. On the other hand, the length and/or the type of the hydrophobic side chain was modified (butyl-, octyl-, or -phenyl chains attached at the repetition unit of a polyampholyte). Finally, the type of charge carried by the chosen polyelectrolytes (anionic, cationic or zwitterionic) is of crucial interest as the polymers synthesized are brought to interact afterwards with different surfactant systems.

In order to study and compare the influence of a cationic polymer, a commercial branched poly(ethyleneimine) was used, too.

This work regroups several results concerning the incorporation of the previously mentioned polyelectrolytes into microemulsion systems consisting of a surfactant, a toluene-pentanol (1:1) oil mixture and an aqueous phase. Depending on the type of polymer, as well as on the type of surfactant used, the presence of the polymer can have a drastic influence on the droplet size, the droplet-droplet interactions, and/or the stability of the surfactant film by the formation of polymer-surfactant complexes. Therefore, the incorporation of a polymer into a microemulsion system usually leads to a modification of the area and properties of the different isotropic phases initially present in this system.

For instance, with increasing hydrophobicity of the polyacrylates, the charged polymers induce a clear diminution of the water solubilization capacity of a CTAB-based microemulsion at a polymer concentration of only 1 weight %. However, titration experiments with a surfactant selective electrode showed that the cooperativity of the interactions between the hydrophobic-modified polyelectrolyte and the surfactant molecules is decreased due to the formation of microdomains. Basing on this knowledge, the decrease of the area of the L_2-phase with increasing hydrophobicity of the PAA becomes plausible due to the precipitation of more hydrophobic polyelectrolyte-surfactant complexes.

Concerning the cationic branched poly(ethyleneimine), its influence was studied on the phase behaviour of a SDS-based microemulsion system. The isotropic microemulsions still exist when water is replaced by aqueous solutions of PEI (up to 30% in weight), but their stability is also significantly influenced. From a polymer concentration of 20 weight %, the polymer enhances the solubilization of water in oil, changes the sign of the spontaneous curvature of

121

the surfactant film and induces an inversion of the microemulsion type from water-in-oil (L_2) to oil-in-water (L_1), by the formation of a bicontinuous channel. Further investigations show that the addition of polymer in the L_2 phase influences the rheological properties of the system and changes the droplet-droplet interactions from attractive to repulsive as conductivity drops and percolation disappears.

Finally, the different hydrophobically modified polyampholytes were incorporated into a SDS-based microemulsion. In general, it can be concluded that the incorporation of the polymers leads to a more or less strong increase of the water solubilization capacity of the inverse microemulsion droplets depending on the type of hydrophobic group carried by the polymer chains. It was also demonstrated that the polymers, interacting with the surfactant film, lead to an increase of the droplet-droplet interactions and hence to an increase of the shear viscosity in the system. Concerning the polymer bearing small hydrophobic side chains (butyl group) along the copolymer backbone, the formation of a bicontinuous channel can be detected when the temperature arises 40°C. This phenomenon can be explained by additional hydrophob-hydrophob interactions affecting the surfactant film stability and increasing the solubilization capacity of the microemulsion droplets, and finally changing the spontaneous curvature of the surfactant film to zero.

In addition, these polymers can be successfully used as stabilizing and/or in particular cases as reducing agents for the formation of nanoparticles in different media: in the polymer-modified microemulsions where the droplets play the role of nanoreactors, or in water.

Thus, the modified poly(sodium acrylates) were successfully used for the controlled single-step synthesis and stabilization of gold nanoparticles in water. Under optimised conditions, nanoparticles with an average size around 18 nm were produced. It was established that the polyelectrolytes were involved into the crystallization process of the nanoparticles, and in the presence of hydrophobic microdomains at the particle surface a better stabilization at higher temperatures was observed.

In the same way, the branched poly(ethyleneimine) was used as reducing and stabilizing agent for the formation of gold nanoparticles. On the one hand, it was shown that the cationic polyelectrolyte acts in water as a reducing and stabilizing agent to produce gold nanoparticles via a nucleation process, with at least an average diameter of 7 nm. On the other hand, it was demonstrated that the polymer acts also as reducing and stabilizing agent in much more complex systems, i.e. in water-in-oil (w/o) microemulsion droplets. The polymer, incorporated into the droplets, exhibits reducing properties, adsorbs on the surface of the

nanoparticles and prevents their aggregation. Consequently, nanoparticles around 9 nm can be redispersed after solvent evaporation without a change of their size. Nevertheless, the polymer acts already as a "template" during the formation of the nanoparticles in water and in microemulsion, so that an additional template effect of the microemulsion was not observed.

Barium sulphate nanoparticles with an average size of 14 nm were also prepared from the PEI-modified microemulsion. Again, one can suppose that the branched polymer acts as a "template" during the nucleation process, which permits the formation of small BaSO$_4$ particles even in the bicontinuous phase.

Finally, the reverse microemulsion droplets modified by the polyampholytes were used as a template for the synthesis of BaSO$_4$ nanoparticles. The polymers, which are involved in the redispersion process, influence again the size and the stability of the nanoparticles formed by preventing their aggregation, and monodisperse BaSO$_4$ nanoparticles with an average size of 5 nm were recovered.

Moreover, it was established that the modified polyampholytes can also act as reducing and stabilizing agents for the formation of gold nanoparticles in water, and particles around 14 nm were produced in presence of the octyl-modified polymer.

To conclude, polymer-modified microemulsions present an undeniable interest as nanoreactors for the synthesis of nanoparticles as demonstrated in this work. By modifying the polymer properties (structure, charge, hydrophobicity…etc) it becomes possible to act on the properties of the isotropic microemulsion itself and to make it suitable for the synthesis of nanoparticles. Finally, the presence of the polymer represents a real advantage to tune the size and under certain conditions the shape of the nanoparticles produced, and to recover them from the microemulsion without a change of their size.

However, it was also demonstrated that in the case of gold an easier way for the production of nanoparticles can be found by using directly the polyelectrolytes as reducing and stabilizing agents, and then avoiding the introduction of still more components in the system used.

Therefore, further research activities should be purchased in the next future on the synthesis of well defined hydrophobically modified polyelectrolytes, especially polyampholytes, to open a door towards new fields of application.

APPENDIX 1: Characterization of the hydrophobically modified poly(sodium acrylates)
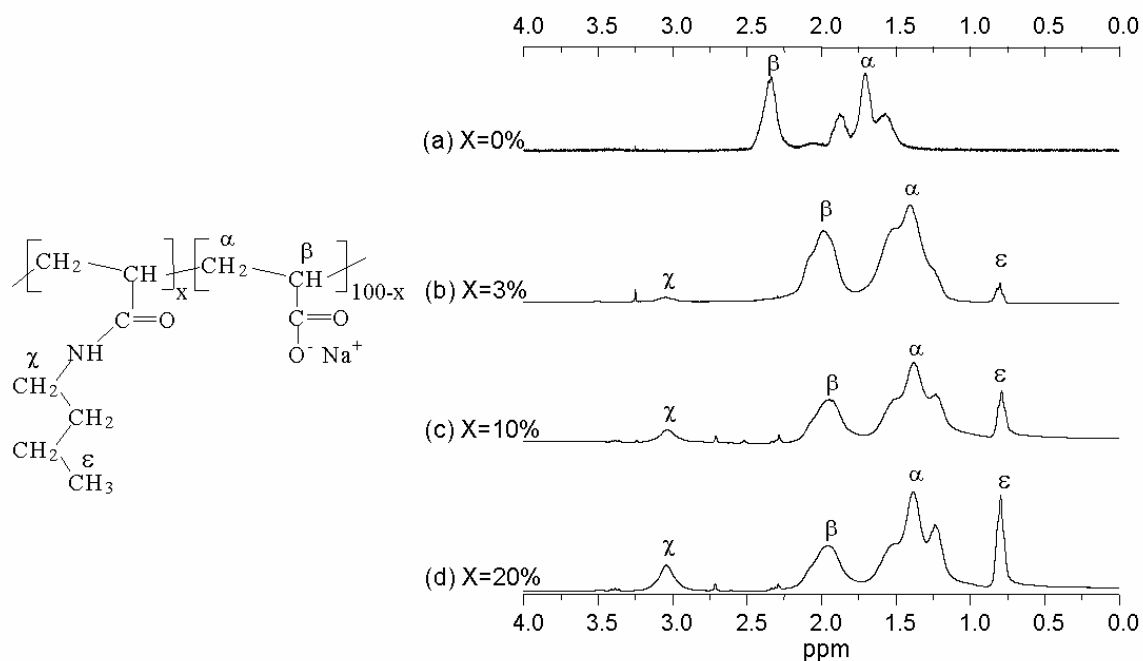
Figure A1-1: ^{1}H NMR spectra in D$_2$O of (a) PAA in comparison to PAA derivatives [(b) PA3C4; (c) PA10C4; (d) PA20C4].
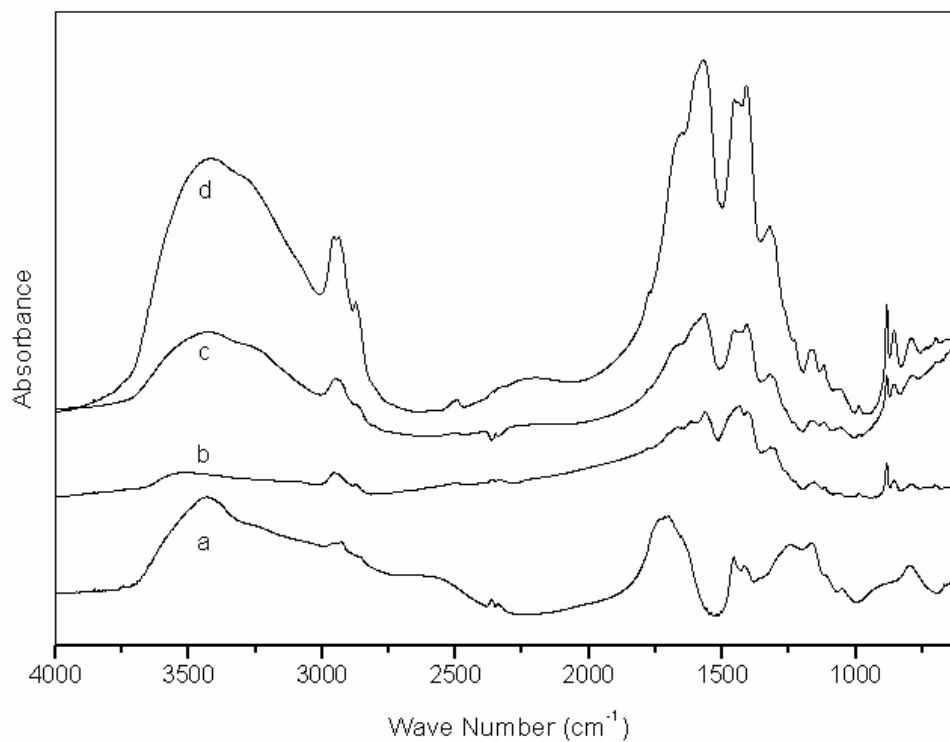
Figure A1-2: FTIR spectra of (a) PAA in comparison to the PAA derivatives [(b) PA3C4; (c) PA10C4; (d) PA20C4].
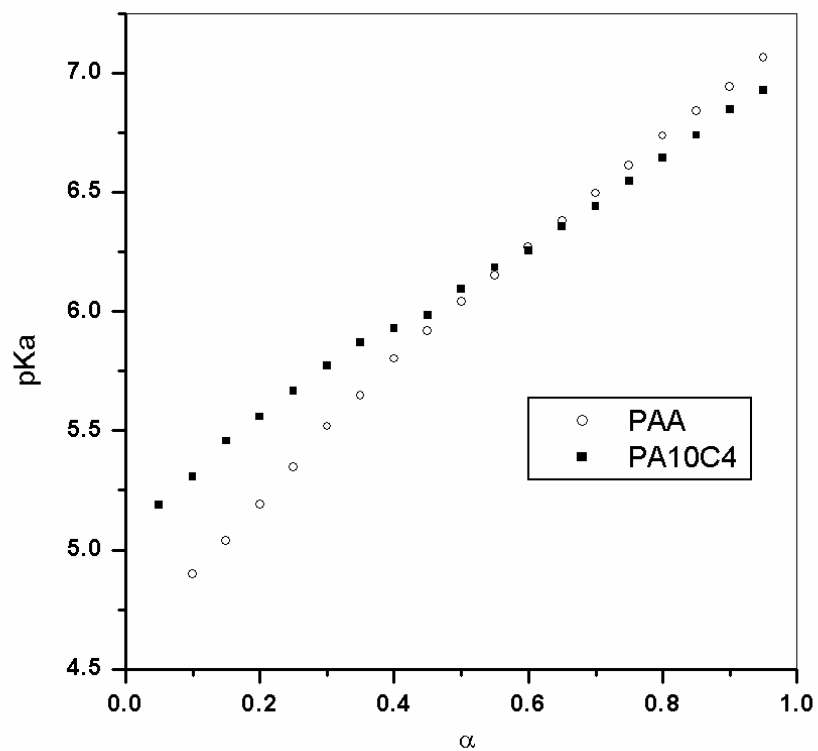
Figure A1-3: Potentiometric titration of (○) PAA and (■) PA10C4 in water.
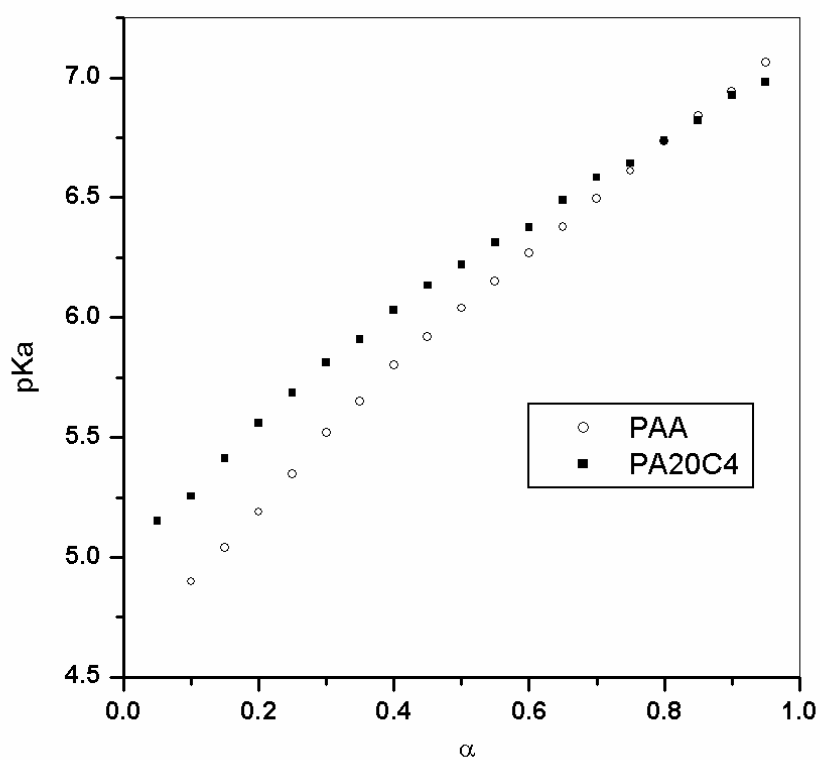
Figure A1-4: Potentiometric titration of (○) PAA and (■) PA20C4 in water.

APPENDIX 2: Determination of the weight molar masses of the polyampholytes by Analytical Ultracentrifugation

Fraction A: 7,889 Da; 23%
Fraction B: 18,502 Da; 75%
Fraction C: 85,898 Da; 2%

For the evaluation, the following values were used
Partial specific volume : 0.732mL/g)
Buffer density : 1.366 g/mL)
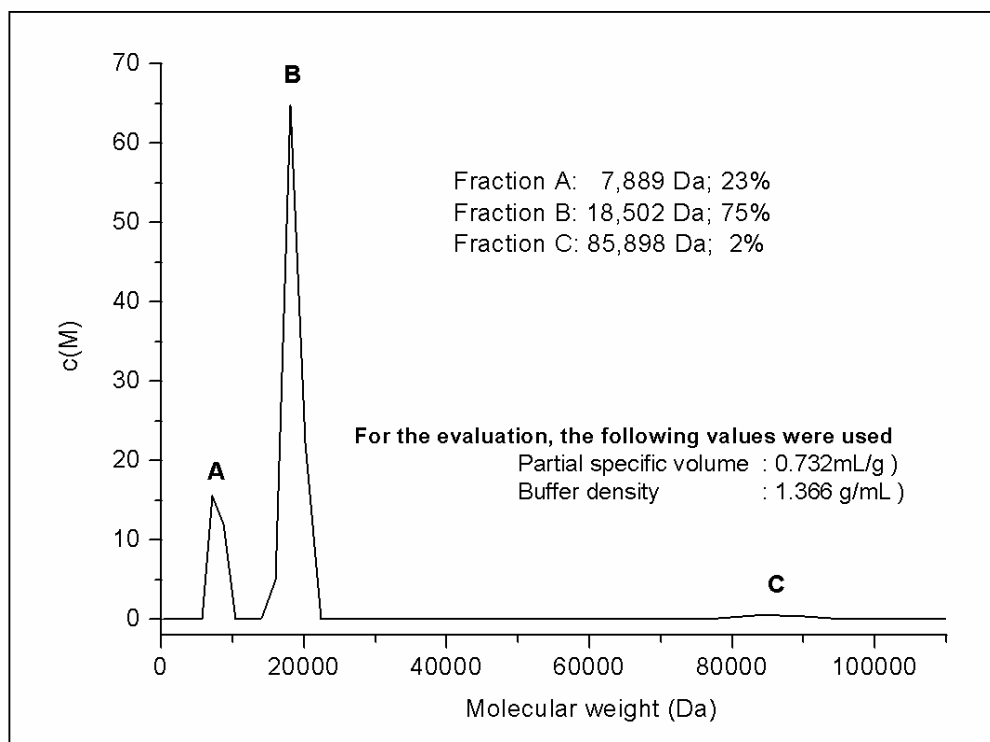
Figure A2-1: Weight molar masses distribution from the sedimentation velocity experiments for the polymer PalH.

Fraction A: 4,599Da; 25%
Fraction B: 12,188Da; 63%
Fraction C: 49,169Da; 12%

For the evaluation, the following values were used
Partial specific volume : 0.794mL/g)
Solution density : 1.260 g/mL)
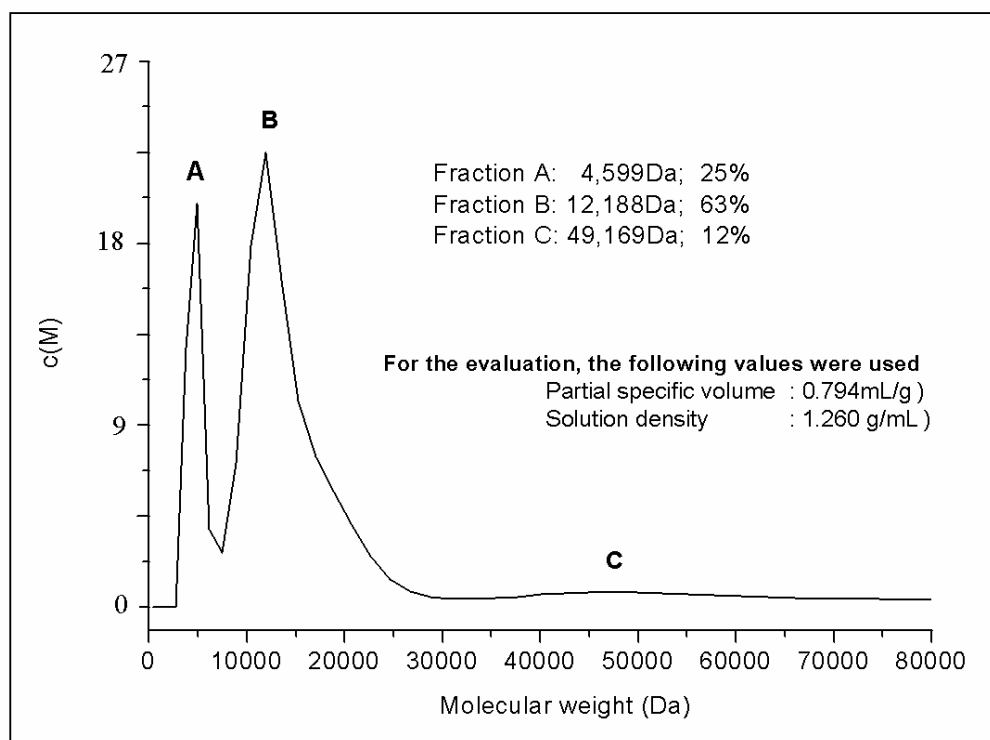
Figure A2-2: Weight molar masses distribution from the sedimentation velocity experiments for the polymer PalBu.
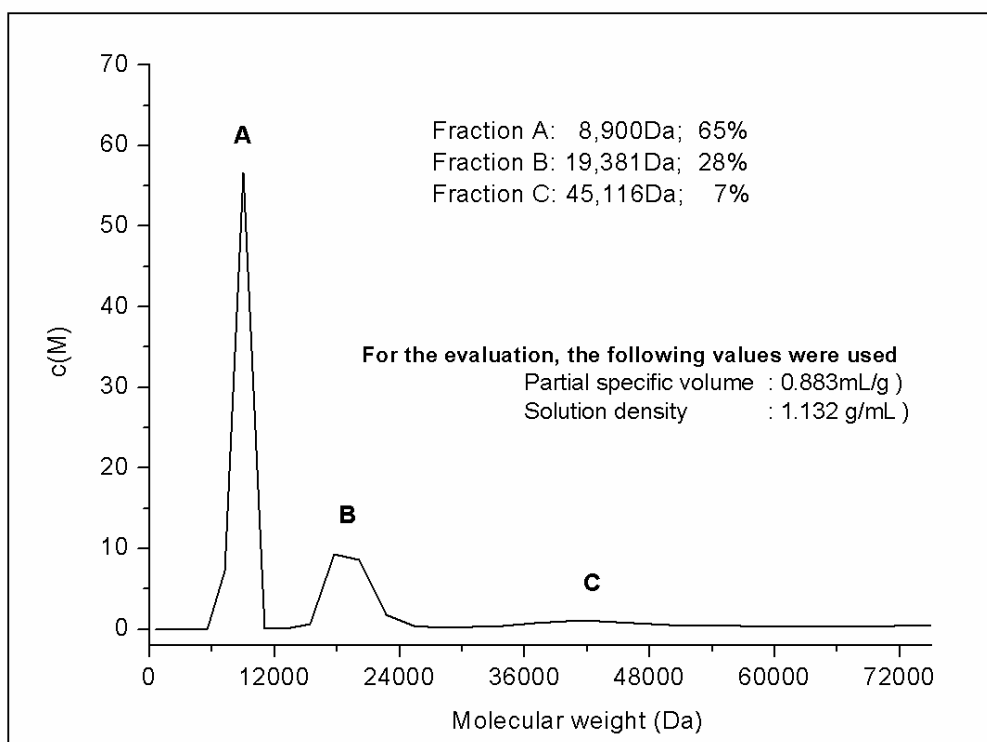
Figure A2-3: Weight molar masses distribution from the sedimentation velocity experiments for the polymer PalOc.
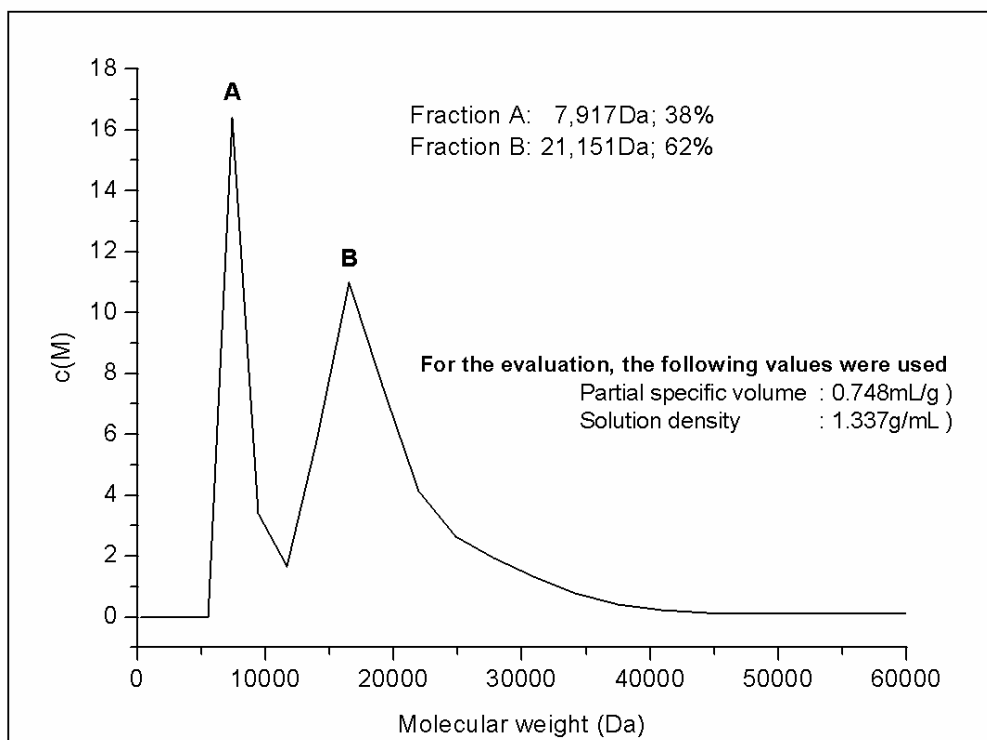
Figure A2-4: Weight molar masses distribution from the sedimentation velocity experiments for the polymer PalPh.

APPENDIX 3: Characterization of the non modified CTAB/toluene-pentanol (1:1)/water microemulsion
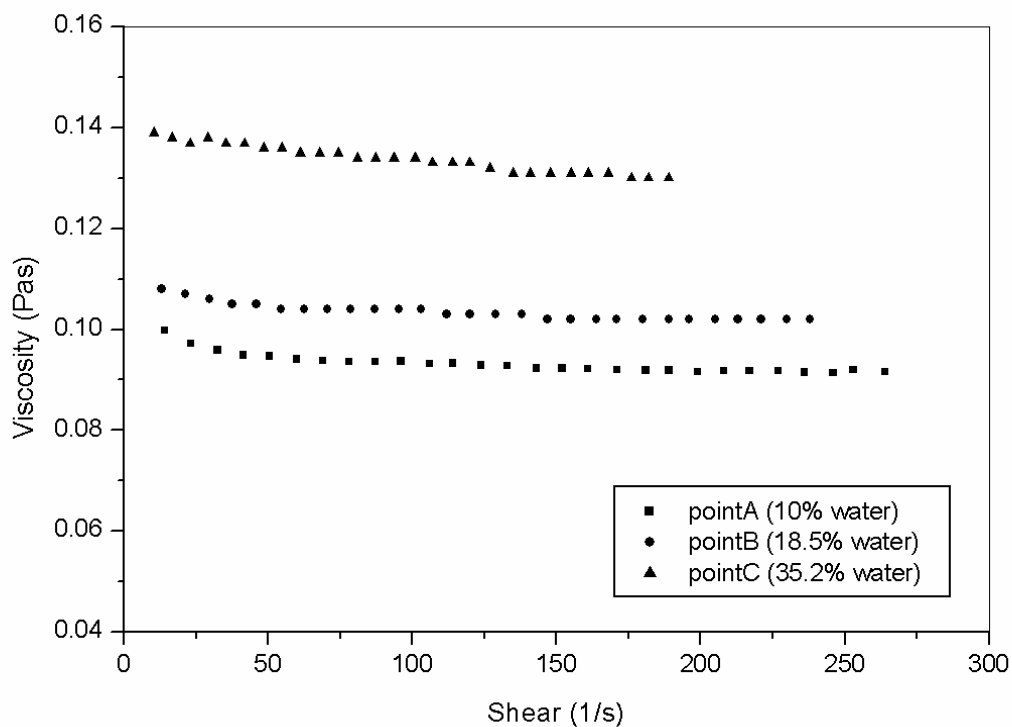
Figure A3-1: Viscosity measurements in the CTAB/toluene-pentanol (1:1)/water inverse microemulsion at different water contents.
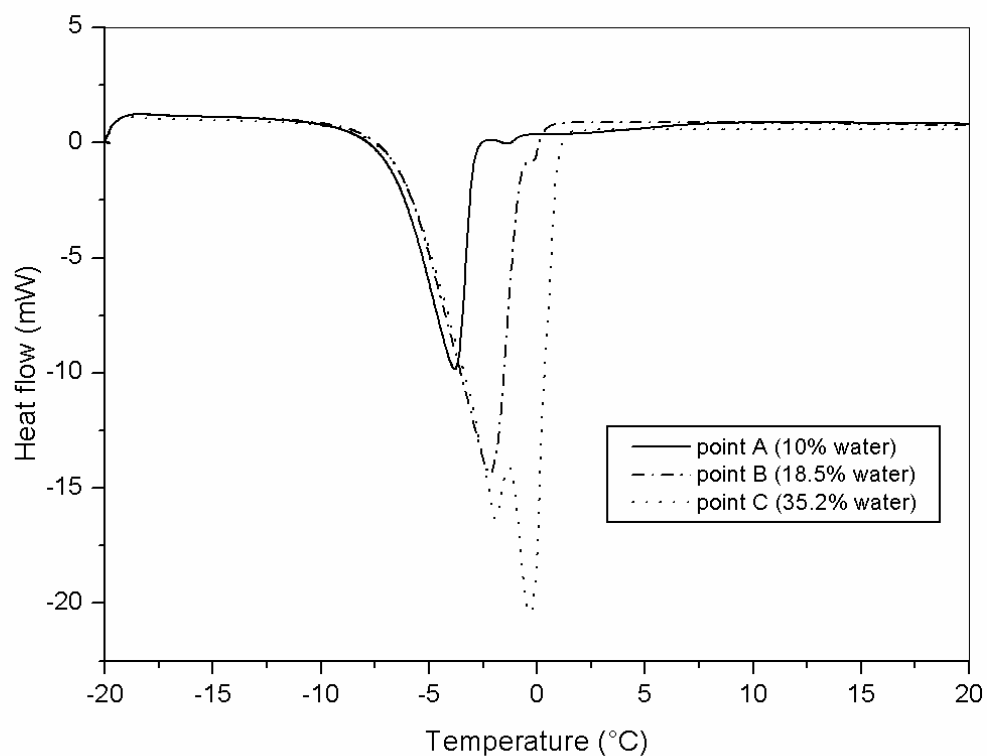
Figure A3-2: DSC heating curves of the CTAB/toluene-pentanol (1:1)/water inverse microemulsion at differentl water contents.

APPENDIX 4: Influence of branched-PEI in different microemulsion systems
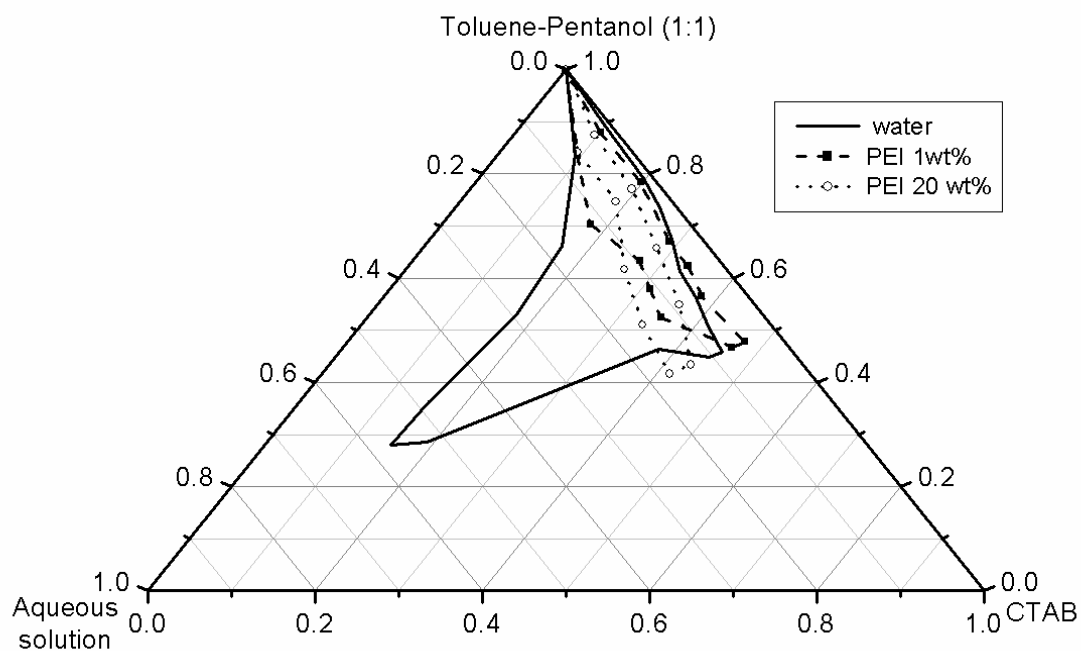
Figure A4-1: Partial phase diagrams of the quasi ternary system CTAB/toluene-pentanol (1:1)/water in presence of different PEI concentrations.
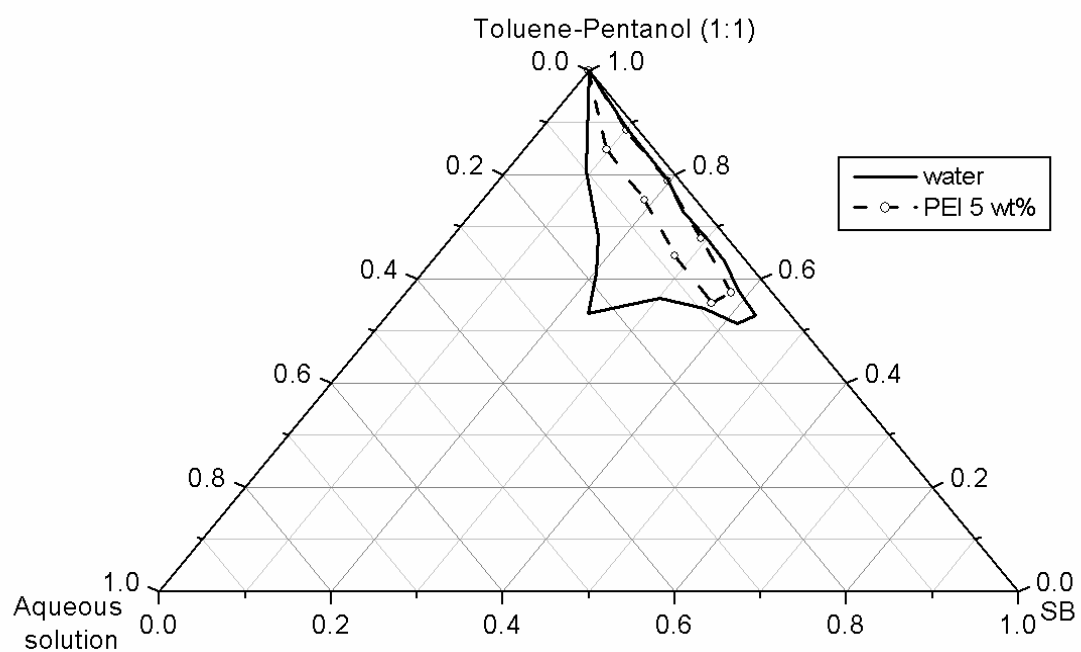
Figure A4-2: Partial phase diagrams of the quasi ternary system SB/toluene-pentanol (1:1)/water with and without polymer.

APPENDIX 5: Influence of the temperature on the SDS/toluene-pentanol (1:1)/water microemulsion
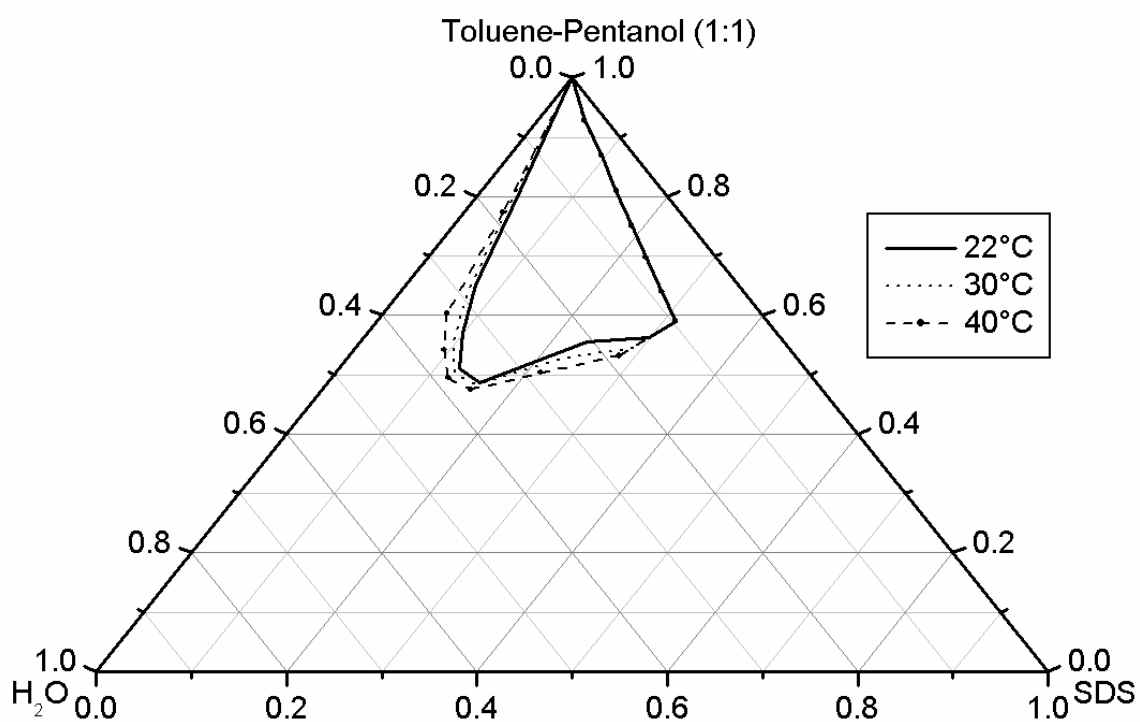
Figure A5-1: Partial phase diagrams of the quasi ternary system SDS/toluene-pentanol (1:1)/water at different temperatures.

APPENDIX 6: Representation of the dilution line ω = 33/67
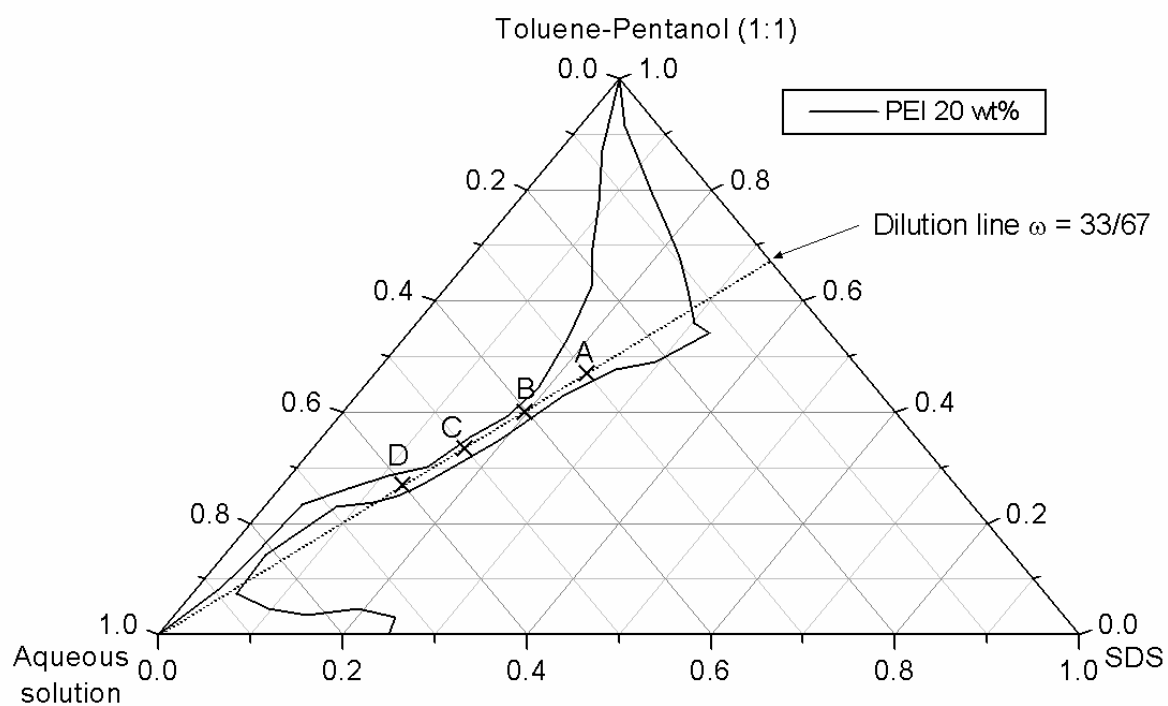
Figure A6-1: Representation of the dilution line ω = 33/67 in the partial phase diagram of the system SDS/toluene-pentanol/PEI 20wt% in water.
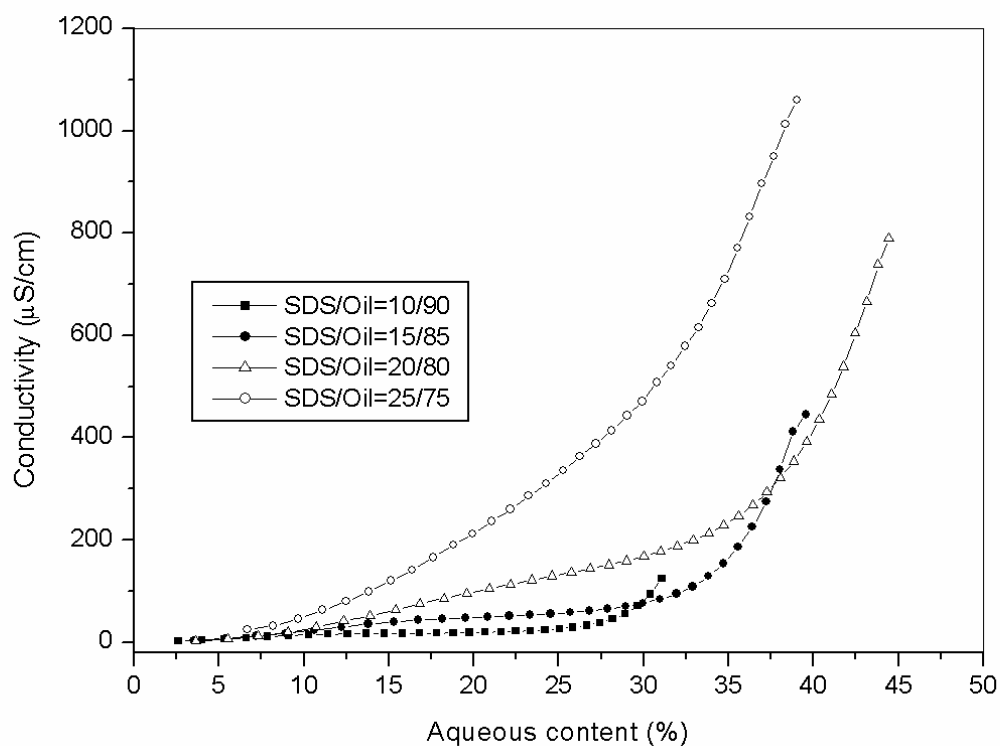
APPENDIX 7: Characterization of the SDS-microemulsion system by conductivity measurements
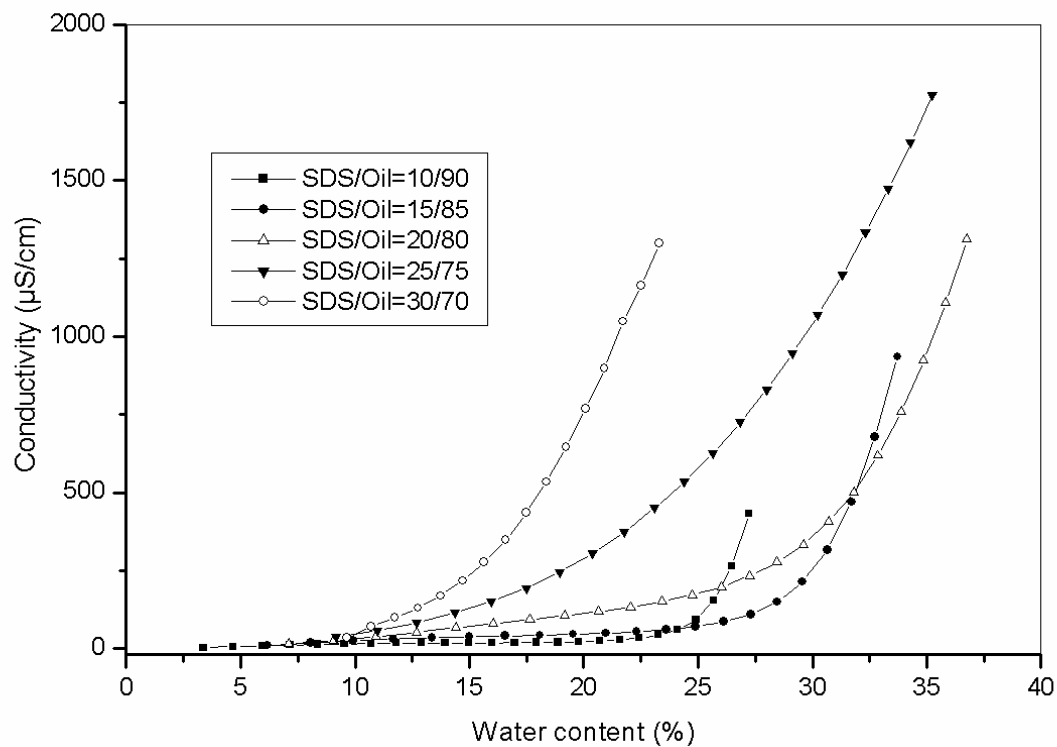
Figure A7-1: Conductivity measurements in the SDS/toluene-pentanol (1:1)/water inverse microemulsion by titration with water.

APPENDIX 8: Influence of the polyampholytes in the CTAB-microemulsion systems
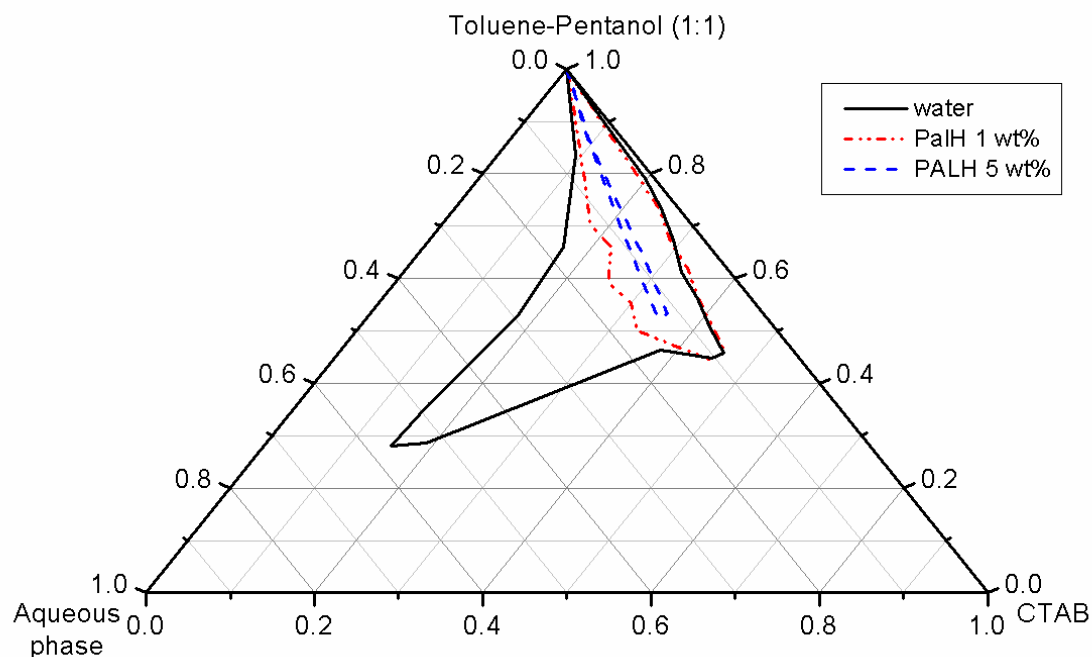
Figure A8-1: Partial phase diagrams at 22°C of the quasi ternary system CTAB/toluene-pentanol (1:1)/water in presence of different PalH concentrations.
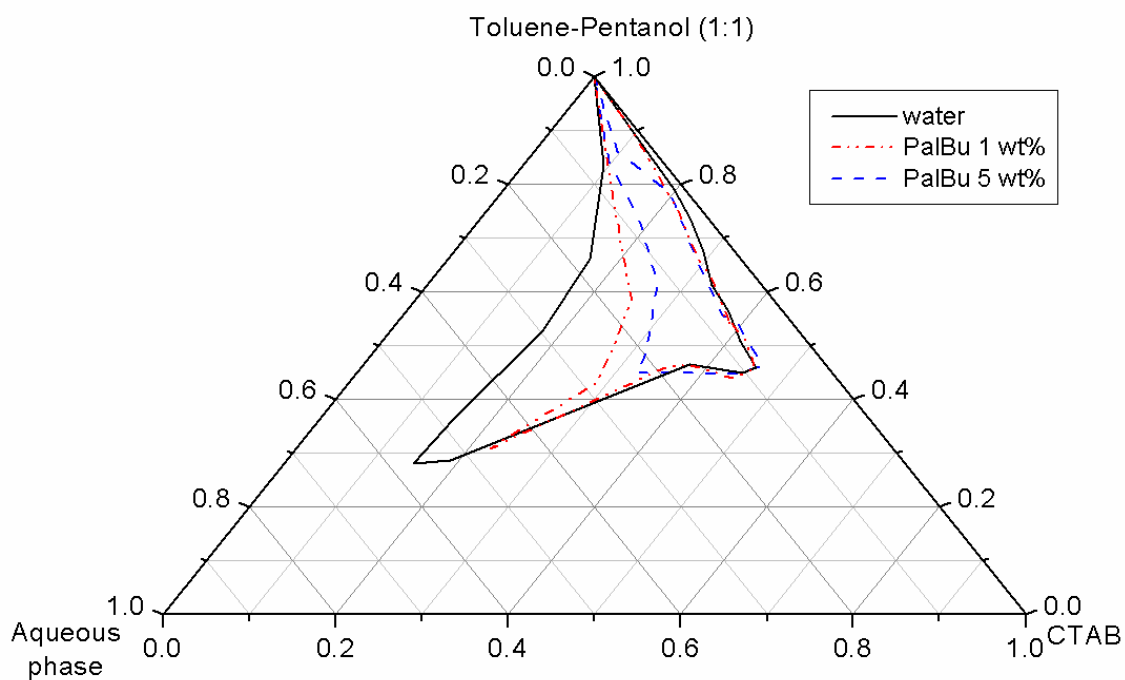
Figure A8-2: Partial phase diagrams at 22°C of the quasi ternary system CTAB/toluene-pentanol (1:1)/water in presence of different PalBu concentrations.

APPENDIX 9: Influence of the temperature in the polyampholyte-modified microemulsions
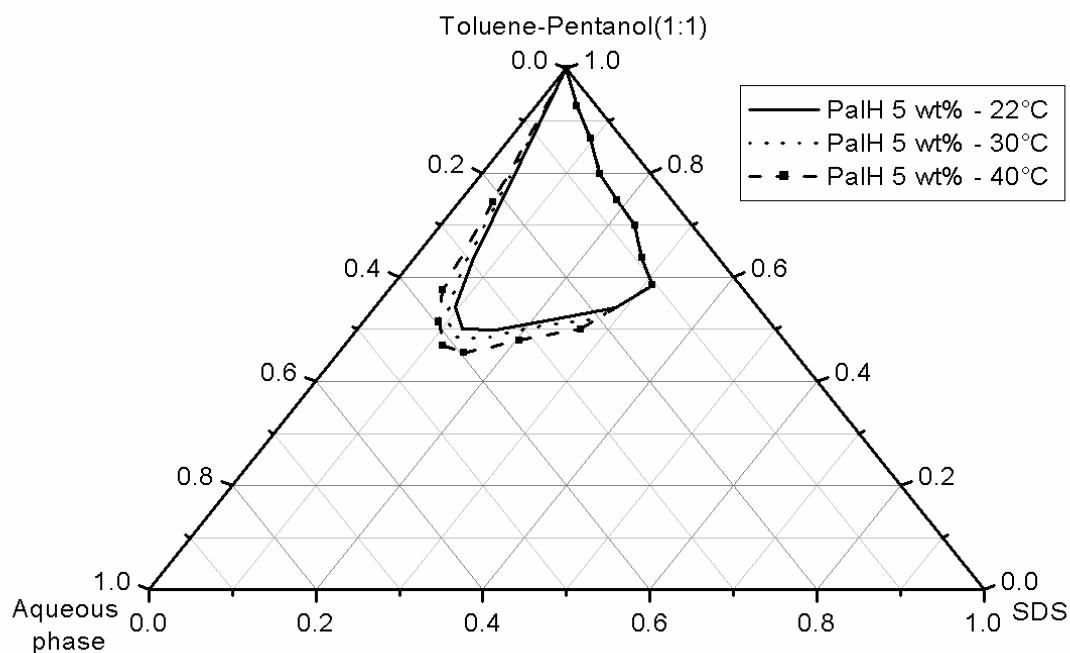
Figure A9-1: Partial phase diagrams at different temperatures of the quasi ternary system SDS/toluene-pentanol (1:1)/PalH 5 wt% in water.
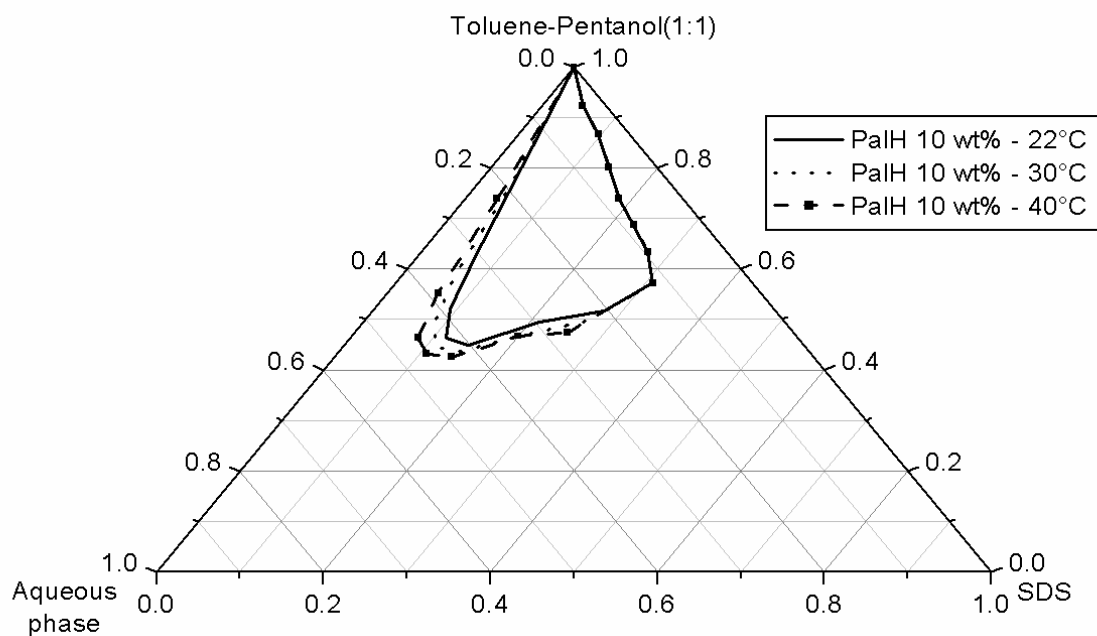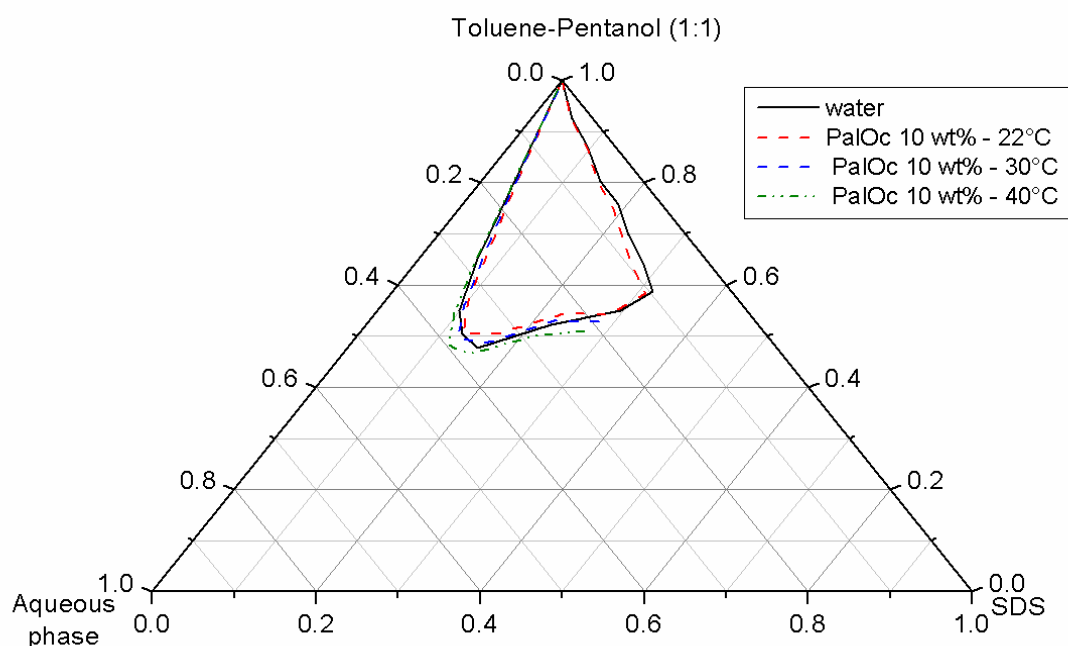

Figure A9-2: Partial phase diagrams at different temperatures of the quasi ternary system SDS/toluene-pentanol (1:1)/PalH 10 wt% in water.
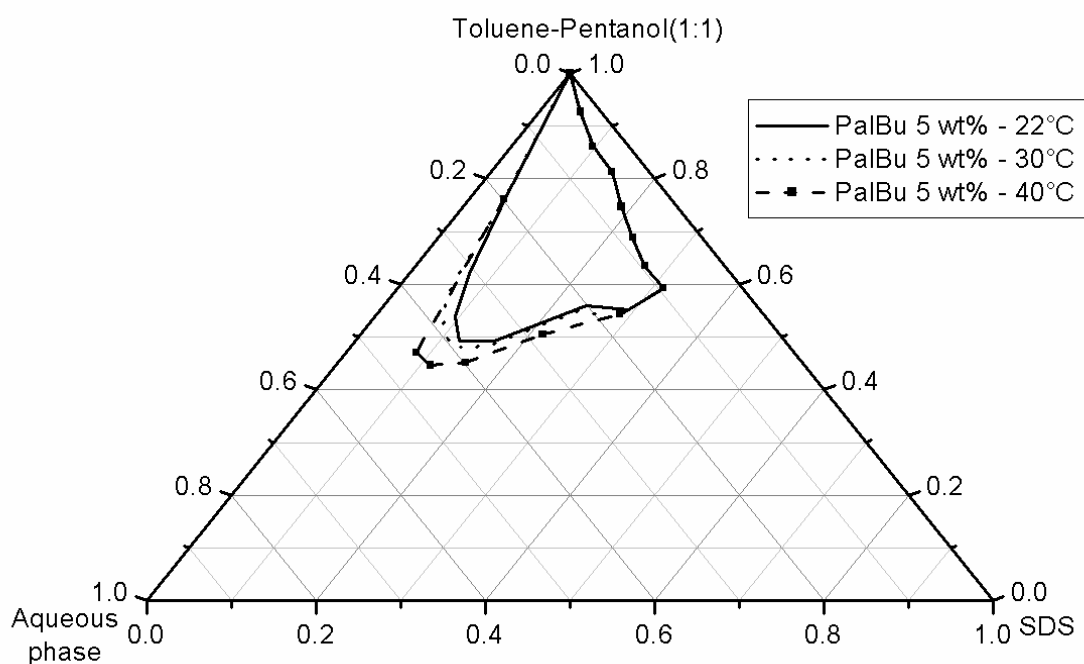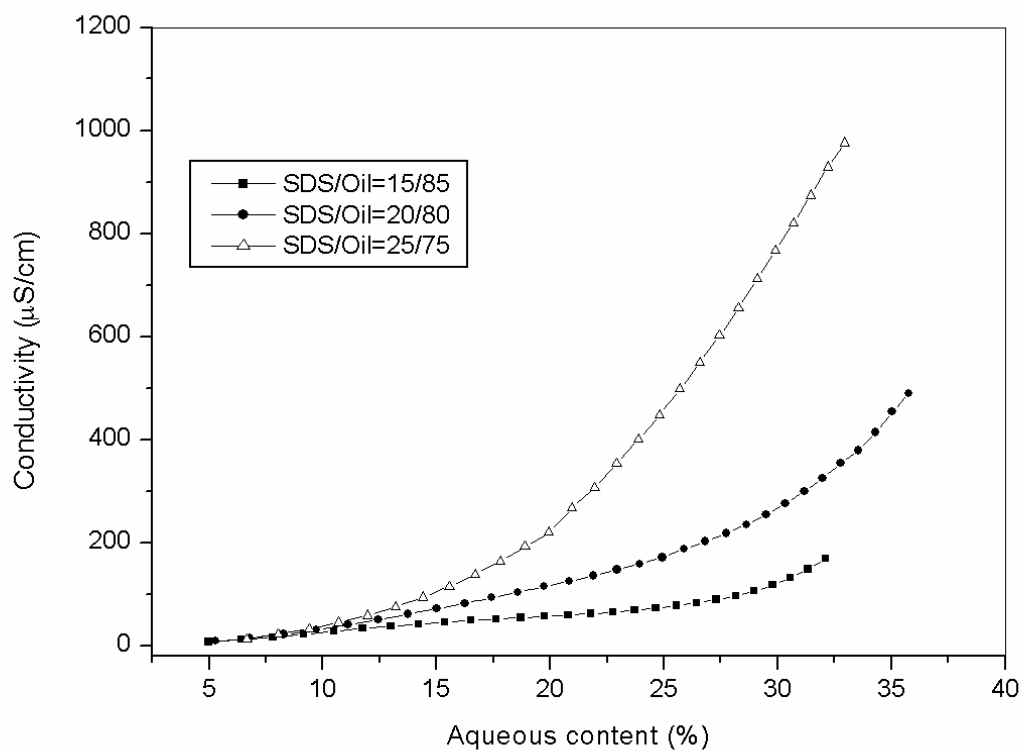
Figure A9-3: Partial phase diagrams at different temperatures of the quasi ternary system SDS/toluene-pentanol (1:1)/PalBu 5 wt% in water.
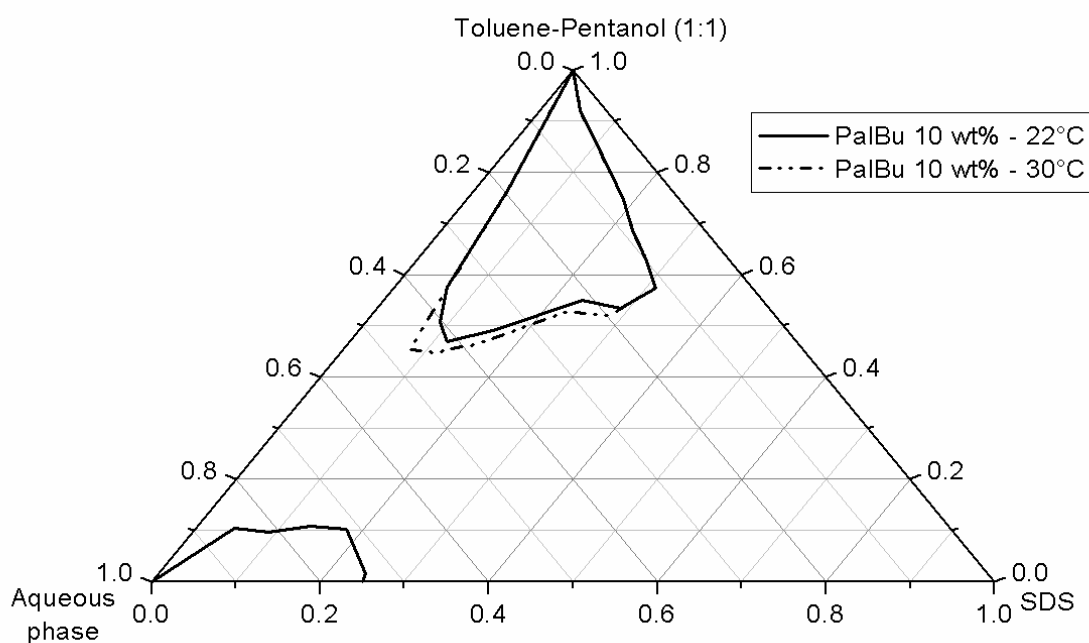
Figure A9-4: Partial phase diagrams at different temperatures of the quasi ternary system SDS/toluene-pentanol (1:1)/PalBu 10 wt% in water.

APPENDIX 10: Characterization of the polyampholyte-modified microemulsion by conductivity measurements

Figure A10-1: Conductivity measurements in the 10 wt% PalH modified W/O microemulsion.
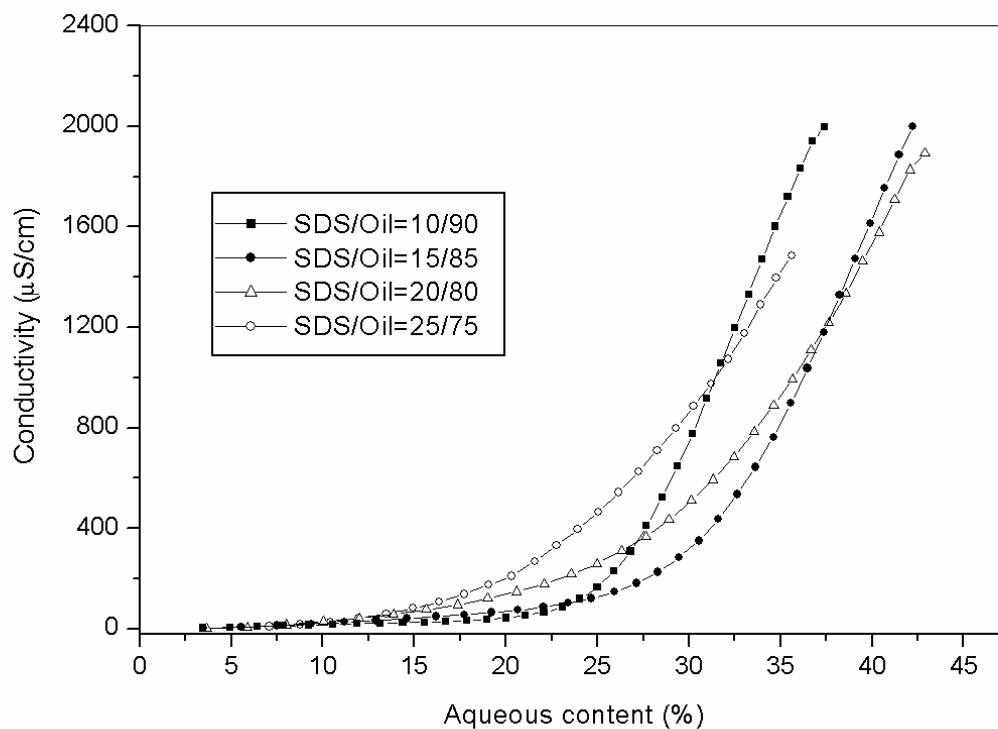
Figure A10-2: Conductivity measurements in the 10 wt% PalBu modified W/O microemulsion.

**APPENDIX 11: Characterization of the PalOc-modified microemulsion systems**

Figure A11-1: Partial phase diagrams at different temperatures of the quasi ternary system SDS/toluene pentanol (1:1)/10 wt% PalOc in water.
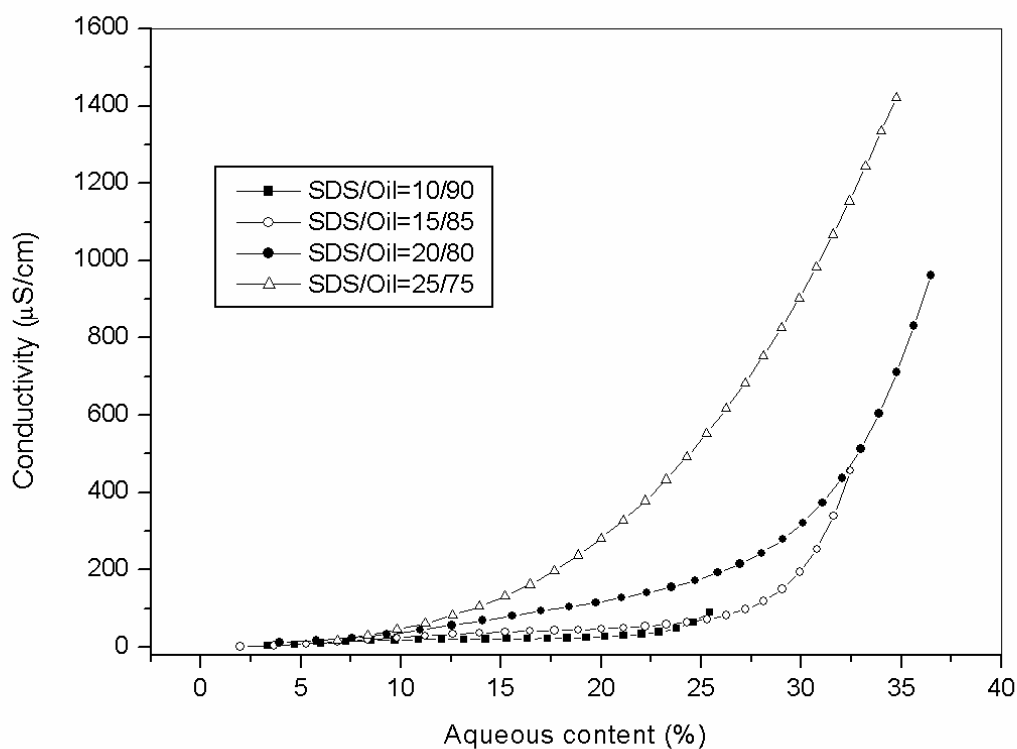
Figure A11-2: Conductivity measurements in the 1 wt% PalOc modified W/O microemulsion.

Figure A11-3: Conductivity measurements in the 10 wt% PalOc modified W/O microemulsion.

APPENDIX 12: Characterization of the PalPh-modified microemulsion systems
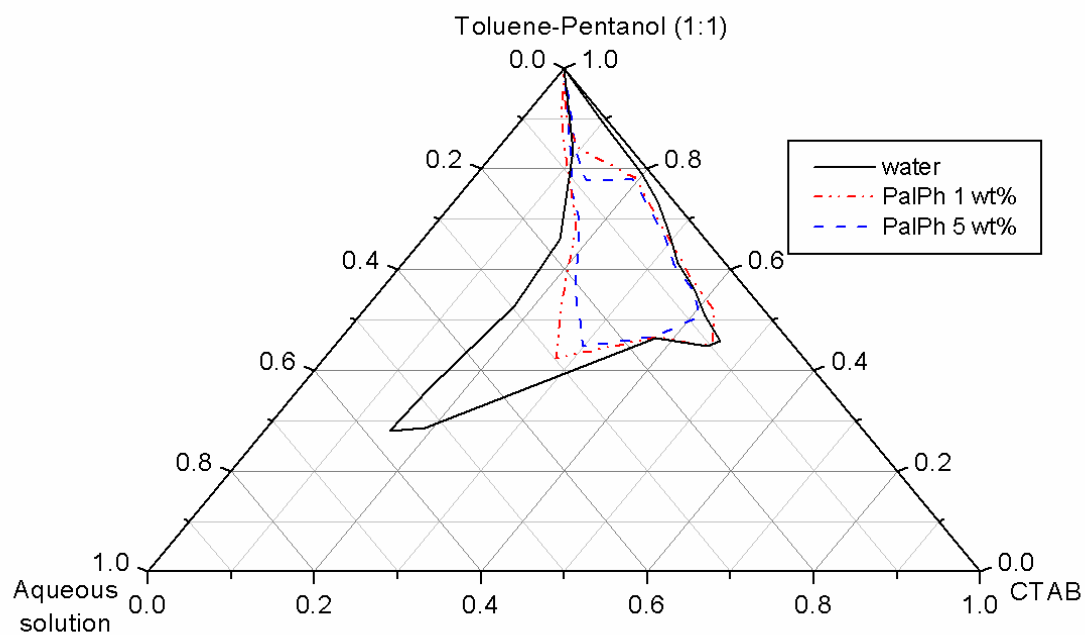
Figure A12-1: Partial phase diagrams at 22°C of the quasi ternary system CTAB/toluene-pentanol (1:1)/water in presence of different PalPh concentrations.
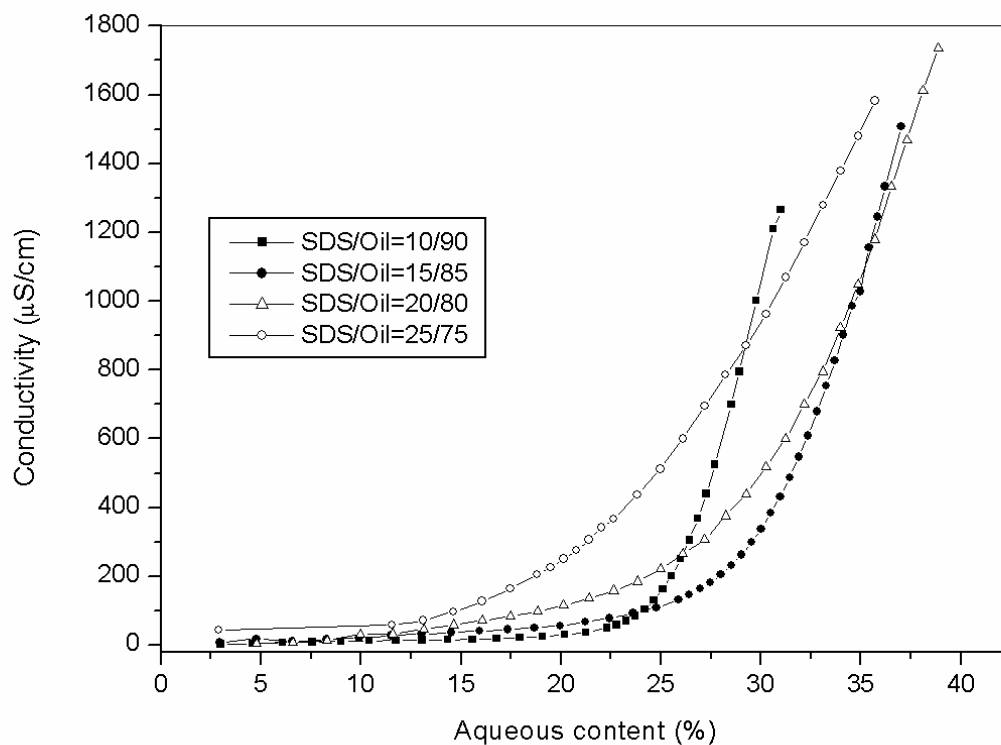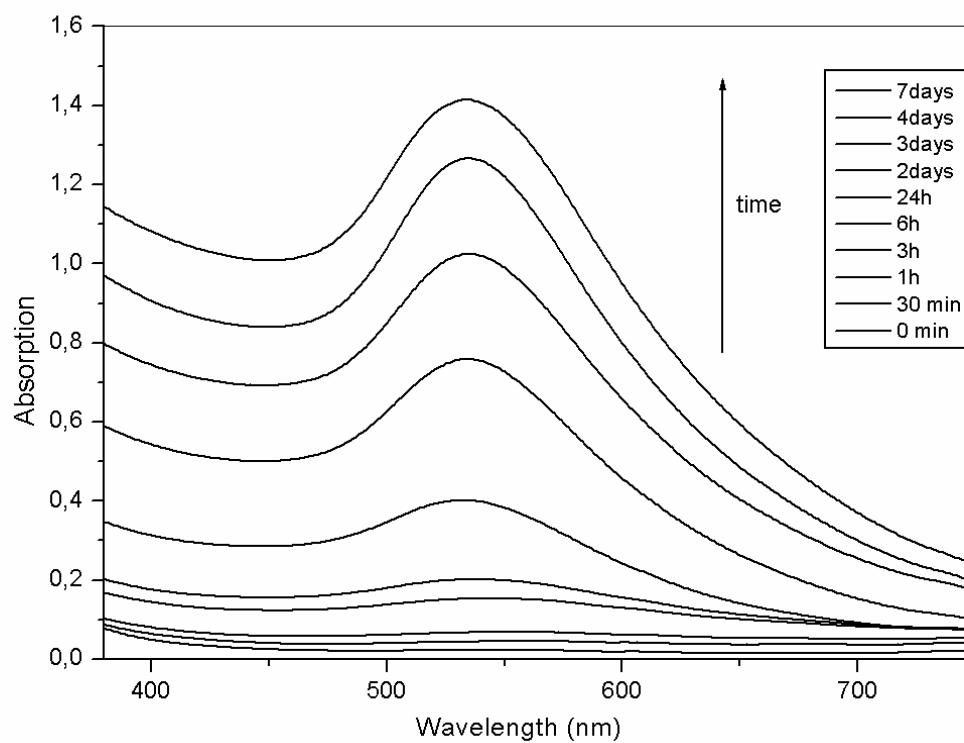

Figure A12-2: Conductivity measurements in the 5 wt% PalPh modified W/O microemulsion.

APPENDIX 13: Gold nanoparticle formation at room temperature with the hydrophobically modified poly(sodium acrylates)

Figure A13-1: Time dependent UV-vis absorption spectra of gold nanoparticles with PA3C4 for the procedure at room temperature.

APPENDIX 14: Communications concerning this thesis

Posters:

<u>C. Note</u>, J. Koetz, S. Kosmella, "Influence of hydrophobically modified polyelectrolytes on self-organized systems", 1. Zsigmondy-Colloquim, 1st-2nd April **2004**, Max-Planck- Institute for Polymer, Mainz, Germany.

<u>C. Note</u>, J. Koetz, S. Kosmella, "Influence of hydrophobically modified polyelectrolytes on self-organized systems", Tag der Chemie, 7. Juli **2004**, Potsdam, Germany.

<u>C. Note</u>, J. Koetz, S. Kosmella, "Influence of hydrophobically-modified polyelectrolytes in microemulsions on the nanoparticle formation", Polydays **2004** (Biannual International Meeting on Polymers), 4th-6th Oct. 2004, Potsdam, Germany.

<u>C. Note</u>, J. Koetz, S. Kosmella, B. Tiersch, "Hydrophobically modified polyelectrolytes used as reducing and stabilizing agent for the formation of gold nanoparticles", Formula IV: Frontiers in Formulation Science (RSC & SFC), 4th-7th July **2005**, King's College London, England.

<u>C. Note</u>, J. Koetz, S. Kosmella, "Influence of hydrophobically modified polyelectrolytes on CTAB-based w/o microemulsions", Formula IV: Frontiers in Formulation Science (RSC & SFC), 4th-7th July **2005**, King's College London, England.

<u>C. Note</u>, J. Koetz, "Poly(ethyleneimine) modified microemulsions as templates for the formation of nanoparticles", 1st European Chemistry Congress (RSC & GDCh), 27th-31st August **2006**, Budapest, Hungary.

<u>C. Note</u>, J. Koetz, "Structural changes in poly(ethyleneimine) modified microemulsions", Polydays **2006** (Biannual International Meeting on Polymers), 4th-6th Oct. 2006, Berlin, Germany.
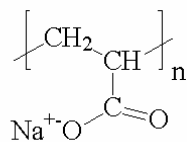
Oral presentations:

<u>C. Note</u>, J. Koetz, S. Kosmella, "Influence of hydrophobically modified polyelectrolytes on self-organized systems", Tag der Chemie, 7. Juli **2004**, Potsdam, Germany.

<u>C. Note</u>, J. Koetz, "Branched poly(ethyleneimine) as reducing and stabilizing agent for the formation of gold nanoparticles", 3. Zsigmondy-Colloquim, 6-7 April **2006**, Technische Universität Berlin, Germany.
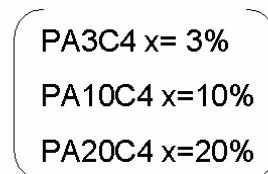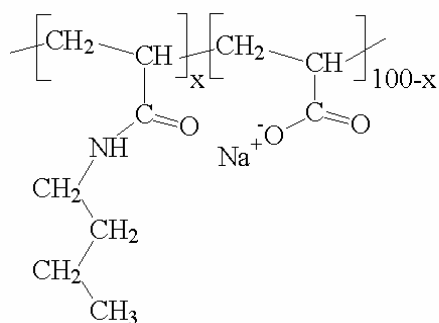
APPENDIX 15: Chemicals commonly used in this work
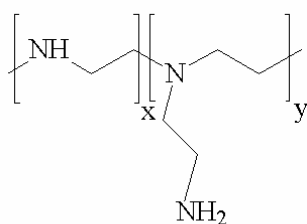
Anionic polymers:

PAA

$$\left[CH_2 - CH \right]_n$$
$$Na^+ {}^-O - C = O$$

PAxC4

$$\left[CH_2 - CH \right]_x \left[CH_2 - CH \right]_{100-x}$$

NH   C = O
CH₂   Na⁺ ⁻O   C = O
CH₂
CH₂
CH₃

PA3C4 x= 3%
PA10C4 x=10%
PA20C4 x=20%

Cationic polymer:

Branched PEI

$$\left[NH \right]_x \left[N \right]_y$$
NH₂

Polyampholytes:

PalR

H₃C   N⁺   CH₃
O⁻   HN
R
O   O
n

PalH   R= hydrogen
PalBu   R= butyl
PalOc   R= octyl
PalPh   R= phenyl

Surfactants:

CTAB

$$CH_3 - \left[CH_2 \right]_{15} - N^+ \begin{array}{c} CH_3 \\ CH_3 \\ CH_3 \end{array} \quad Br^-$$

SDS

$$CH_3 - \left[CH_2 \right]_{11} - O - S - O^- \quad Na^+$$
(with O above and O below the S)

SB

$$CH_3 - \left[CH_2 \right]_{11} - N^+ \left[CH_2 \right]_3 - S - O^-$$
(with CH₃ above and CH₃ below the N; O above and O below the S)

Oils:

Pentanol

$$CH_3 - (CH_2)_4 - OH$$

Toluene

CH₃